Electrophoresis 1991, 12, 907–930

N. Leigh Anderson
Ricardo Esquer-Blasco
Jean-Paul Hofmann
Norman G. Anderson

Large Scale Biology Corporation,
Rockville, MD

A two-dimensional gel database of rat liver proteins useful in gene regulation and drug effects studies

A standard two-dimensional (2-D) protein map of Fischer 344 rat liver (F344MST3) is presented, with a tabular listing of more than 1200 protein species. Sodium dodecyl sulfate (SDS) molecular mass and isoelectric point have been established, based on positions of numerous internal standards. This map has been used to connect and compare hundreds of 2-D gels of rat liver samples from a variety of studies, and forms the nucleus of an expanding database describing rat liver proteins and their regulation by various drugs and toxic agents. An example of such a study, involving regulation of cholesterol synthesis by cholesterol-lowering drugs and a high-cholesterol diet, is presented. Since the map has been obtained with a widely used and highly reproducible 2-D gel system (the Iso-Dalt® system), it can be directly related to an expanding body of work in other laboratories.

Contents

Correspondence: Dr. N. Leigh Anderson, Large Scale Biology Corporation, 9620 Medical Center Drive, Rockville, MD 20850, USA

Abbreviations: CBB, Coomassie Brilliant Blue; CPK, creatine phosphokinase; 2-D, two-dimensional; IEF, isoelectric focusing; MSN, master spot number; NP-40, Nonidet P-40; SDS, sodium dodecyl sulfate

0173-0835/91/1111-0907 $3.50+.25/0

1 Introduction

High-resolution two-dimensional electrophoresis of proteins, introduced in 1975 by O'Farrell and others [1–4], has been used over the ensuing 16 years to examine a wide variety of biological systems, the results appearing in more than 5000 published papers. With the advent of computerized systems for analyzing two-dimensional (2-D) gel images and constructing spot databases, it is also possible to plan and assemble integrated bodies of information describing the appearance and regulation of thousands of protein gene products [5, 6]. Creating such databases involves amassing and organizing quantitative data from thousands of 2-D gels, and requires a substantial commitment in technology and resources.

Given the long-term effort required to develop a protein database, the choice of a biological system takes on considerable importance. While *in vitro* systems are ideal for answering many experimental questions, especially in cancer research and genetics, our experience with cell cultures and tissue samples suggests that some *in vivo* approaches could have major advantages. In particular, we have noticed that liver tissue samples from rats and mice appear to show greater quantitative reproducibility (in terms of individual protein expression) than replicate cell cultures. This is perhaps a natural result of the homeostasis maintained in a complete animal *vs.* the well-known variability of cell cultures, the latter due principally to differences in reagents (*e.g.*, fetal bovine serum), conditions (*e.g.*, pH) and genetic "evolution" of cell lines while in culture. It is also more difficult to generate adequate amounts of protein from cell culture systems (particularly with attached cells), forcing the investigator to resort to radioisotope-based or silver-based stain-detection methods. While these methods are more sensitive (sometimes much more sensitive) than the Coomassie Brilliant Blue (CBB) stain typically used for protein detection in "large" protein samples, they are generally more variable, more labor-intensive and, in the case of radiographic methods, may generate highly "noisy" images, due to the properties of the films used. By contrast, large protein samples can easily be prepared from liver using urea/Nonidet P-40 (NP-40) solubilization and stained with CBB, which has the advantage of being easily reproducible [8]. Finally, there remains the question of the "truthfulness" of many *in vitro* systems as compared to their *in vivo* analogs; how great are the changes caused by the introduction into a cul-

ture and the associated shift to strong selection for growth, and how do these affect experimental outcomes? Hence the apparent advantages of *in vitro* systems, in terms of experimental manipulation, may be counterbalanced by other factors relating to 2-D data quality.

There is a second important class of reasons for exploring the use of an *in vivo* biological system such as the liver. Historically, there have been two broad approaches to the mechanistic dissection of biochemical processes in intact cellular systems: genetics (a search for informative mutants) and the use of chemical agents (drugs and chemical toxins). Both approaches help us to understand complex systems by disrupting some specific functional element and showing us the result. With the development of techniques for genetic manipulation and cloning, the genetic approach can be effectively applied either *in vitro* or *in vivo*, although the *in vitro* route is usually quicker. The chemical approach can also be applied to either sort of biological system; here, however, the bulk of consistently acquired information is in experimental animals (rats and mice). While most biologists know a short list of compounds having specific, experimentally useful effects (*e.g.*, inhibitors of protein synthesis, ionophores, polymerase inhibitors, channel blockers, nucleotide analogs, and compounds affecting polymerization of cytoskeletal proteins), there is a much larger number of interesting chemically-induced effects, most of them characterized by toxicologists and pharmacologists in rodent systems. Just as a thorough genetic analysis would involve saturating a genome with mutations, it is possible to imagine a saturating number of drugs, the analysis of whose actions would reveal the complete biochemistry of the cell. While organized drug discovery efforts usually target specific desired effects, the nature of the process, with its dependence on screening large numbers of compounds, necessarily produces many unanticipated effects. It is therefore reasonable to suppose that the required broad range of compounds necessary to achieve "biochemical saturation" may be forthcoming; in fact, it may already exist among the hundreds of thousands of compounds that failed to qualify as drugs.

Among organs, the liver is an obvious choice for the study of chemical effects because of its well-known plasticity and responsiveness. The brain appears to be quite plastic (*e.g.* [7]), but it is a complicated mixture of cell types requiring skillful dissection for most experiments. The kidney, while quite responsive, also presents a potentially confounding mixture of cell types. The liver, by contrast, is made up of one predominant cell type which is easy to solubilize: the hepatocyte, representing more than 95% of its mass. Most importantly, the liver performs many homeostatic functions that require rapid modulation of gene expression. It appears that most chemical agents tested affect gene expression in the liver at some dosage (N. Leigh Anderson, unpublished observations), an interesting contrast to our earlier work with lymphocytes, for example, which seem to be much less responsive. Such results conform to the expectation that cells with a homeostatic, physiological role should be more plastic than cells differentiated for a purpose dependent on the action of a limited number of specific genes.

The liver also allows the parallels between *in vitro* and *in vivo* systems to be examined in detail. Significant progress has been made in the development of mouse, rat and human hepatocyte culture systems, as well as in precision-cut tissue slices. Using such an array of techniques, it is possible to assemble a matrix of mammalian systems including mouse and rat *in vivo* on one level and mouse, rat and human *in vitro* on a second level, and to compare effects between species and between systems. This approach allows us to draw informed conclusions regarding the biochemical "universality" of biological responses among the mammals and to offer some insight into the validity of *in vitro* approaches for toxicological screening. We believe this data will be necessary if *in vitro* alternatives are to achieve wider usage in government-mandated safety testing of drugs, consumer products and industrial and agricultural chemicals.

A number of interesting studies have been published using 2-D mapping to examine effects in the rodent liver. A number of investigarors have made use of the technique to screen for existing genetic variants [8–11] or induced mutations [12–14], mainly in the mouse. This work builds on the wealth of genetic information available on the mouse and its established position as a mammalian mutation-detection system. While some studies of chemical effects have been undertaken in the mouse [15–17], most have used the rat [18–23]. The examination of the cytochrome p-450 system, in particular, has been carried out almost exclusively on the rat [24, 25].

These considerations lead us to conclude that rodent liver offers the best opportunity to systematically examine an array of gene regulation systems, and ultimately to build a predictive model of large-scale mammalian gene control. The basic underlying foundation of such a project is a reliable, reproducible master 2-D pattern of liver, to which ongoing experimental results can be referred. In this paper, we report such a master pattern for the acidic and neutral proteins of rat liver (pattern F344MST3). In future, this master will be supplemented by maps of basic proteins, and analogous maps of mouse and human liver.

2 Materials and methods

2.1 Sample preparation

Liver is an ideal sample material for most biochemical studies, including 2-D analysis. A sample is taken of approximately 0.5 g of tissue from the apical end of the left lobe of the liver. Solubilization is effected as rapidly as practical: a delay of 5–15 min appears to cause no major alteration in liver protein composition if the liver pieces are kept cold (*e.g.*, on ice) in the interim. In the solubilization process, the liver sample is weighed, placed in a glass homogenizer (*e.g.*, 15 mL Wheaton); 8 volumes of solubilizing solution*

* The solubilizing solution is composed of 2% NP-40 (Sigma), 9 M urea (analytical grade, *e.g.*, BDH or Bio-Rad), 0.5% dithiothreitol (DTT: Sigma) and 2% carrier ampholytes (pH 9–11 LKB: these come as a 20% stock solution, so 2% final concentration is achieved by making the final solution 10% 9–11 Ampholine by volume). A large batch of solubilizer (several hundred mL) is made and stored frozen at −80°C in aliquots sufficient to provide enough for one day's estimated sample preparation requirement. The solution is never allowed to become warmer than room temperature at any stage during preparation or thawing for use, since heating of concentrated urea solutions can produce contaminants that covalently modify proteins producing artifactual charge shifts. Once thawed, any unused solubilizer is discarded.

dded (*i.e.*, 4 mL per 0.5 g tissue) and the mixture is ho-genized using first the loose- and then then the tight-fit-g glass pestle. This takes approximately 5 strokes with ch pestle and is carried out at room temperature because would crystallize out in the cold. Once the liver sample thoroughly homogenized in the solubilizer, it is assumed at all the proteins are denatured (by the chaotropic effect the urea and NP-40 detergent) and the enzymes inacti-ted by the high pH (~9.5). Therefore these samples may kept at room temperature until they can be centrifuged frozen as a group (within several hours of preparation). ie samples are centrifuged for 6×10^4 *g* min (*e.g.*, 500 000 *g* for 12 min using a Beckman TL-100 centrifuge). The ntrifuge rotor is maintained at just below room tempera-re (*e.g.*, 15–20°C), but not too cold, so as to prevent the ecipitation of urea. The centrifuge of choice is a Beckman L-100 because of the sample tube sizes available, but any ltracentrifuge accepting smallish tubes will suffice. When appropriate centrifuge is not available near the site of mple preparation, samples can be frozen at −80°C and awed prior to centrifugation and collection of superna-nts. Each supernatant is carefully removed following cen-ifugation and aliquoted into at least 4 clean tubes for stor-ge. This is done by transferring all the supernatant to one lean tube, mixing this gently (to assure homogeneous omposition) and then dividing it into 4 aliquots. The ali-uots are frozen immediately at −80°C. These multiple ali-uots can provide insurance against a failed run or a freezer reakdown.

2.2 Two-dimensional electrophoresis

ample proteins are resolved by 2-D electrophoresis using he 20 × 25 cm Iso-Dalt[3] 2-D gel system ([26–29]; pro-uced by LSB and by Hoefer Scientific Instruments, San rancisco) operating with 20 gels per batch. All first-dimen-ional isoelectric focusing (IEF) gels are prepared using the ame single standardized batch of carrier ampholytes BDH 4–8A in the present case, selected by LSB's batch-esting program for rat and mouse database work**). A 10 L sample of solubilized liver protein is applied to each gel, and the gels are run for 33 000 to 34 500 volt-hours using a rogressively increasing voltage protocol implemented by a programmable high-voltage power supply. An Ange-ique™ computer-controlled gradient-casting system (pro-uced by LSB) is used to prepare second-dimensional sod-um dodecyl sulfate (SDS) polyacrylamide gradient slab gels in which the top 5% of the gel is 11%T acrylamide, and he lower 95% of the gel varies linearly from 11% to 18%T.

his system has recently been modified so as to employ a ommercially available 30.8%T acrylamide/*N,N'*-methyle-ebisacrylamide prepared solution (thus avoiding the han-ling of the solid acrylamide monomer) and three addi-onal stock solutions: buffer (made from Sigma pre-set Tris), persulfate and *N,N,N',N'*-tetramethylethylenedi-mine (TEMED). Each gel is identified by a computer-inted filter paper label polymerized into the lower left cor-r of the gel. First-dimensional IEF tube gels are loaded directly (as extruded) onto the slab gels without equilibration, and held in place by polyester fabric wedges (Wedgies™, produced by LSB) to avoid the use of hot agarose. Second-dimensional slab gels are run overnight, in groups of 20, in cooled DALT tanks (10°C) with buffer circulation. All run parameters, reagent source and lot information, and notations of deviation from expected results are entered by the technician responsible on a detailed, multi-page record of the experiment.

2.3 Staining

Following SDS-electrophoresis, slab gels are stained for protein using a colloidal Coomassie Blue G-250 procedure in covered plastic boxes, with 10 gels (totalling approximately 1 L of gel) per box. This procedure (based on the work of Neuhoff [30, 31]) involves fixation in 1.5 L of 50% ethanol and 2% phosphoric acid for 2 h, three 30 min washes, each in 2 L of cold tap water, and transfer to 1.5 L of 34% methanol, 17% ammonium sulfate and 2% phosphoric acid for 1 h, followed by the addition of a gram of powdered Coomassie Blue G-250 stain. Staining requires approximately 4 days to reach equilibrium intensity, whereupon gels are transferred to cool tap water and their surfaces rinsed to remove any particulate stain prior to scanning. Gels may be kept for several months in water with added sodium azide. The water washes remove ethanol that would dissolve the stain (and render the system noncolloidal, with high backgrounds). The concentrated ammonium sulfate and methanol solution is diluted by equilibration with the water volume of the gels to automatically achieve the correct final concentrations for colloidal staining. Practical advantages of this staining approach can be summarized as follows: (i) the low, flat background makes computer evaluation of small spots (max OD < 0.02) possible, especially when using laser densitometry; (ii) up to 1500 spots can be reliably detected on many gels (*e.g.*, rat liver) at loadings low enough to preserve excellent resolution; and (iii) reproducibility appears to be very good: at least several hundred spots have coefficients of reproducibility less than 15%. This value is at least as good as previous CBB methods, and significantly better than many silver stain systems.

2.4 Positional standardization

The carbamylated rabbit muscle creatine phosphokinase (CPK) standards [32] are purchased from Pharmacia and BDH. Amino acid compositions, and numbers of residues present in proteins used for internal standardization, are taken from the Protein Identification Resource (PIR) sequence database [33].

2.5 Computer analysis

Stained slab gels are digitized in red light at 134 micron resolution, using either a Molecular Dynamics laser scanner (with pixel sampling) or an Eikonix 78/99 CCD scanner. Raw digitized gel images are archived on high-density DAT tape (or equivalent storage media) and a greyscale videoprint prepared from the raw digital image as hard-copy backup of the gel image. Gels are processed using the Kepler[®] software system (produced by LSB), a commercially available workstation-based software package built on

This material (succeeding certified batches of which are available from Hoefer Scientific Instruments) has the most linear pH gradient produced by any ampholyte tested except for the Pharmacia wide range (which has an unacceptable tendency to bind high-molecular weight acidic proteins, causing them to streak).

some of the principles of the earlier TYCHO system [34–41]. Procedure PROC008 is used to yield a spotlist giving position, shape and density information for each detected spot. This procedure makes use of digital filtering, mathematical morphology techniques and digital masking to remove the background, and uses full 2-D least-squares optimization to refine the parameters of a 2-D Gaussian shape for each spot. Processing parameters and file locations are stored in a relational database, while various log files detailing operation of the automatic analysis software are archived with the reduced data. The computed resolution and level of Gaussian convergence of each gel are inspected and archived for quality control purposes.

Experiment packages are constructed using the Kepler experiment definition database to assemble groups of 2-D patterns corresponding to the experimental groups (*e.g.*, treated and control animals). Each 2-D pattern is matched to the appropriate "master" 2-D pattern (pattern F344MST3 in the case of Fischer 344 rat liver), thereby providing linkage to the existing rodent protein 2-D databases. The software allows experiments containing hundreds of gels to be constructed and analyzed as a unit, with up to 100 gels displayed on the screen at one time for comparative purposes and multiple pages to accommodate experiments of > 1000 gels. For each treatment, proteins showing significant quantitative differences *vs.* appropriate controls are selected using group-wise statistical parameters (*e.g.*, Student's t-test, Kepler[2] procedure STUDENT). Proteins satisfying various quantitative criteria (such as $P < 0.001$ difference from appropriate controls) are represented as highlighted spots onscreen or on computer-plotted protein maps and stored as spot populations (*i.e.*, logical vectors) in a liver protein database. Quantitative data (spot parameters, statistical or other computed values) are stored as real-valued vectors in the database. Analysis of coregulation is performed using a Pierson product-moment correlation (Kepler procedure CORREL) to determine whether groups of proteins are coordinately regulated by any of the treatments. Such groups can be presented graphically on a protein map, and reported together with the statistical criteria used to assess the level of coregulation. Multivariate statistical analysis (*e.g.*, principal components' analysis) is performed on data exported to SAS (SAS Institute).

2.6 Graphical data output

Graphical results are prepared in GKS and translated within Kepler[2] into output for any of a variety of devices. Linedrawing output is typically prepared as Postscript and printed on an Apple Laserwriter. Detailed maps presented here have been generated using an ultra-high-resolution Postscript-compatible Linotronic output device. Greyscale graphics are reproduced from the workstation screen using a Seikosha videoprinter. Patterns are shown in the standard orientation, with high molecular mass at the top and acidic proteins to the left.

2.7 Experiment LSBC04

In the study described here 12-week-old Charles River male F344 rats were used. Diets were prepared at LSB, based on a Purina 5755M Basal Purified Diet. Lovastatin and cholestyramine were obtained as prescription pharmaceuticals, ground and mixed with the diet at concentrations of 0.075% and 1%, respectively. The high cholesterol diet was Purina 5801M-A (5% cholesterol plus 1% sodium cholate in the control diet). Animal work was carried out by Microbiological Associates (Bethesda, MD). Animals were acclimatized for one week on the control diet, fed test or control diets for one week, and sacrificed on day 8. Average daily doses of lovastatin and cholestyramine in appropriate groups were 37 mg/kg/day and 5 g/kg/day, respectively, based on the weight of the food consumed. Liver samples were collected and prepared for 2-D electrophoresis according to the standard liver protocol (homogenization in 8 volumes of 9 M urea, 2% NP-40, 0.5% dithiothreitol, 2% LKB pH 9–11 carrier ampholytes, followed by centrifugation for 30 min at 80 000 × *g*). Kidney, brain and plasma samples were frozen. Gels were run as described above, and the data was analyzed using the Kepler[2] system. Gels were scaled, to remove the effect of differences in protein loading, by setting the summed abundances of a large number of matched spots equal for each gel (linear scaling).

3 Results and discussion

3.1 The rat liver protein 2-D map

F344MST3 is a standard 2-D pattern of rat liver proteins, based on the Fischer 344 strain. This pattern was initiated from a single 2-D gel and extensively edited in an experiment comparing it to a range of protein loads, so as to include both small spots and well-resolved representations of high-abundance spots. More than 700 rat liver 2-D patterns have been matched to F344MST3 in a series of drug effects and protein characterization experiments, and numerous new spots (induced by specific drugs, for instance) have been added as a result. A modified version including additional spots present in the Sprague-Dawley outbred rat has also been developed (data not shown). Figure 1 shows a greyscale representation and Fig. 2 a schematic plot of the master pattern. More than 1200 spots are included, most of which are visible on typical gels loaded with 10 µL of solubilized liver protein prepared by the standard method and stained with colloidal Coomassie Blue. Master spot numbers (MSN's) have been assigned to all proteins, and appear in the following figures, each showing one quadrant of the pattern. Figure 3 shows the upper left (acidic, high molecular mass) quadrant, Fig. 4 the upper right (basic, high molecular mass) quadrant, Fig. 5 the lower left (acidic, low molecular mass) quadrant, and Fig. 6 the lower right (basic, low molecular mass) quadrant. The quadrants overlap as an aid to moving between them. The gel position (in 100 micron units), isoelectric point (relative to the CPK internal p*I* standards) and SDS molecular mass (from the calibration curve in Fig. 8) are listed for each spot (Table 1). Because of the precision of the CPK-p*I* values, these parameters can be used to relate spot locations between gel systems more reliably than using p*I* measurements expressed as pH. A major objective of current studies is the identification of all major spots corresponding to known liver proteins, as well as rigorous definitions of subcellular organelle contents. Of particular interest to us is the parallel development of identifications in the rat and mouse liver maps, allowing detailed comparisons of gene expression effects in the two systems. The results of these studies will be presented systematically in a later edition of this database.

we include here a useful series of 22 orienting identifications as an aid to other users of the rat liver pattern (Table

2 Carbamylated charge standards, computed p*I*s and molecular mass standardization

We have previously shown that the use of a system of close-spaced internal p*I* markers (made by carbamylating a basic protein) offers an accurate and workable solution to the problem of assigning positions in the p*I* dimension [32]. The same system, based on 36 protein species made by carbamylating rabbit muscle CPK has been used here to assign p*I*s to most rat liver acidic and neutral proteins. The standards were coelectrophoresed with total liver proteins, and the standard spots added to a special version of the master pattern F344MST3. The gel *X*-coordinates of all liver protein spots lying within the CPK charge train were then transformed into CPK p*I* positions by interpolation between the positions of immediately adjacent standards (Table 1) using a Kepler[2] vector procedure.

It has proven possible to compute fairly accurate p*I* values for many proteins from the amino acid composition [42]. We have attempted here to test a further elaboration of this approach, in which we computed p*I*s for the CPK standards themselves, based on our knowledge of the rabbit muscle CPK sequence and the fact that adjacent members of the charge train typically differ by blockage of one additional lysine residue (Table 3). We compared these values to similar computed p*I*s for an additional set of carbamylated standards made from human hemoglobin beta chains and a series of rat liver and human plasma proteins of known position and sequence (Fig. 7, Table 4). The result demonstrates good concordance between these systems. Two proteins show significant deviations: liver fatty-acid binding protein (FABP; #1 in Table 4) and protein disulphide isomerase (#20 in the table). The FABP spot present on F344MST3 may represent a charge-modified version of a more basic parent spot closer to the expected p*I*, not resolved in the IEF/SDS gel. Of particular importance is the fact that, by comparing computed p*I*s of sequenced but unlocated proteins with the CPK p*I*s, we can assign a probable gel location without making any assumptions regarding the actual gel pH gradient. This offers a useful shortcut, given the vagaries of pH measurement on small diameter IEF gels. We have used this approach to compute the CPK p*I*s of all rat and mouse proteins in the PIR sequence database, as an aid to protein identification (data not shown).

In order to standardize SDS molecular weight (SDS-MW), we have used a standard curve fitted to a series of identified proteins (Fig. 8). Rather than using molecular mass *per se*, we have elected to use the number of amino acids in the polypeptide chain, as perhaps a better indication of the length of the SDS-coated rod that is sieved by the second dimension slab. The resulting values were multiplied by 112 (the weighted average mass of amino acids in sequenced proteins) to give predicted molecular masses. Because we use gradient slabs, we have not constrained the fitted curve to conform to any predetermined model; rather we tried many equations and selected the best using the program "Tablecurve" on a PC. The equation chosen was $y = a + bx + c/x^2$, where y is the number of residues, x is the gel *Y* coordinate, a is 511.83, b is −0.2731 and c is 33183801. The resulting fit appears to be fairly good over a broad range of molecular mass.

3.3 An example of rat liver gene regulation: Cholesterol metabolism

Experiment LSBC04 was designed as a small-scale test of the regulation of cholesterol metabolism *in vivo* by three agents included in the diet: lovastatin (Mevacor®, an inhibitor of HMG-CoA reductase); cholestyramine (a bile acid sequestrant that has the effect of removing cholesterol from the gut-liver recirculation); and cholesterol itself. The first two agents should lower available cholesterol and the third should raise it, allowing manipulation of relevant gene expression control systems in both directions. Such an experiment offers an interesting test of the 2-D mapping system since most of the pathway enzymes are present in low abundance, many are membrane-bound and difficult to solubilize, and the pathway itself is complex. Approximately 1000 proteins were separated and detected in liver homogenates. Twenty-one proteins were found to be affected by at least one treatment, and these could be divided into several coregulated groups.

3.3.1 MSN 413 (putative cytosolic HMG-CoA synthase) and sets of spots regulated coordinately or inversely

One group of spots (including a spot assigned to the cytosolic HMG-CoA synthase, MSN 413) showed the expected increase in abundance with lovastatin or cholestyramine, the synergistic further increase with lovastatin and cholestyramine, and a dramatic decrease with the high cholesterol diet. Spot number 413 is the most strongly regulated protein in the present experiment, showing a 5- to 10-fold induction after a 1 week treatment with 0.075% lovastatin and 1% cholestyramine in the diet (Figs. 9 and 10). Its expression follows precisely the expectation for an enzyme whose abundance is controlled by the cholesterol level; it is progressively increased from the control levels by cholestyramine, lovastatin and lovastatin plus cholestyramine, and it sinks below the threshold of detection in animals fed the high cholesterol diet. This spot has been tentatively identified as the cytosolic HMG-CoA synthase, based on a reaction with an antiserum to that protein provided by Dr. Michael Greenspan at Merck Sharp & Dohme Research Laboratories. This enzyme lies immediately before HMG-CoA reductase in the liver cholesterol biosynthesis pathway, and is known to be co-regulated with it. Spot 413 has an SDS molecular weight of about 54 000 and a CPK p*I* of −11.4, in reasonably close agreement with a molecular weight of 57300 and a CPK p*I* of −15.7 computed from the known sequence of the hamster enzyme [43].

Using a classical product-moment correlation test (Kepler procedure CORREL), a series of five additional spots was found to be coregulated with 413. The level of correlation was exceedingly high (> 95%). Two of these, 1250 and 933, are at similar molecular weights and approximately one charge more acidic than 413 (Fig. 9), indicating that they may be covalently modified forms of the 413 polypeptide. This suspicion is strengthened by the observation that both spots are also stained by the antibody to cytosolic HMG-CoA synthase. The remaining three correlated spots appear

to comprise an additional related pair (1253 and 1001) of around 40 kDa and a single spot (1119) of around 28 kDa. Because these two presumed proteins are present at substantially lower abundances than 413, and because the cytosolic HMG-CoA synthase is reported to consist of only one type of polypeptide, they are likely to represent other, very tightly coregulated enzymes. A second group of six spots was selected based on a regulatory pattern close to the inverse of that for spot 413 (MSN's 34, 79, 178, 182, 204, 347; data not shown). For these proteins, the lowest level of expression occurs with exposure to lovastatin plus cholestyramine and the highest level upon exposure to the high-cholesterol diet. Spots 182 and 79 are highly correlated and lie about one charge apart at the same molecular weight; they may thus be isoforms of a single protein. The other four spots probably represent additional enzymes or subunits.

3.3.2 MSN 235 and coregulated spots

A third group of five spots, mainly comprised of mitochondrial proteins including putative mitochondrial HMG-CoA synthase spots, showed a modest induction by lovastatin alone, but little or no effect with any of the other treatments (including the combination of lovastatin and cholestyramine; Fig. 12). This result is intriguing because lovastatin was expected to affect only the regulation of enzymes of cholesterol synthesis, which is entirely extra-mitochondrial. Three of the spots (235, 134, 144) form a closely-packed triad at approximately 30 kDa, and are likely to represent isoforms of one protein. All three spots are stained by an antibody to the mitochondrial form of HMG-CoA synthase obtained from Dr. Greenspan. Subcellular fractionation indicates a mitochondrial location. The other two spots (633 at about 38 kDa and 724 at about 69 kDa) are each present at lower abundance than the members of the triad.

3.3.3 An example of an anti-synergistic effect

A sixth spot (367) shows strong induction by lovastatin (two- to threefold), and about half as much induction with lovastatin plus cholestyramine, but without sharing the animal-animal heterogeneity pattern of the 235-set (Fig. 13). This protein is also mitochondrial, and represents the clearest example of an anti-synergistic effect of lovastatin and cholestyramine. The existence of such an effect demonstrates that lovastatin and cholestyramine do not act exclusively through the same regulatory pathway.

3.3.4 Complexity of the cholesterol synthesis pathway

Taken together, these results suggest that treatment with lovastatin alone can affect both cytosolic and mitochondrial pathways using HMG-CoA, while cholestyramine, on the other hand, either alone or in combination with lovastatin, produces a strong effect on the putative cytosolic pathway, but little or no effect on the putative mitochondrial pathway. An explanation for this difference may lie in lovastatin's effect on levels of HMG-CoA and related precursor compounds that are exchanged between the cytosol and the mitochondrion, whereas cholestyramine should affect only the cytosolic pathways directly controlled by cholesterol and bile acid levels. It remains to be explained why some proteins of the putative mitochondrial pathway are so much more variable in their expression in all groups. An examination of all the coregulated groups suggests that quantitative statistical techniques can extract a wealth of interesting information from large sets of reproducible gels. The abundance of spots in the 413 coregulation group, for example, shows an amazing level of concordance in their relative expression among the five individuals of the lovastatin and cholestyramine treatment group. This effect is not due to differences in total protein loading, since they have already been removed by scaling, and since proteins with quite different regulation patterns can be demonstrated (*e.g.*, Fig. 13). Such effects raise the possibility that many gene coregulation sets may be revealed through the study of a sufficiently large population of control animals (*i.e.*, without any experimental manipulation). This approach, exploiting natural biological variation in protein expression instead of drug effects, offers an important incentive for the construction of a large library of control animal patterns.

4 Conclusions

Because of the widespread use of rat liver in both basic biochemistry and in toxicology, there is a long-term need for a comprehensive database of liver proteins. The rat liver master pattern presented here has proven to be an accurate representation of this system, having been matched to more than 700 gels to date. As the number of proteins identified and the number of compounds tested for gene expression effects grows, we expect this database to contribute valuable insights into gene regulation. Its practical utility in several areas of mechanistic toxicology is already being demonstrated.

Received September 11, 1991

5 References

[1] O'Farrell, P., *J. Biol. Chem.* 1975, *250*, 4007–4021.
[2] Klose, J., *Humangenetik* 1975, *26*, 231–243.
[3] Scheele, G. A., *J. Biol. Chem.* 1975, *250*, 5375–5385.
[4] Iborra, G. and Buhler, J. M., *Anal. Biochem.* 1976, *74*, 503–511.
[5] Anderson, N. G. and Anderson, N. L., *Behring. Inst. Mitt.* 1979, *63*, 169–210
[6] Anderson, N. G. and Anderson, N. L., *Clin. Chem.* 1982, *28*, 739–748
[7] Heydorn, W. E., Creed, G. J. and Jacobowitz, D. M., *J. Pharmacol. Exp. Therap.* 1984, *229*, 622–628.
[8] Anderson, N. L., Nance, S. L., Tollaksen, S. L., Giere, F. A. and Anderson, N. G., *Electrophoresis* 1985, *6*, 592–599.
[9] Racine, R. R. and Langley, C. H., *Biochem. Genet.* 1980, *18*, 185–197.
[10] Klose, J., *Mol. Evol.* 1982, *18*, 315–328.
[11] Neel, J. V., Baier, L., Hanash, S. and Erickson, R. P., *J. Hered.* 1985, *76*, 314–320.
[12] Marshall, R. R., Raj, A. S., Grant, F. J. and Heddle, J. A., *Can. J. Genet. Cytol.* 1983, *25*, 457–446.
[13] Taylor, J., Anderson, N. L., Anderson, N. G., Gemmell, A., Giometti, C. S., Nance, S. L. and Tollaksen, S. L., in: Dunn, M. J. (Ed.), *Electrophoresis '86*, Verlag Chemie, Weinheim 1986, pp. 583–587.
[14] Giometti, C. S., Gemmell, M. A., Nance, S. L., Tollaksen, S. L. and Taylor, J., *J. Biol. Chem.* 1987, *262*, 12764–12767.
[15] Anderson, N. L., Giere, F. A., Nance, S. L., Gemmell, M. A., Tollaksen, S. L. and Anderson, N. G., in: Galteau, M.-M. and Siest, G. (Eds.), *Progrès Récents en Electrophorèse Bidimensionelle*, Presses Universitaires de Nancy, Nancy 1986, pp. 253–260.
[16] Anderson, N. L., Swanson, M., Giere, F. A., Tollaksen, S., Gemmell, A., Nance, S. L. and Anderson, N. G., *Electrophoresis* 1986, *7*, 44–48.

Anderson, N. L., Giere, F. A., Nance, S. L., Gemmell, M. A., Tollaksen, S. L. and Anderson, N. G., *Fundam. Appl. Toxicol.* 1987, *8*, 39–50.
Anderson, N. L., in: *New Horizons in Toxicology*, Eli Lilly Symposium, 1991, in press.
Antoine, B., Rahimi-Pour, A., Siest, G., Magdalou, J. and Galteau, M. M., *Cell. Biochem. Funct.* 1987, *5*, 217–231.
Elliott, B. M., Ramasamy, R., Stonard, M. D. and Spragg, S. P. *Biochim. Biophys. Acta* 1986, *870*, 135–140.
Huber, B. E., Heilman, C. A., Wirth, P. J., Miller, M. J. and Thorgeirsson, S. S., *Hepatology* 1986, *6*, 206–219.
Wirth, P. J. and Vesterberg, O., *Electrophoresis* 1988, *9*, 47–53.
Witzmann, F. A. and Parker, D. N., *Toxicol. Lett.* 1991, *57*, 29–36.
Rampersaud, A., Waxman, D. J., Ryan, D. E., Levin, W. and Walz, F. G., Jr., *Arch. Biochem. Biophys.* 1985, *243*, 174–183.
Vlasuk, G. P. and Walz, F. G., Jr., *Anal. Biochem.* 1980, *105*, 112–120.
Anderson, N. G. and Anderson, N. L., *Anal. Biochem.* 1978, *85*, 331–340.
Anderson, N. L. and Anderson, N. G., *Anal. Biochem.* 1978, *85*, 341–354.
Anderson, L., Hofmann, J.-P., Anderson, E., Walker, B. and Anderson, N. G., in: Endler, A. T. and Hanash, S. (Eds.), *Two-Dimensional Electrophoresis*, VCH Verlagsgesellschaft, Weinheim 1989, pp. 288–297.
Anderson, L., *Two-Dimensional Electrophoresis: Operation of the ISO-DALT® System*, Large Scale Biology Press, Washington, DC 1988, ISBN 0-945532-00-8, 170pp.
Neuhoff, V., Stamm, R. and Eibl, H., *Electrophoresis* 1985, *6*, 427–448.
[31] Neuhoff, V., Arold, N., Taube, D. and Ehrhardt, W., *Electrophoresis* 1988, *9*, 255–262.
[32] Anderson, N. L. and Hickman, B. J., *Anal. Biochem.* 1979, *93*, 312–320.
[33] Sidman, K. E., George, D. E., Barker, W. C. and Hunt, L. T., *Nucl. Acids Res.* 1988, *16*, 1869–1871.
[34] Taylor, J., Anderson, N. L., Coulter, B. P., Scandora, A. E. and Anderson, N. G., in: Radola, B. J. (Ed.), *Electrophoresis '79*, de Gruyter, Berlin 1980, pp. 329–339.
[35] Taylor, J., Anderson, N. L. and Anderson, N. G., in: Allen, R. C. and Arnaud, P. (Eds.), *Electrophoresis '81*, de Gruyter, Berlin 1981, pp. 383–400.
[36] Anderson, N. L., Taylor, J., Scancora, A. E., Coulter, B. P. and Anderson, N. G., *Clin. Chem.* 1981, *27*, 1807–1820.
[37] Taylor, J., Anderson, N. L., Scandora, A. E., Jr., Willard, K. E. and Anderson, N. G., *Clin. Chem.* 1982, *28*, 861–866.
[38] Taylor, J., Anderson, N. L. and Anderson, N. G., *Electrophoresis* 1983, *4*, 338–345.
[39] Anderson, N. L. and Taylor, J., in: *Proceedings of the Fourth Annual Conference and Exposition of the National Computer Graphics Association*, Chicago, June 26–30, 1983, pp. 69–76.
[40] Anderson, N. L., Hofmann, J.-P., Gemmell, A. and Taylor, J., *Clin. Chem.* 1984, *30*, 2031–2036.
[41] Anderson, L., in: Schafer-Nielsen, C. (Ed.), *Electrophoresis '88*, VCH Verlagsgesellschaft, Weinheim 1988, pp. 313–321.
[42] Neidhardt, F. C., Appleby, D. A., Sankar, P., Hutton, M. E. and Phillips, T. A., *Electrophoresis* 1989, *10*, 116–121.
[43] Gil, G., Goldstein, J. L., Slaughter, C. A. and Brown, M. S., *J. Biol. Chem.* 1986, *261*, 3710–3716.

6 Addendum 1: Figures 1–13

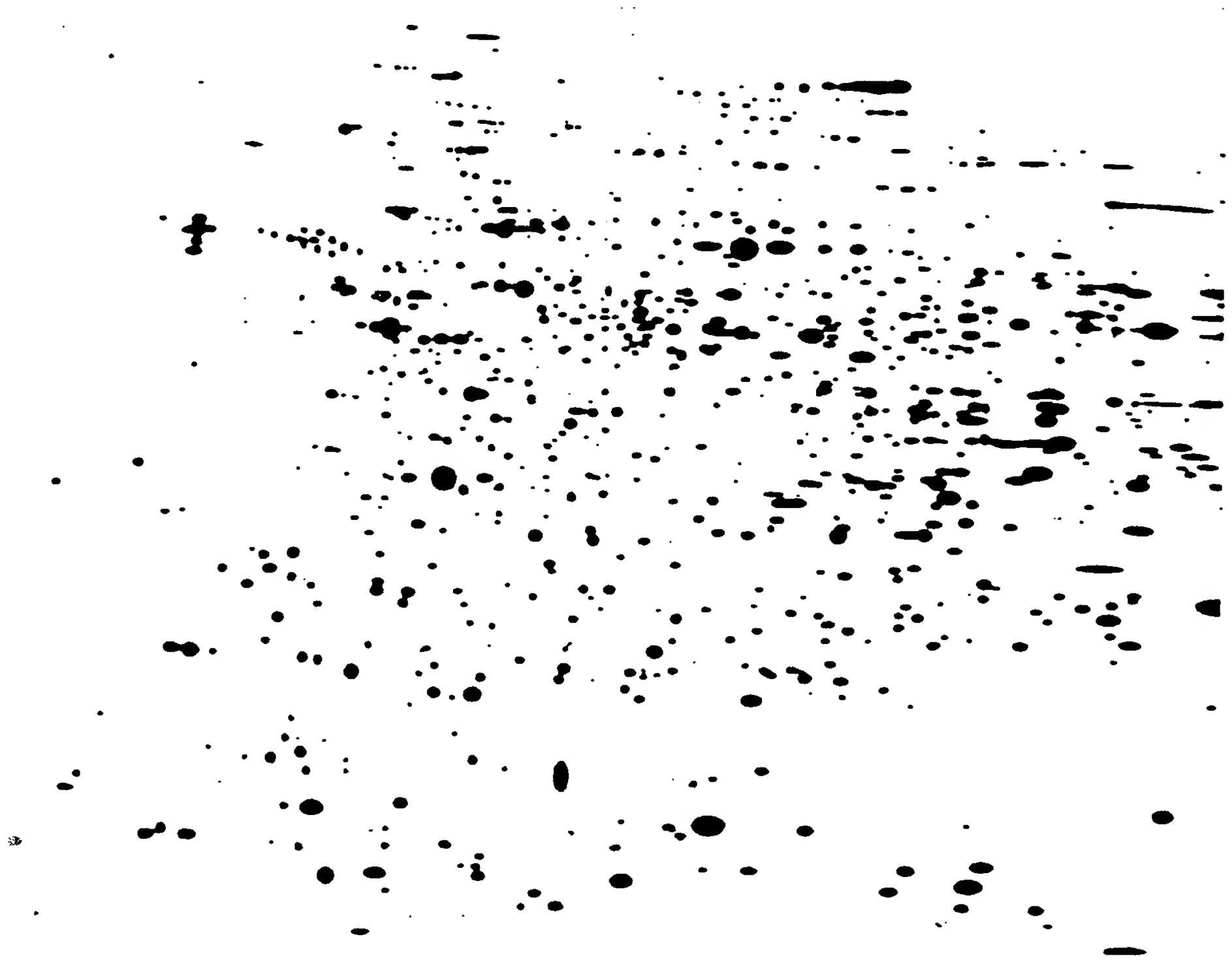

Figure 1. Synthetic representation of the standard rat liver 2-D master pattern, rendered as a greyscale image using a videoprinter.

Figure 2. Schem
grams.

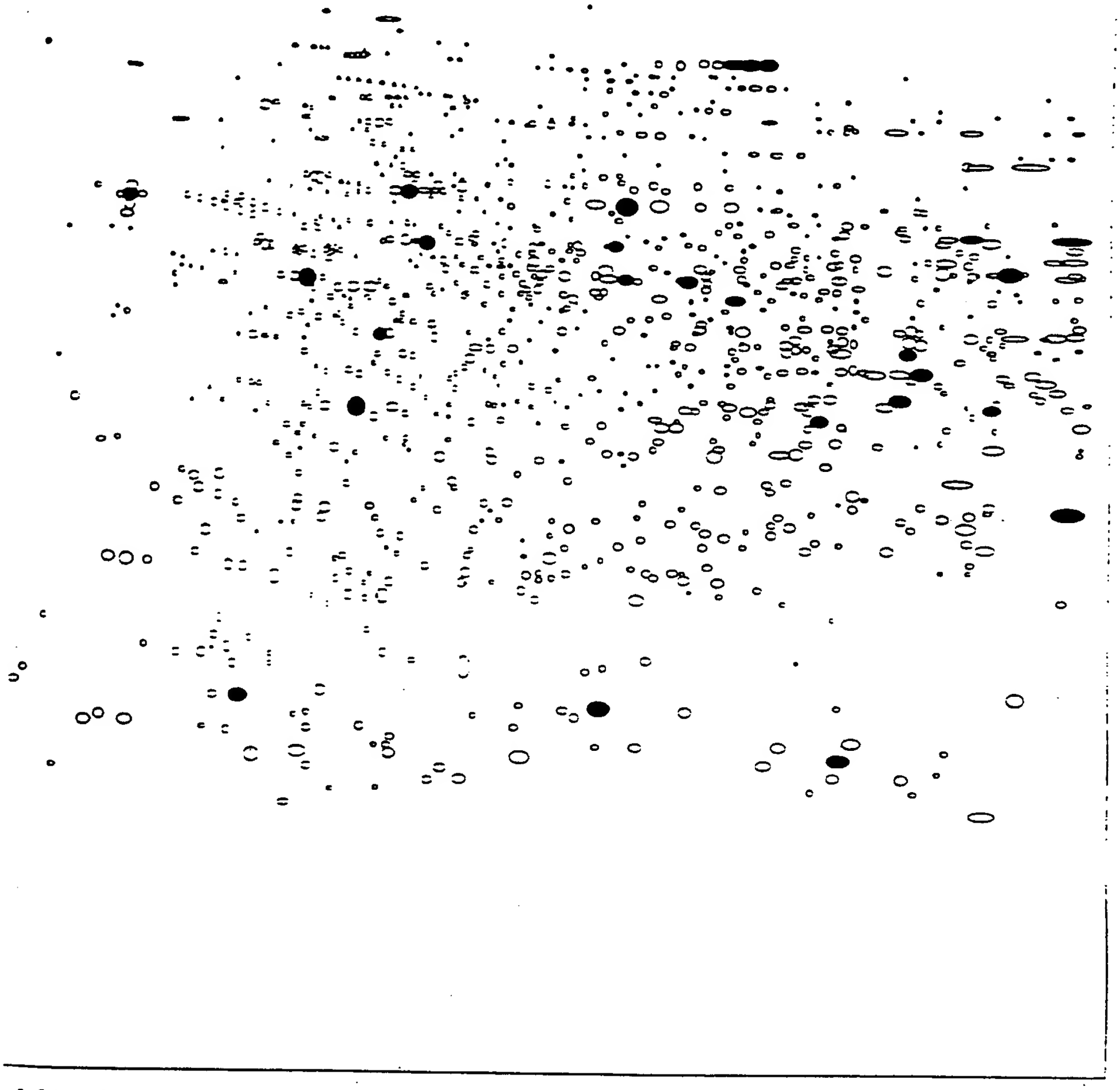

re 2. Schematic representation of the master pattern (the same as Fig. 1), useful as an aid in relating specific areas of Fig. 1 and the following detailed
fronts.

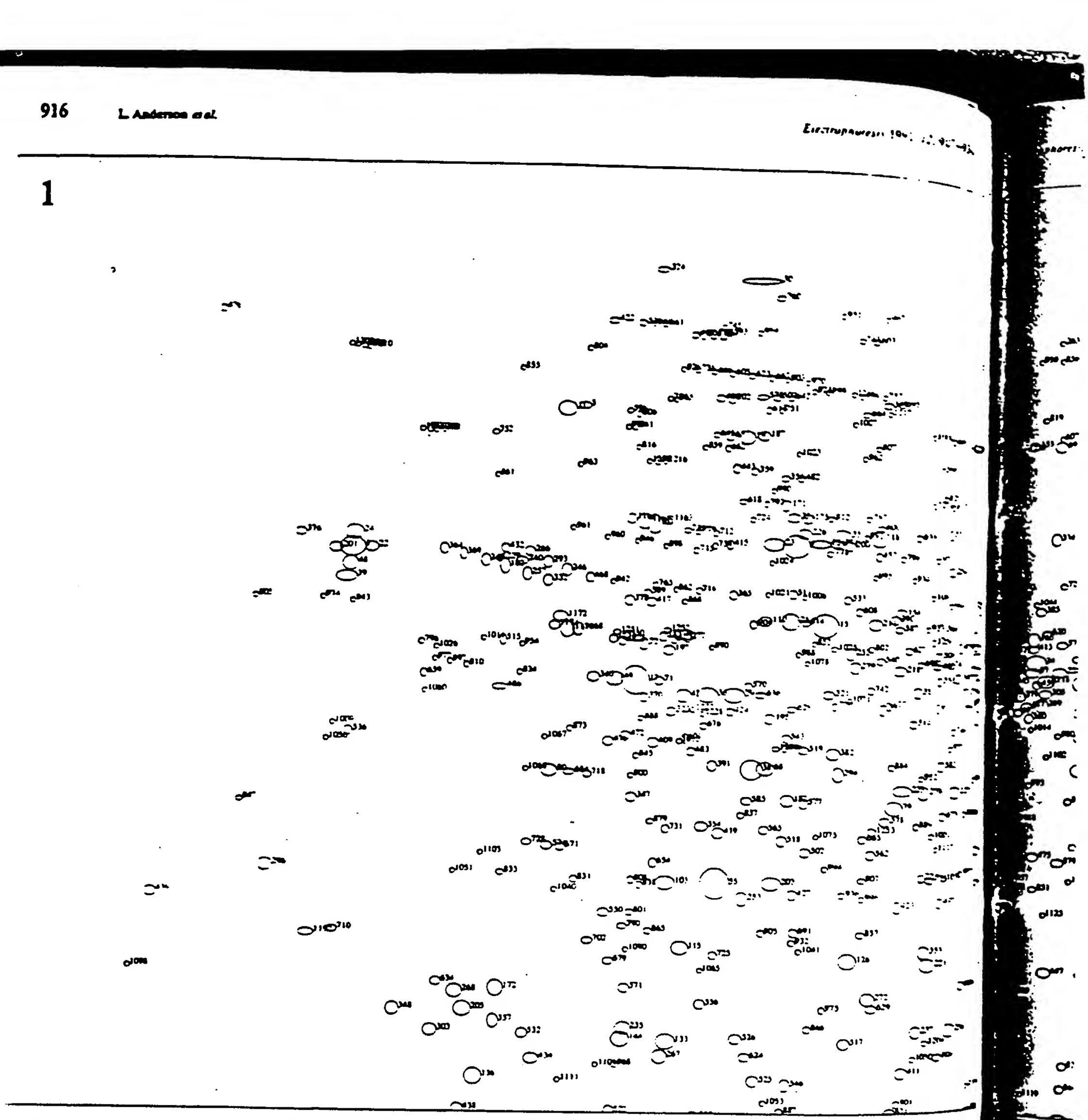

Figure 3. Upper left (high molecular weight, acidic) quadrant (#1) of the rat liver map, showing spot numbers.

4. Up

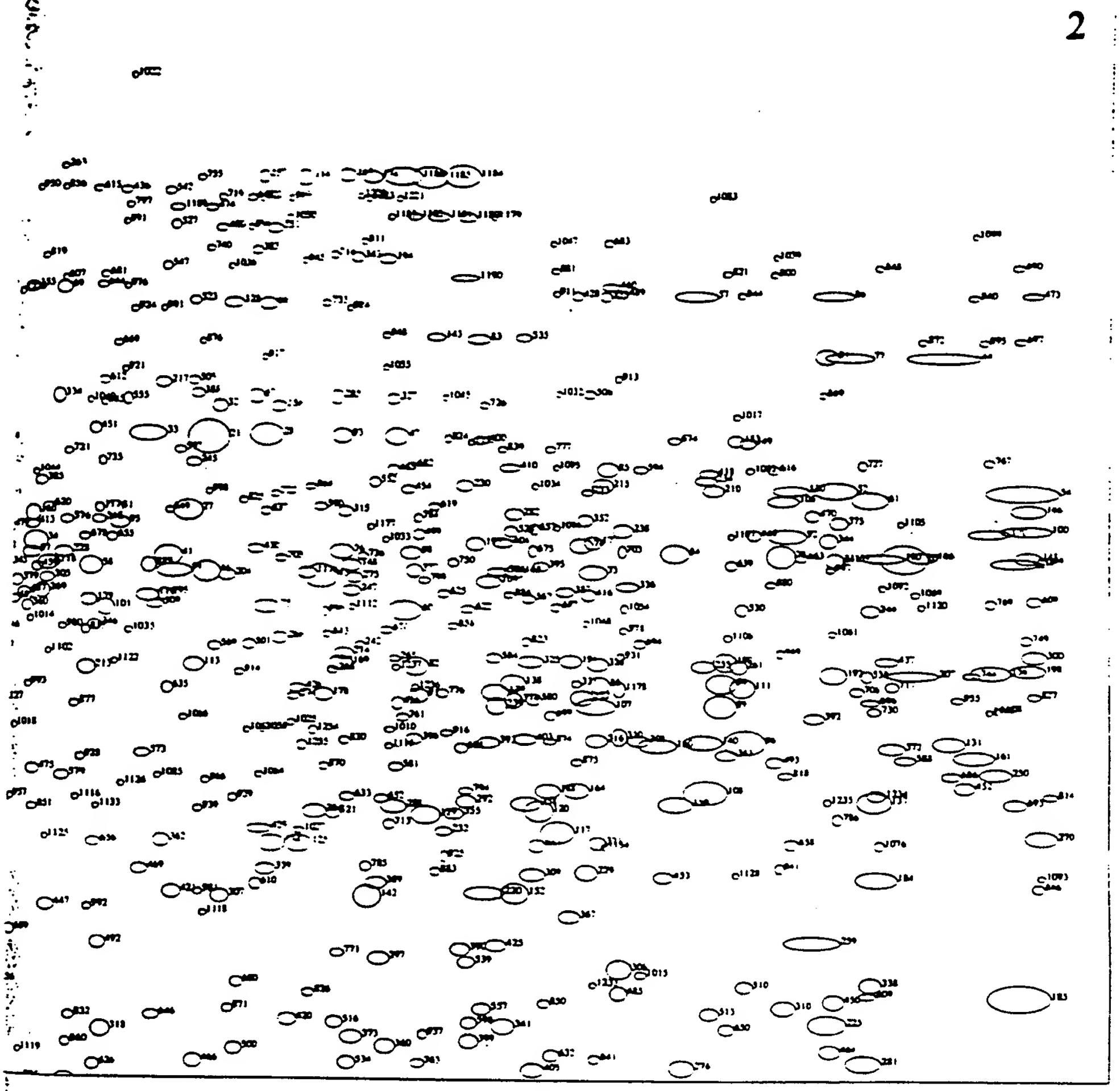

Figure 4. Upper right (high molecular weight, basic) quadrant (#2) of the rat liver map, showing spot numbers.

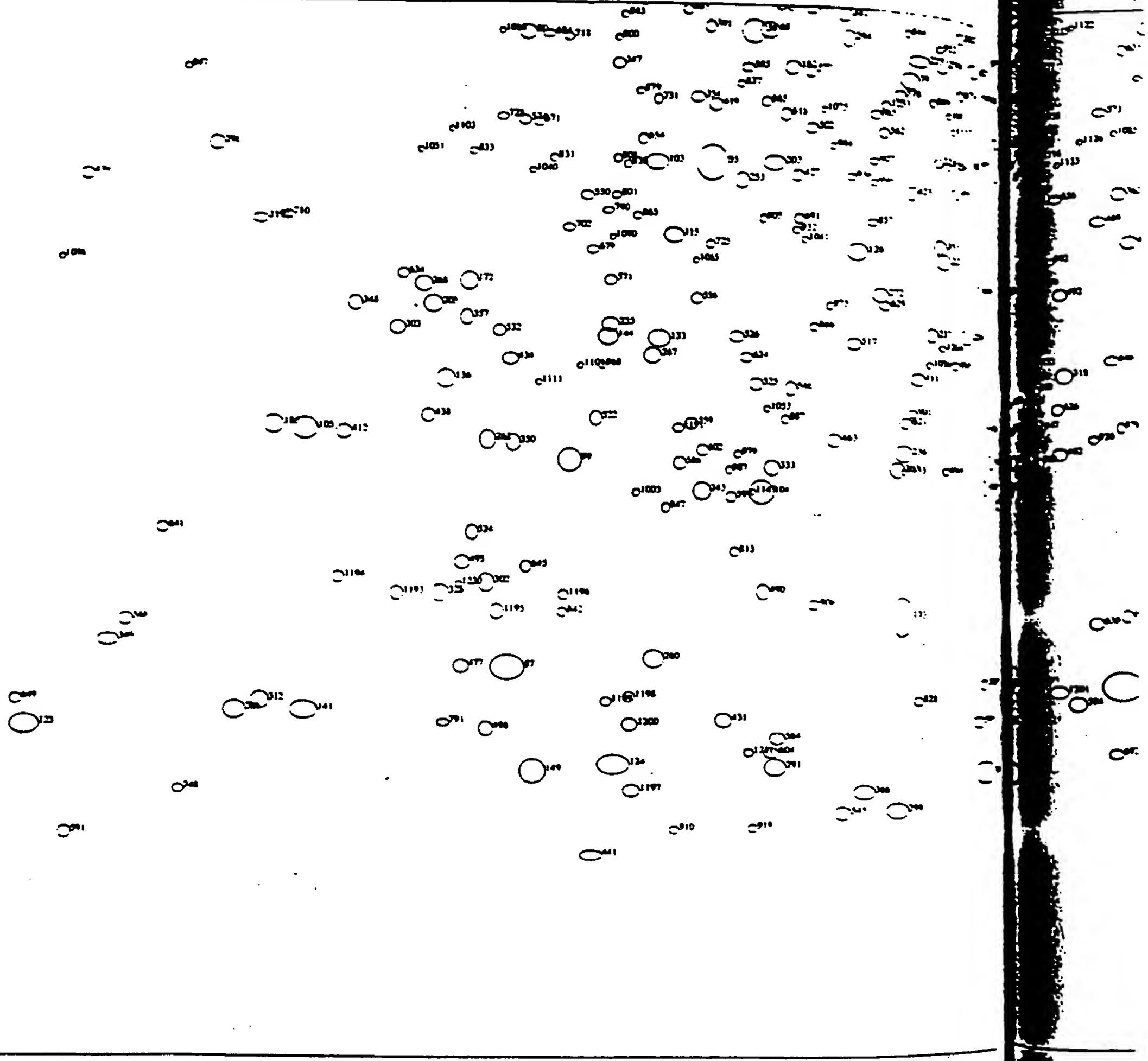

Figure 5. Lower left (low molecular weight, acidic) quadrant (#3) of the rat liver map, showing spot numbers.

6. Lower r

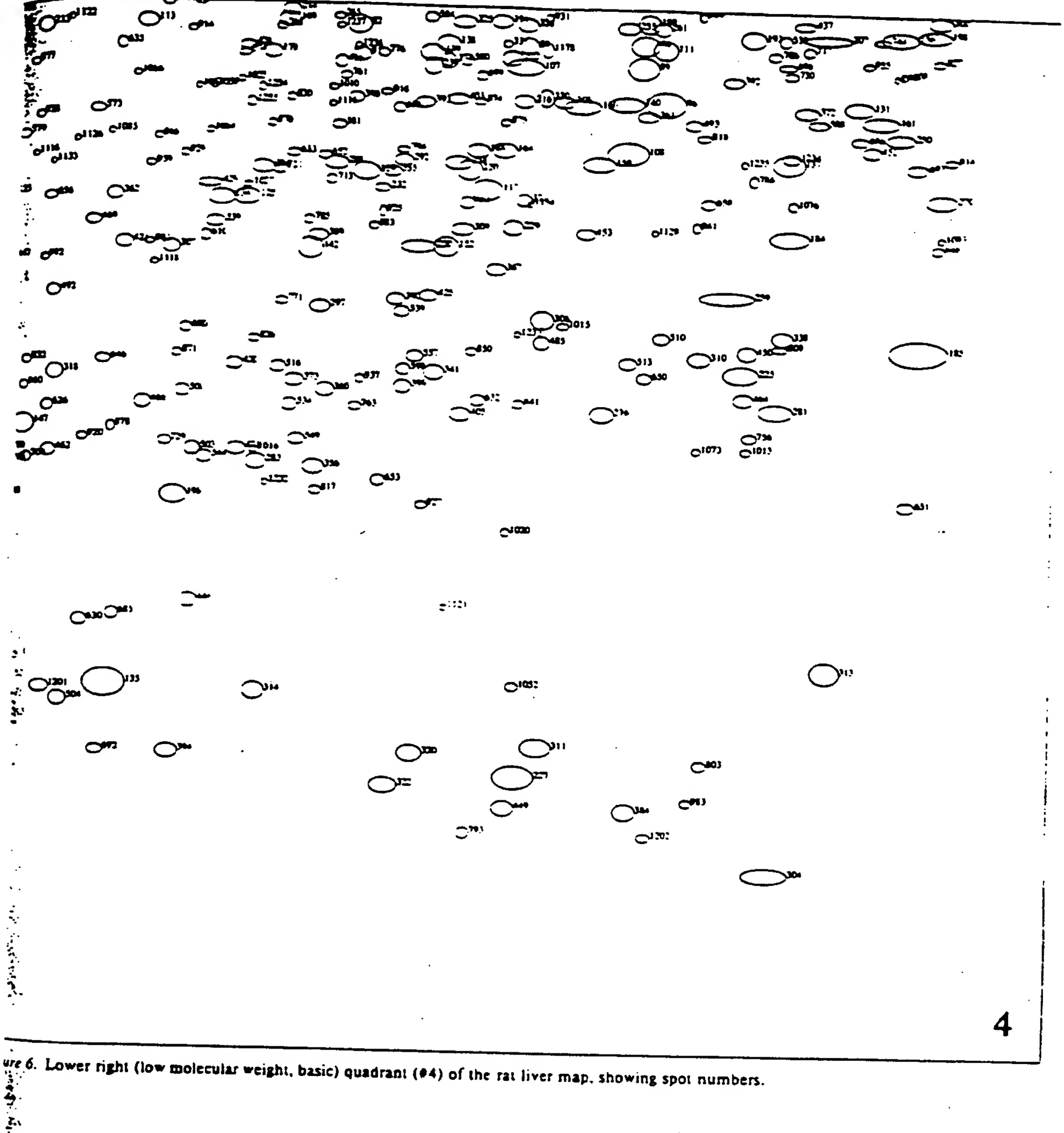

ure 6. Lower right (low molecular weight, basic) quadrant (#4) of the rat liver map, showing spot numbers.

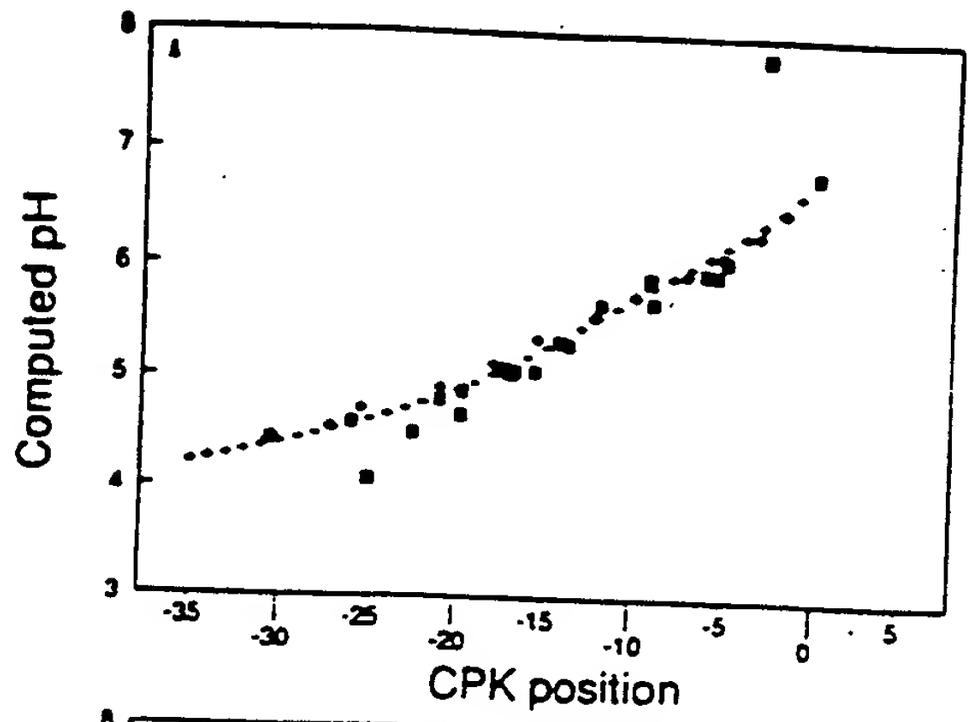

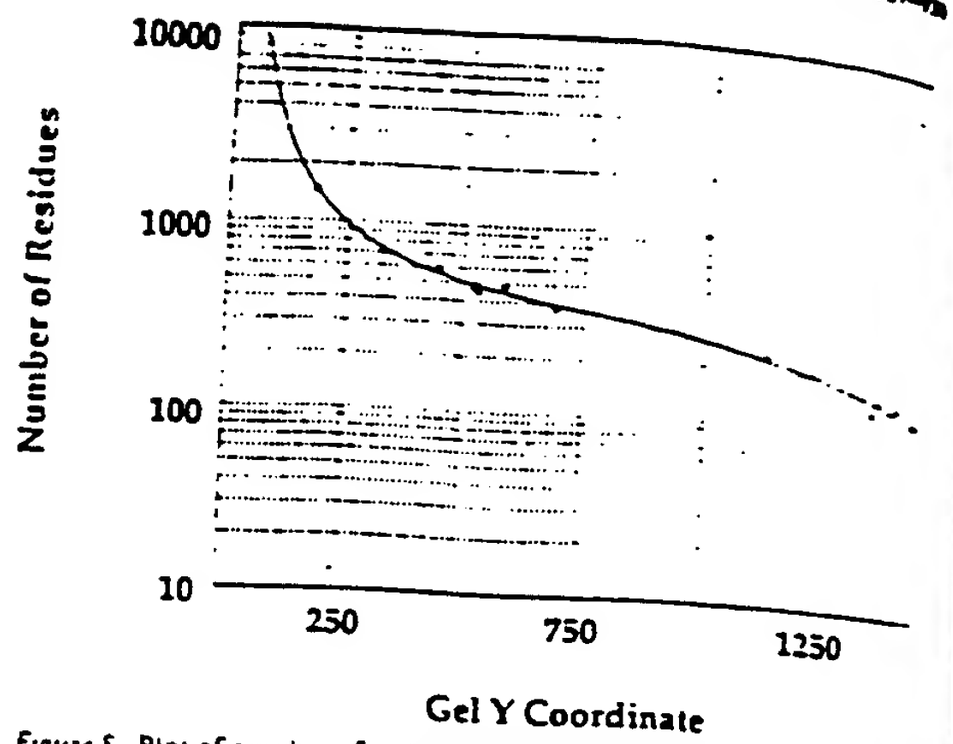

Figure 8. Plot of number of amino acids versus gel Y-position, with fitted curve used to predict molecular mass of unidentified proteins

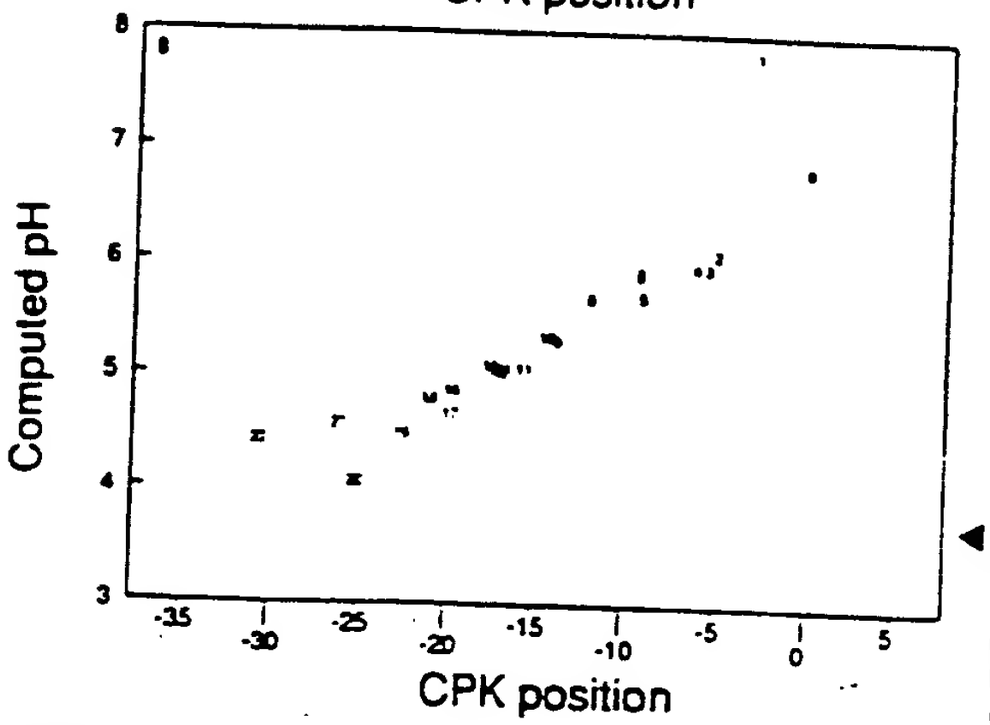

◀ *Figure 7.* (a) Plot of computed isoelectric point versus gel X-position for two sets of carbamylated standard proteins (rabbit muscle CPK [–] and human hemoglobin β chain, filled diamonds) and several other proteins (shaded squares). (b) The identities of the various proteins represented by the squares are indicated by the numbers in corresponding positions on (a); these refer to Table 4.

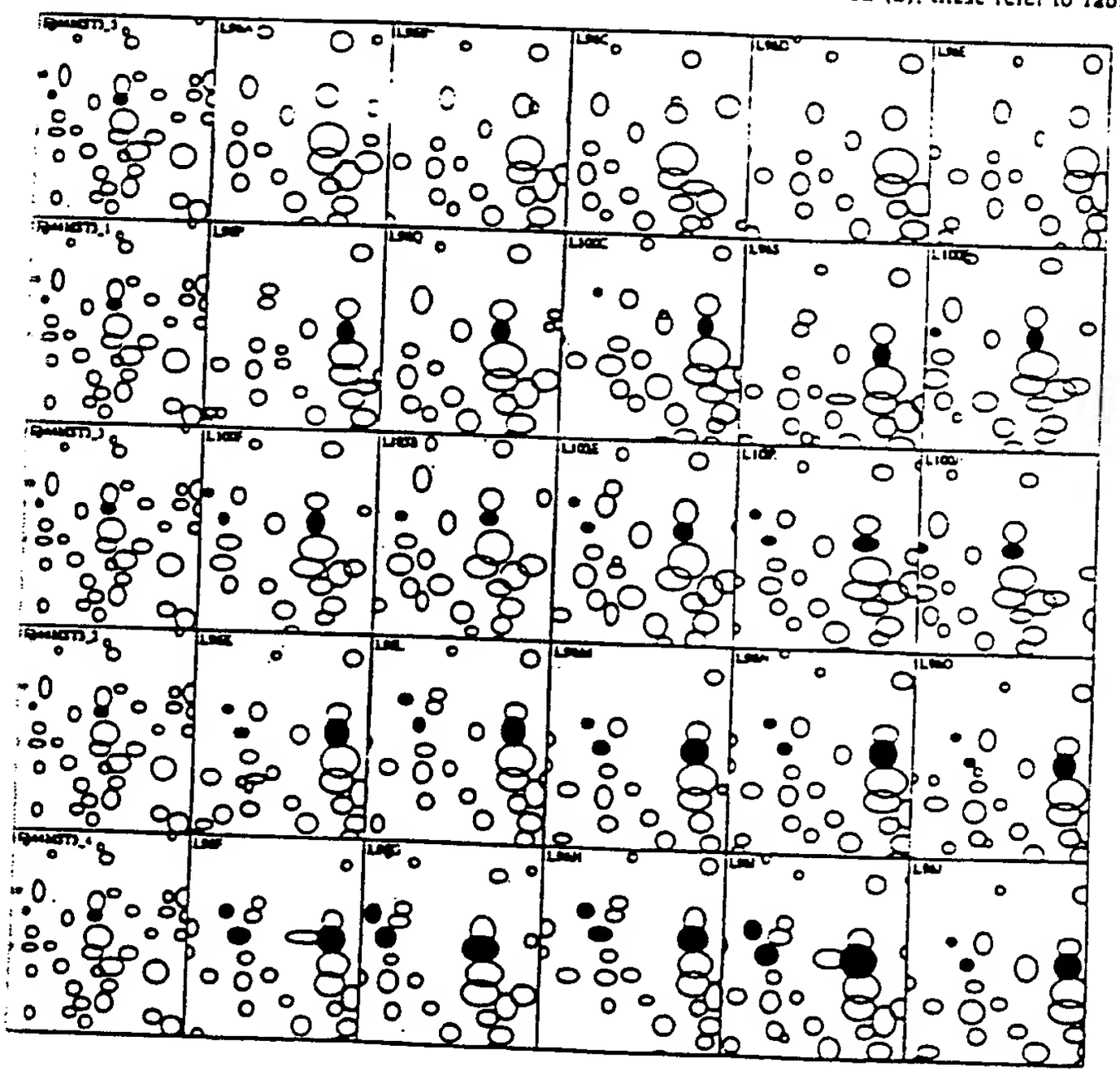

Figure 9. Montage showing effects in the region of MSN:413. The montage shows a small window into one portion of the 2-D pattern, one row of windows for each experimental group, and one panel for each gel in the experiment. The left-most pattern in each row is a group-specific copy of the master pattern followed by the patterns for the five individual rats in the group. The highlighted protein spots (filled circles) are spot 413 (on the right of each panel; identified as cytosolic HMG-CoA synthase) and two modified forms of it (1250 and 933). From the top, the rows (experimental groups) are: high cholesterol, controls, cholestyramine, lovastatin, and lovastatin plus cholestyramine.

413

1119

...ersis 1991, 12, 907–930

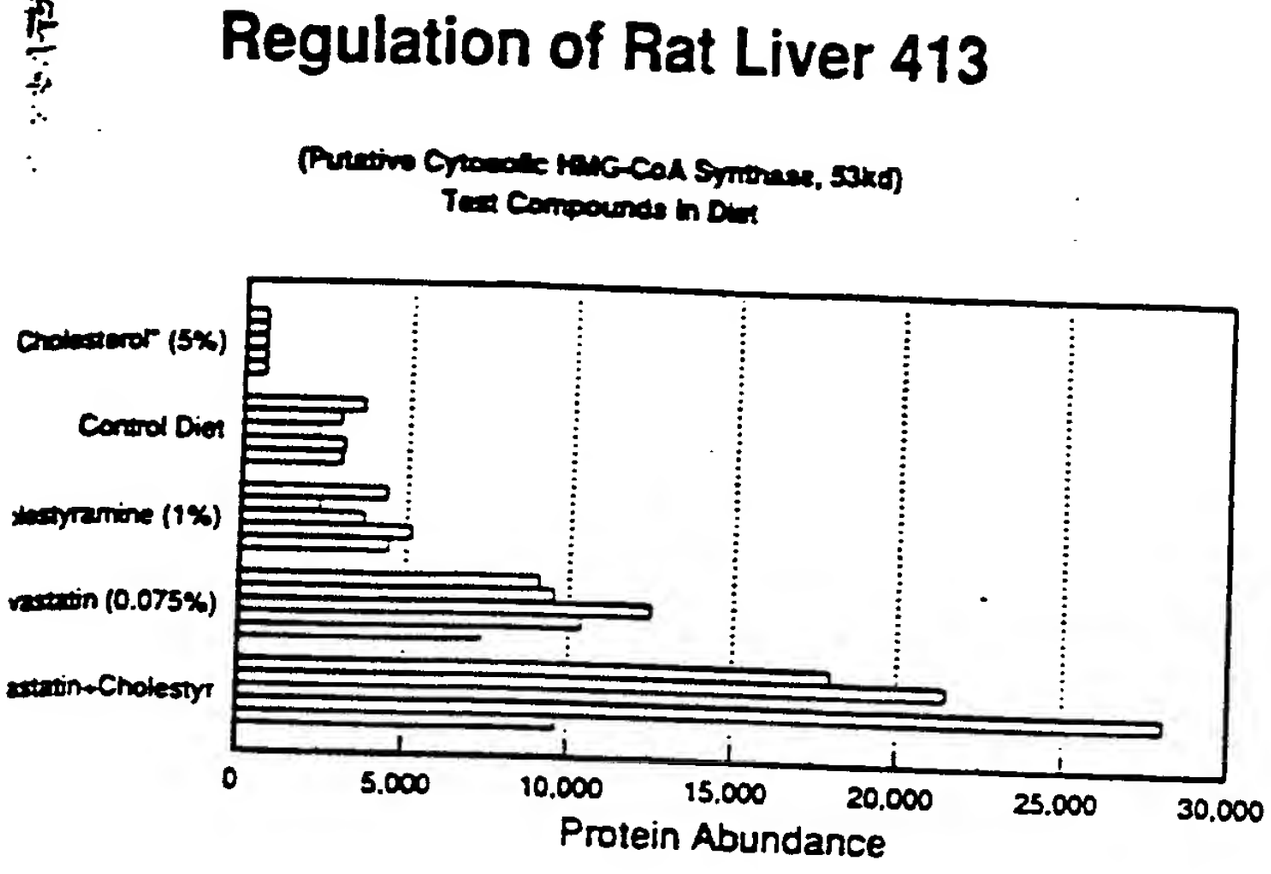

Figure 10. Bargraph showing the quantitative effects of various treatments on the abundance of MSN:413 (cytosolic HMG-CoA synthase) in the gels of Fig. 9.

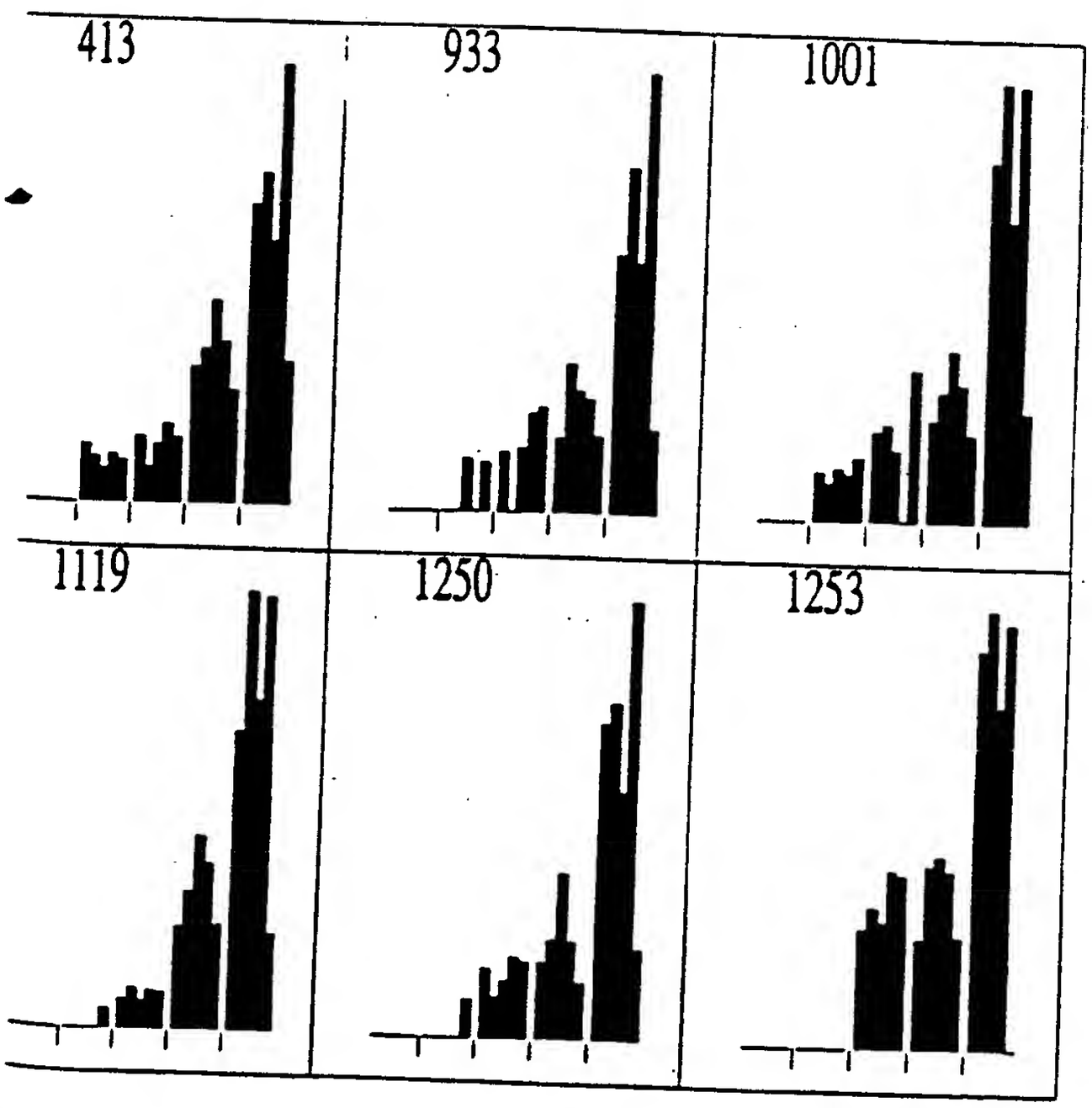

Figure 11. Bargraphs of a series of six coregulated spots including MSN:413. In the bargraphs, the abundances of the appropriate spot (master spot number shown at the top of the panel) in each animal are shown. The five five-animal groups are in the order (left to right): high cholesterol, controls, cholestyramine, lovastatin, and lovastatin plus cholestyramine. Each bar within a group represents one experimental animal liver (one 2-D gel). Note the correlated expression of the 6 spots, especially in the two far right (most strongly induced) groups.

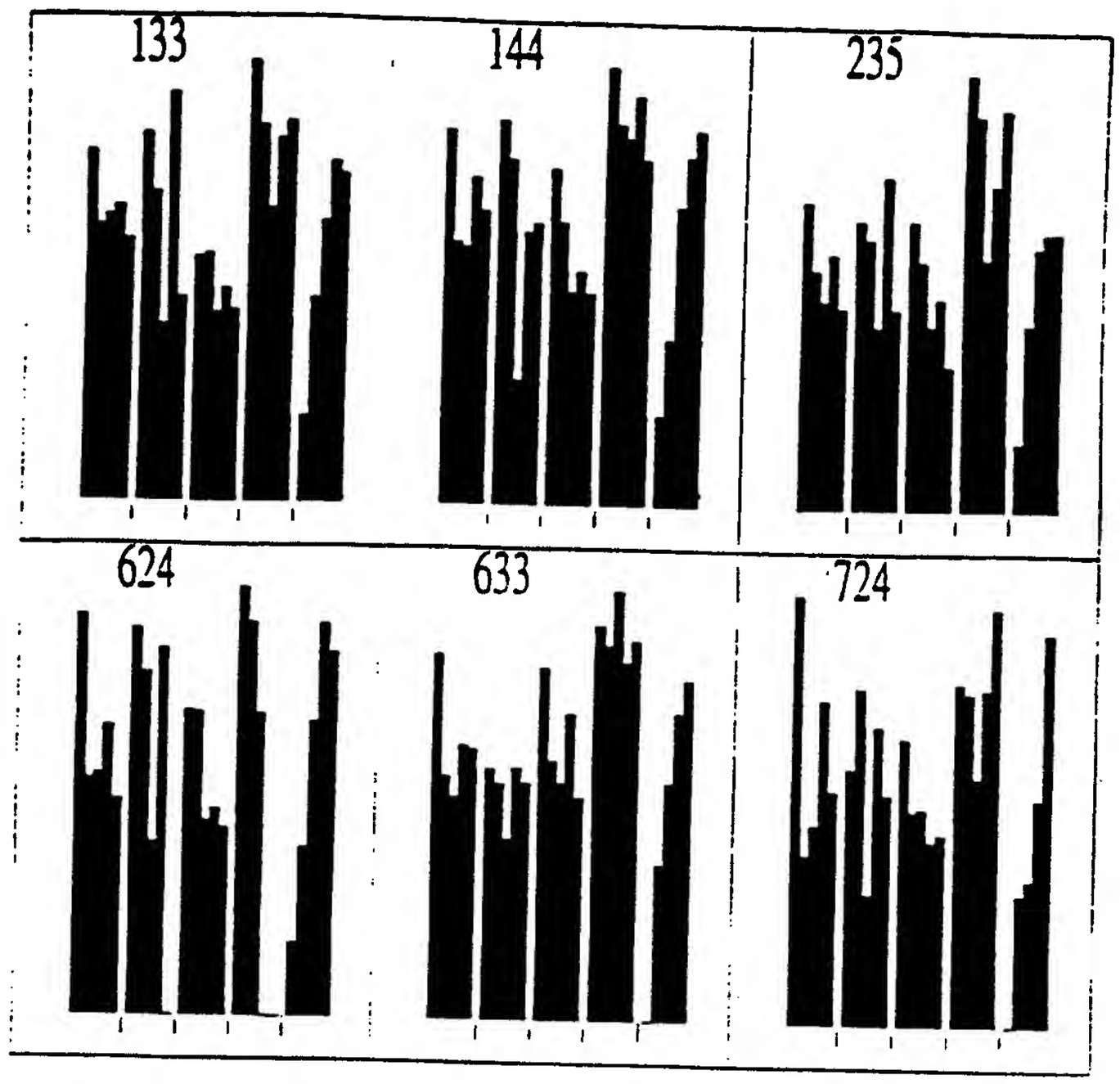

Figure 12. Data on a second coregulated group of spots, presented as in Fig. 11. The fourth experimental group (lovastatin) shows a modest induction, while the fifth group (lovastatin plus cholestyramine) does not.

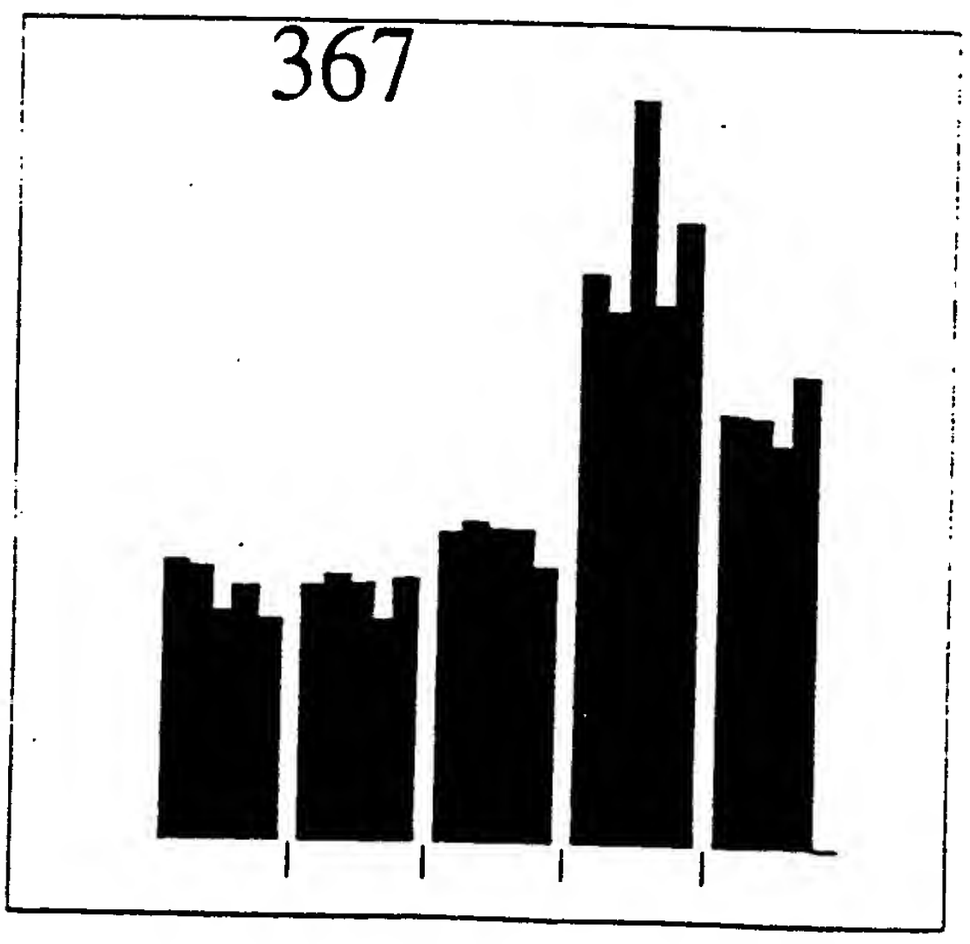

Figure 13. Data on spot MSN:367, presented as in Fig. 11. This protein shows unambiguously the anti-synergistic effect of lovastatin and cholestyramine (fifth group) as compared to lovastatin (fourth group). This response contrasts strongly with the regulation pattern seen in Fig. 11.

Addendum 2: Tables 1–4

Table 1. Master table of proteins in the rat liver database[a]

MSN	X	Y	CPKol	SDSMW
3	311	434	<-35.0	63,800
5	568	263	-24.3	102,900
8	812	426	-16.0	64,800
11	549	268	-25.2	101,000
15	845	520	-15.3	55,200
17	629	589	-21.6	50,000
18	906	414	-14.0	66,300
19	755	298	-17.5	90,200
20	649	403	-20.9	67,900
21	1204	448	-8.7	62,100
22	332	434	<-35.0	63,800
23	787	424	-16.6	65,000
24	313	417	<-35.0	66,000
25	807	516	-16.1	56,500
27	1184	524	-9.0	54,900
28	1263	446	-8.0	62,400
29	743	605	-17.8	49,000
30	768	112	-17.2	348,600
32	1216	417	-8.6	66,000
33	1145	445	-9.5	62,500
34	1037	555	-11.3	52,400
35	863	412	-14.9	66,600
36	712	606	-18.7	48,900
38	763	694	-17.3	43,800
39	304	470	<-35.0	59,800
41	1165	569	-9.2	51,400
42	684	607	-19.6	48,800
43	1318	589	-7.3	50,000
44	1924	362	-0.1	74,600
46	1203	586	-8.7	50,200
47	1391	447	-6.3	62,300
48	309	454	<-35.0	61,500
49	605	587	-22.5	50,100
50	621	535	-21.8	53,900
51	1113	522	-10.0	55,000
52	1820	499	-0.9	57,000
53	725	177	-18.3	170,800
54	2001	500	>0.0	56,900
55	722	830	-18.4	37,300
56	678	533	-19.8	54,100
57	1682	302	-2.5	89,000
58	1091	580	-10.3	50,600
59	1171	585	-9.2	50,300
60	1400	624	-6.2	47,800
61	1853	508	-0.6	56,200
62	1888	567	-0.4	51,500
65	735	297	-18.1	90,500
66	1263	312	-8.0	85,900
67	1252	407	-8.1	67,300
68	779	682	-16.8	43,900
69	1064	296	-10.8	90,800
71	656	589	-20.6	50,000
72	638	545	-21.2	53,100
73	1582	583	-3.6	50,400
74	1570	556	-3.8	52,300
75	1264	621	-8.0	48,000
76	1338	564	-7.0	51,800
77	1833	363	-0.8	74,400
78	1767	565	-1.5	51,700
79	925	738	-13.6	41,600
80	534	698	-26.1	43,600
81	1811	363	-1.0	74,500
82	1412	681	-6.0	44,500
83	1471	347	-5.0	77,500
84	1662	563	-2.7	51,800
85	1596	479	-3.4	58,900
86	1817	301	-0.9	89,100
87	516	1371	-27.0	17,400
88	1589	698	-3.5	43,600
89	1706	719	-2.2	42,500
90	651	329	-20.8	81,700
91	1415	710	-6.0	43,000
92	1773	545	-1.4	53,200
93	1338	446	-7.0	62,300
94	1708	696	-2.2	43,700
95	1119	536	-9.9	53,800
96	1731	756	-2.0	40,700
97	1033	566	-11.4	51,600
98	1406	565	-6.1	51,700
99	578	1149	-23.8	25,000
100	2004	538	>0.0	53,700
101	1106	623	-10.1	47,900
102	482	455	-28.5	61,300
103	665	830	-20.2	37,300
104	773	1182	-17.0	23,800
105	312	1117	<-35.0	26,100
106	1769	509	-1.5	56,100
107	1585	720	-3.6	42,500
108	1692	807	-2.4	38,300
109	1482	583	-4.8	49,700
110	778	516	-16.9	55,500
111	1728	700	-2.0	43,500
113	1191	680	-8.9	44,500
114	1298	185	-7.5	160,800
115	682	907	-19.6	34,100
116	1146	610	-9.5	48,700
117	1548	849	-4.1	36,500
118	1050	577	-11.1	50,800
120	1530	828	-4.3	37,400
121	838	423	-15.4	65,200
122	1572	712	-3.8	42,900
123	23	1433	<-35.0	15,300
124	621	1474	-21.9	13,900
125	1298	862	-7.5	36,000
126	872	921	-14.7	33,500
127	1000	717	-12.0	42,600
128	1229	311	-8.4	86,100
129	1422	832	-5.8	37,300
130	1776	499	-1.4	57,000
131	1930	757	-0.1	40,700
132	660	537	-20.4	53,800
133	666	1019	-20.2	29,700
134	1271	862	-7.9	36,000
135	1161	1389	-9.3	16,800
136	453	1063	-29.7	28,100
137	1858	823	-0.6	37,700
138	1504	697	-4.6	43,700
139	1488	707	-4.8	43,200
140	1689	756	-2.4	40,700
141	311	1417	<-35.0	15,800
142	1366	915	-6.7	33,800
143	1429	346	-5.7	77,900
144	615	1017	-22.1	29,800
145	2006	566	>0.0	51,600
146	2006	518	>0.0	55,300
147	1070	1108	-10.7	26,500
148	1347	578	-6.9	50,800
149	541	1481	-25.7	13,700
150	1645	760	-2.8	40,500
151	1269	236	-7.9	117,000
152	1507	911	-4.5	33,900
153	1722	448	-2.1	62,100
154	932	503	-13.5	56,600
155	1031	294	-11.4	91,400
156	1970	684	>0.0	44,400
157	1258	183	-8.1	162,400
158	1275	417	-7.8	65,900
159	1663	820	-2.6	37,800
160	1034	527	-11.4	54,600
161	1953	771	>0.0	40,000
162	1020	1482	-11.6	13,700
164	1566	806	-3.8	38,400
166	1905	565	-0.2	51,700
167	1340	181	-7.0	164,900
168	1506	583	-4.6	50,400
169	1338	678	-7.0	44,700
170	1969	541	>0.0	53,500
171	800	378	-16.3	71,800
172	476	958	-28.7	32,100
173	919	1314	-13.7	19,300
174	1364	183	-6.7	162,900
175	825	393	-15.7	69,300
177	1562	553	-3.6	52,600
178	1321	710	-7.2	43,000
179	1089	615	-10.4	48,300
180	1866	567	-0.5	51,600
181	411	295	-32.1	91,200
182	804	730	-16.2	42,000
184	1860	896	-0.6	34,500
185	1997	1017	>0.0	29,800
186	279	1113	<-35.0	26,300
187	773	296	-17.0	90,800
188	1538	807	-4.2	38,400
191	1560	674	-3.9	44,900
192	1818	687	-0.9	44,200
193	1469	555	-5.0	52,400
194	1380	266	-6.4	101,600
195	784	632	-16.7	47,300
196	1227	1185	-8.4	23,700
197	667	553	-20.1	52,600
198	2006	681	>0.0	44,500
199	1711	674	-2.2	44,900
200	872	424	-14.7	65,000
201	292	435	<-35.0	63,700
202	736	253	-18.0	107,800
203	786	829	-16.7	37,400
204	1224	589	-8.5	50,000
205	439	983	-30.9	31,100
206	1994	571	>0.0	51,300
207	1895	687	-0.3	44,200
208	240	1418	<-35.0	15,800
210	1700	499	-2.3	57,000
211	902	517	-14.1	55,400
213	1087	684	-10.4	44,400
214	1340	668	-7.0	45,200
215	1591	495	-3.5	57,300
216	1585	755	-3.6	40,700
217	1159	393	-9.3	69,300
218	931	572	-13.5	51,200
219	713	177	-18.7	170,500
220	1479	911	-4.9	33,900
221	965	927	-12.8	33,300
223	934	716	-13.5	42,700
225	1812	1045	-1.0	28,800
226	821	411	-15.8	66,800
227	1586	1483	-3.6	13,600
228	1065	567	-10.8	51,600
229	1577	890	-3.7	34,800
230	1458	496	-5.2	57,300
232	1440	849	-5.5	36,500
234	1692	489	-2.4	57,900
235	618	1004	-22.0	30,300
236	920	1138	-13.7	25,400
237	952	1008	-13.1	30,200
238	1611	541	-3.2	53,500
239	1489	720	-4.8	42,500
240	501	448	-27.7	62,100
241	1820	569	-0.9	51,400
242	1357	658	-6.8	45,800
243	711	1182	-18.7	23,800
244	1855	621	-0.6	48,000
245	1189	474	-8.9	59,300
246	551	459	-25.1	61,000
247	1348	604	-6.9	49,100
248	460	448	-29.3	62,100
249	1733	451	-1.9	61,800
250	1974	788	>0.0	39,200
251	808	392	-16.1	69,500
252	874	553	-14.6	52,500
253	753	848	-17.6	36,500
254	995	450	-12.1	61,900
255	1690	679	-2.4	44,600
256	994	1006	-12.1	30,200
257	508	464	-27.4	60,400
258	1517	820	-4.4	37,800

[a] Master table of proteins in the rat liver database, showing spot master number, gel position (x and y), isoelectric point relative to CPK standards, and predicted molecular mass (from the standard curve of Fig. 8).

MSN	X	Y	CPKol	SDSMW
259	1796	861	-1.1	31,900
260	661	1361	-20.4	17,700
261	1725	679	-2.0	44,600
262	496	1127	-28.0	25,800
263	1063	172	-10.9	177,400
265	1390	673	-6.3	45,000
266	510	437	-27.3	63,400
267	660	1038	-20.4	29,000
268	430	961	-31.0	31,900
269	1044	806	-11.2	48,900
270	2019	853	>0.0	36,300
271	857	422	-15.0	65,200
272	895	988	-14.2	31,700
274	1292	712	-7.6	42,900
275	1350	580	-6.9	49,900
276	1670	1089	-2.6	27,100
277	688	538	-19.4	53,700
278	961	718	-13.0	42,600
279	879	570	-14.5	51,300
281	1848	1084	-0.7	27,300
282	1505	525	-4.6	54,800
283	1313	1147	-7.3	25,100
284	1314	829	-7.3	37,400
285	1332	408	-7.1	67,200
286	1277	652	-7.8	46,100
288	1391	824	-6.3	37,600
289	1147	579	-9.5	50,700
290	925	511	-13.6	55,900
291	787	1476	-16.6	13,900
292	1462	818	-5.1	37,800
293	531	449	-26.3	62,000
294	860	688	-14.9	43,600
295	1162	609	-9.3	48,700
296	218	814	<-35.0	38,000
297	1377	979	-6.5	31,300
299	913	1523	-13.9	12,400
300	2012	667	>0.0	45,300
301	702	178	-19.0	169,200
302	494	1280	-28.1	20,400
303	403	1008	-32.6	30,100
304	1843	1585	-0.7	10,300
305	1049	583	-11.1	49,800
306	1608	989	-3.3	30,900
307	1219	916	-8.5	33,700
308	1627	755	-3.0	40,700
309	1524	892	-4.4	34,700
310	1769	1028	-1.5	29,400
311	1609	1451	-3.3	14,700
312	266	1408	<-35.0	16,100
313	1902	1365	-0.3	17,600
314	1316	1395	-7.3	16,600
315	1341	523	-7.0	54,900
318	1104	1053	-10.1	28,500
320	1480	1459	-4.9	14,400
321	850	603	-15.1	49,100
322	1454	1494	-5.3	13,300
323	670	626	-20.0	47,700
324	655	101	-20.6	420,500
325	1521	675	-4.4	44,800
326	1587	677	-3.6	44,700
327	1388	409	-6.3	67,000
328	448	1291	-30.0	20,100
330	1608	751	-3.3	40,900
331	1566	697	-3.8	43,700
332	531	471	-26.3	59,600
333	784	1156	-16.7	24,700
334	1059	407	-10.9	67,300
335	1583	303	-3.5	88,500
336	1616	598	-3.2	49,400
338	1854	1004	-0.6	30,300
339	1265	888	-8.0	34,900
340	581	585	-23.6	50,300
341	1497	1047	-4.7	28,700
343	1351	265	-6.8	102,200
344	1813	549	-0.9	52,800
345	1006	578	-11.9	50,800
346	1095	640	-10.3	46,800
347	625	728	-21.7	42,000
348	361	983	-35.3	31,100
349	110	1343	<-35.0	18,300
350	521	1130	-26.7	25,700
351	912	619	-13.9	48,100
352	1574	530	-3.7	54,300
353	961	912	-12.9	33,900
354	706	762	-18.9	40,400
355	1450	830	-5.3	37,300
356	1374	1152	-6.5	24,900
357	474	997	-28.7	30,600
358	798	346	-16.3	77,800
359	764	338	-17.3	79,400
360	1384	1068	-6.4	27,900
361	1713	769	-2.1	40,100
362	1161	859	-9.3	36,100
363	914	1156	-13.8	24,800
364	412	435	-32.0	63,700
365	741	486	-17.9	58,200
366	878	1503	-14.6	13,000
367	1560	935	-3.9	33,000
368	983	520	-12.4	55,200
369	434	441	-31.0	63,000
370	639	610	-21.2	48,700
371	1587	860	-3.6	36,100
372	1875	762	-0.5	40,400
373	1351	1059	-6.8	28,300
374	1506	715	-4.6	42,700
375	1823	532	-0.9	54,200
376	254	417	<-35.0	65,900
377	1409	583	-6.1	50,400
378	621	494	-21.8	57,500
379	1017	595	-11.7	49,600
381	953	598	-13.1	49,400
382	856	674	-15.0	44,900
383	1252	258	-8.1	105,300
384	1699	1518	-2.3	12,500
385	1042	493	-11.2	57,500
386	1490	583	-4.7	50,400
387	1554	603	-4.0	49,100
388	1193	404	-8.9	67,700
389	1374	902	-6.5	34,300
390	1456	969	-5.2	31,700
391	718	690	-18.5	44,000
392	1799	732	-1.1	41,900
393	1482	758	-4.8	40,600
394	1227	1461	-8.4	14,400
395	1530	577	-4.3	50,800
396	1410	755	-6.0	40,800
397	912	256	-13.9	106,400
399	1465	1063	-5.0	28,100
400	1473	450	-4.9	61,900
401	1029	1140	-11.5	25,300
403	1516	754	-4.4	40,800
404	1495	554	-4.7	52,500
405	1525	1092	-4.3	27,100
406	723	252	-18.4	108,000
409	650	663	-20.8	45,500
410	1501	478	-4.6	59,000
411	936	1057	-13.4	28,300
412	350	1120	-35.9	26,000
413	1033	538	-11.4	53,700
415	737	425	-18.0	64,900
416	1578	606	-3.7	48,900
417	646	496	-21.0	57,300
418	1695	482	-2.3	58,600
419	725	770	-18.3	40,000
420	1289	1041	-7.7	28,900
421	1171	912	-9.1	33,900
422	599	162	-22.8	193,700
423	929	856	-13.6	36,200
424	739	625	-17.9	47,700
425	1490	965	-4.7	31,800
426	1286	704	-7.6	43,200
427	810	843	-16.0	36,800
428	1565	303	-3.9	88,700
429	1259	847	-8.0	36,800
430	1253	562	-8.1	51,900
431	734	1426	-18.1	15,500
432	483	433	-28.5	63,900
434	518	1041	-26.9	28,800
435	1020	1170	-11.6	24,300
436	1122	196	-9.8	147,600
437	1870	673	-0.5	45,000
438	435	1102	-31.0	26,700
439	86	847	<-35.0	36,600
440	1740	544	-1.8	53,200
441	599	1571	-22.8	10,800
443	743	335	-17.8	80,100
446	801	668	-16.2	45,200
447	1050	926	-11.1	33,300
448	1245	1298	-8.2	19,800
449	1576	1516	-3.7	12,800
450	1818	1021	-0.9	29,800
451	1094	440	-10.3	63,100
452	1945	802	>0.0	38,800
453	1652	894	-2.8	34,800
454	1403	500	-6.1	56,900
456	1394	718	-6.3	42,600
457	905	436	-14.0	63,500
459	1038	581	-11.3	50,500
460	1598	294	-3.4	91,400
461	1528	863	-4.3	35,900
462	1098	1137	-10.2	25,400
463	849	1125	-15.2	25,800
464	1814	1072	-0.9	27,800
465	1388	481	-6.3	58,700
466	1194	1084	-8.9	27,300
468	577	467	-23.9	60,100
469	1140	888	-9.6	34,900
470	1797	524	-1.1	54,800
471	1293	1133	-7.6	25,500
472	618	655	-21.9	46,000
473	2009	299	>0.0	89,900
474	1205	215	-8.7	131,300
475	1035	788	-11.4	39,200
476	160	155	<-35.0	207,800
477	469	1370	-28.9	17,400
478	599	662	-22.8	45,800
479	1009	540	-11.8	53,500
480	1216	235	-8.6	117,400
482	816	346	-15.9	77,800
483	683	673	-19.3	44,900
485	1608	1013	-3.3	30,000
486	478	599	-28.6	49,300
487	1025	607	-11.5	48,800
488	1045	1186	-11.2	23,700
489	1609	301	-3.3	89,200
490	775	1289	-17.0	20,100
491	692	178	-19.3	169,300
492	1100	964	-10.2	31,800
493	1760	776	-1.6	39,700
494	882	247	-14.5	110,700
495	470	1258	-28.9	21,200
496	494	1436	-28.1	15,200
497	980	852	-12.5	36,400
499	1414	546	-6.0	53,100
500	1234	1072	-8.3	27,800
501	1246	659	-8.2	45,700
502	824	792	-15.7	39,000
503	1246	1134	-8.2	25,500
504	1115	1407	-9.9	16,200
505	1189	391	-8.9	69,700
506	1578	402	-3.7	69,000
507	787	250	-16.6	109,000
508	979	552	-12.5	52,800
509	1153	619	-9.4	49,100
510	1730	1006	-2.0	30,200

809
1099
1696
948
481
1334
868
798
822
632
1332
803
1190
479
768
747
1170
1502
1728
507
870
1347
1513
308
1851
1463
909
625
1164
803
1259
856
803
1162
128
1355
595
1369
992
1125
705
1477
980
700
1028
898
789
777
980
1519
1212
780
618
1142
532
771
1068
822
914
1064
1524
1392
982
1487
758
687
830
1888
642
1317
85
1014
732
1627
1009

MSN	X	Y	CPKdl	SDSMW
511	809	484	-16.0	58,400
512	1099	533	-10.2	54,100
513	1696	1034	-2.3	29,200
514	948	636	-13.2	47,100
515	481	543	-28.5	53,400
516	1334	1044	-7.1	28,800
517	868	1021	-14.8	29,700
518	798	779	-16.3	39,600
519	822	670	-15.7	45,100
520	632	165	-21.5	189,000
521	1332	830	-7.1	37,300
522	603	1104	-22.6	26,600
523	1190	309	-8.9	86,800
524	479	1226	-28.6	22,300
525	768	1066	-17.2	28,000
526	747	1016	-17.7	29,800
527	1170	231	-9.2	119,600
528	1502	542	-4.6	53,400
530	1728	620	-2.0	48,000
532	507	1011	-27.4	30,000
533	870	489	-14.7	57,900
534	1347	1085	-6.9	27,300
535	1513	346	-4.5	77,800
536	308	654	<-35.0	46,000
538	1851	689	-0.7	44,100
539	1463	982	-5.1	31,100
540	909	561	-13.9	52,000
541	625	289	-21.7	93,100
542	1164	198	-9.2	146,200
543	803	655	-16.2	45,900
544	1259	1143	-8.0	25,200
545	856	1526	-15.0	12,200
546	803	1071	-16.2	27,800
547	1162	274	-9.3	98,400
548	128	1321	<-35.0	19,000
549	1355	1122	-6.8	25,900
550	595	866	-23.0	35,800
552	1369	494	-6.6	57,500
553	992	405	-12.2	67,600
555	1125	410	-9.8	66,900
556	705	975	-18.9	31,400
557	1477	1030	-4.9	29,300
558	980	583	-12.5	50,400
559	700	1109	-19.1	26,400
560	1028	621	-11.5	48,000
562	898	794	-14.1	38,900
564	789	1446	-16.6	14,900
565	777	766	-16.9	40,200
566	980	328	-12.5	81,900
567	1519	611	-4.4	48,600
569	1212	661	-8.6	45,600
570	760	594	-17.4	49,700
571	618	956	-21.9	32,100
573	1142	771	-9.6	40,000
574	532	787	-26.2	39,300
575	771	250	-17.1	109,200
576	1068	534	-10.8	54,100
577	822	734	-15.7	41,800
578	914	754	-13.8	40,800
579	1064	794	-10.8	38,900
580	1524	714	-4.4	42,800
581	1392	783	-6.3	39,400
582	982	686	-12.4	44,200
584	1487	672	-4.8	45,000
585	758	731	-17.4	41,900
586	687	1152	-19.5	24,900
587	930	523	-13.5	55,000
588	1888	774	-0.4	39,900
589	642	485	-21.1	58,300
590	1317	519	-7.3	55,300
591	65	1548	<-35.0	11,500
592	1014	814	-11.7	48,400
593	732	176	-18.1	172,300
594	1627	478	-3.0	59,000
595	1009	1426	-11.8	15,500
596	619	269	-21.9	100,500
597	1176	461	-9.1	60,700
598	1465	1044	-5.0	28,800
599	741	1188	-17.9	23,600
600	807	402	-14.0	68,000
601	687	658	-19.5	45,800
602	712	1138	-18.7	25,400
603	898	181	-14.1	165,200
604	783	1461	-16.7	14,400
605	736	223	-18.0	125,300
606	629	273	-21.6	98,700
607	1064	286	-10.8	94,000
608	883	503	-14.5	56,700
609	2012	610	>0.0	48,700
610	1255	903	-8.1	34,200
612	1103	391	-10.1	69,600
613	778	265	-16.9	102,000
614	824	518	-15.7	55,400
615	1095	195	-10.3	149,100
616	1759	478	-1.6	59,000
617	994	372	-12.1	72,900
618	751	374	-17.6	72,400
619	1429	518	-5.7	55,300
620	1050	520	-11.1	55,200
621	923	1105	-13.7	26,600
622	1462	622	-5.1	47,900
623	759	225	-17.4	124,000
624	758	1038	-17.4	29,000
625	1438	606	-5.5	48,900
626	1096	1089	-10.2	27,200
627	942	548	-13.3	53,000
628	809	621	-16.0	48,000
629	899	979	-14.1	31,300
630	1135	1321	-9.6	19,100
631	979	615	-12.5	48,300
632	1542	1076	-4.1	27,600
633	1345	814	-6.9	38,000
634	409	950	-32.2	32,400
635	1165	704	-9.2	43,300
636	774	604	-17.0	49,000
637	1263	524	-8.0	54,800
638	952	411	-13.1	66,700
639	1717	575	-2.1	51,000
640	994	292	-12.1	92,000
641	165	1224	<-35.0	22,400
642	803	251	-16.2	108,900
643	719	296	-18.5	90,700
644	1100	294	-10.2	91,400
645	534	1263	-26.1	21,000
646	1153	1038	-9.4	29,000
648	1246	204	-8.2	140,000
649	14	1406	<-35.0	16,200
650	1713	1049	-2.1	28,600
651	1986	1183	>0.0	23,800
652	1378	816	-6.5	38,000
653	1442	1165	-5.5	24,400
654	650	806	-20.8	38,400
655	1111	551	-10.0	52,700
656	1095	861	-10.3	36,000
657	1524	540	-4.4	53,600
658	1777	860	-1.4	36,000
659	391	584	-33.4	50,400
660	977	565	-12.5	51,700
661	658	166	-20.5	187,500
662	732	312	-18.1	86,100
663	1787	567	-1.2	51,500
664	888	268	-14.4	100,900
665	889	775	-14.3	39,800
666	715	221	-18.6	126,300
667	781	227	-16.8	122,400
668	646	165	-21.0	189,100
669	1116	353	-9.9	76,300
670	1382	643	-6.4	46,600
671	547	789	-25.3	39,200
673	984	746	-12.4	41,200
674	1661	448	-2.7	62,100
675	1523	562	-4.4	51,900
676	708	642	-18.8	46,700
677	919	615	-13.7	48,300
678	1085	551	-10.5	52,700
679	600	823	-22.7	33,400
680	1237	1004	-8.3	30,300
681	1103	283	-10.1	95,100
682	1406	477	-6.1	59,100
683	1596	249	-3.4	109,800
684	555	699	-24.8	43,500
685	1167	1313	-9.2	19,300
686	1932	790	0.0	39,100
687	1545	619	-4.1	48,100
688	1456	764	-5.2	40,300
689	1011	953	-11.8	32,300
690	1995	270	>0.0	100,200
691	812	888	-16.0	34,900
692	1154	1461	-9.4	14,400
693	1993	819	>0.0	37,800
694	1628	656	-3.0	45,900
695	928	254	-13.6	107,000
696	1854	715	-0.6	42,700
697	1997	345	>0.0	78,000
698	957	563	-13.0	51,800
699	1540	730	-4.2	42,000
702	577	900	-23.8	34,400
703	1610	562	-3.2	51,900
705	1278	571	-7.8	51,200
706	1841	704	-0.7	43,300
707	1018	1386	-11.7	16,900
709	1074	1145	-10.7	25,100
710	293	889	<-35.0	34,800
712	720	412	-18.5	66,600
713	1386	841	-6.4	36,800
714	1328	263	-7.1	103,100
715	698	433	-19.1	63,900
716	701	481	-19.0	58,700
717	1875	699	-0.5	43,600
718	575	702	-23.9	43,400
719	1216	204	-8.6	140,400
721	1069	464	-10.8	60,400
722	1272	506	-7.9	56,400
723	958	822	-13.0	37,700
724	763	395	-17.3	69,100
725	720	916	-18.5	33,700
726	1476	415	-4.9	66,200
727	1846	473	-0.7	59,400
728	510	783	-27.3	39,400
729	1217	1126	-8.6	25,800
730	1858	724	-0.6	42,300
731	665	765	-20.2	40,300
733	1321	312	-7.2	85,900
734	719	427	-18.5	64,600
735	1101	473	-10.2	59,500
736	1359	569	-6.7	51,400
738	696	220	-19.2	127,600
739	687	409	-19.5	67,000
740	1205	256	-8.7	106,200
741	995	563	-12.1	51,900
742	898	596	-14.1	49,500
743	881	181	-14.5	165,900
744	1951	686	>0.0	44,200
745	726	168	-18.3	183,600
746	999	643	-12.0	46,600
748	182	1503	<-35.0	13,000
749	2005	649	>0.0	46,300
750	1448	575	-5.4	51,000
751	792	266	-16.5	101,900
752	469	296	-28.9	90,600
754	664	254	-20.3	107,000
755	1195	184	-8.8	161,000
756	1821	1113	-0.9	26,300
757	909	246	-13.9	111,000
760	790	133	-16.5	264,900

MSN	X	Y	CPKdl	SDSMW
761	1399	733	-6.2	41,800
763	1416	1085	-5.9	27,300
764	2020	569	>0.0	51,400
765	651	475	-20.8	59,300
766	1052	1149	-11.1	25,000
767	1968	468	>0.0	59,900
768	1330	685	-7.1	44,300
769	1970	613	>0.0	48,500
770	857	617	-15.0	48,200
771	1337	974	-7.0	31,500
773	1576	502	-3.7	56,700
775	969	824	-12.8	37,600
776	1438	708	-5.5	43,100
777	1539	458	-4.2	61,000
778	850	434	-15.1	63,800
779	700	411	-19.1	66,800
780	1052	1136	-11.1	25,500
784	1413	529	-6.0	54,400
785	1364	885	-6.7	35,000
786	1822	835	-0.9	37,100
787	893	392	-14.3	69,500
790	616	882	-22.0	35,100
791	451	1429	-29.8	15,400
792	777	377	-16.9	72,000
793	1536	1543	-4.2	11,700
794	1461	807	-5.1	38,300
796	388	546	-33.6	53,100
797	1126	212	-9.8	133,700
798	933	437	-13.5	63,400
799	1420	583	-5.9	49,800
800	1759	279	-1.6	96,500
801	624	865	-21.7	35,800
802	898	547	-14.2	53,000
803	1775	1468	-1.4	14,200
804	573	196	-24.0	148,400
805	203	494	<-35.0	57,400
806	980	1039	-12.5	29,000
807	902	308	-14.1	87,200
808	625	827	-21.7	37,500
809	1851	1015	-0.7	29,900
810	440	573	-30.9	51,100
811	1358	249	-6.8	109,700
812	851	393	-15.1	69,400
813	745	1246	-17.8	21,600
814	2028	810	>0.0	38,200
815	1086	645	-10.4	46,500
816	629	313	-21.6	85,700
817	1376	1177	-6.5	24,000
818	1771	790	-1.4	39,100
819	1045	263	-11.2	103,100
820	984	362	-12.4	74,600
821	1712	279	-2.2	96,700
822	1256	205	-8.1	139,200
823	1517	654	-4.4	46,000
824	1442	449	-5.5	62,000
825	1240	513	-8.3	55,800
826	1309	1014	-7.4	29,900
827	2012	708	>0.0	43,100
828	937	1405	-13.4	16,200
830	1342	756	-7.0	40,700
831	562	826	-24.5	37,500
832	1073	1039	-10.7	29,000
833	481	820	-28.5	37,800
834	501	581	-27.8	50,500
837	751	748	-17.6	41,100
838	635	833	-21.3	37,200
839	1494	459	-4.7	60,900
840	1952	301	>0.0	89,300
841	1585	1080	-3.6	27,500
842	571	1312	-24.1	19,400
843	1325	649	-7.2	46,300
844	1727	301	-2.0	89,200
845	630	679	-21.5	44,600
846	2016	905	>0.0	34,200
847	673	1200	-19.9	23,200
848	1863	271	-0.6	99,500
849	1166	523	-9.2	54,900
850	1535	1024	-4.2	29,600
851	1035	826	-11.4	37,500
852	834	542	-15.5	53,400
855	499	220	-27.8	127,100
856	1063	194	-10.9	150,500
857	887	890	-14.4	34,800
858	1448	639	-5.4	46,900
859	706	311	-18.9	86,200
860	1070	1066	-10.7	28,000
861	472	347	-28.8	77,600
862	674	480	-19.9	58,800
864	1307	499	-7.4	57,000
865	645	887	-21.0	34,900
866	827	1004	-15.6	30,300
868	685	494	-19.5	57,400
869	1807	402	-1.0	68,000
870	1323	783	-7.2	39,400
871	1228	1031	-8.4	29,300
872	1904	346	-0.3	77,700
873	556	647	-24.8	46,400
874	1540	756	-4.2	40,700
875	1566	777	-3.8	39,700
876	1198	351	-8.8	76,800
877	1076	720	-10.6	42,500
878	1161	1111	-9.3	26,400
879	647	757	-20.9	40,700
880	1756	594	-1.6	49,700
881	1543	278	-4.1	97,100
883	1432	890	-5.7	34,800
884	922	689	-13.7	44,100
885	1103	414	-10.1	66,400
886	1501	607	-4.6	48,900
887	798	1103	-16.3	26,600
888	636	634	-21.3	47,200
889	951	759	-13.1	40,600
890	717	548	-18.6	52,900
891	1123	229	-9.8	121,200
892	891	413	-14.3	66,400
894	1245	234	-8.2	117,800
895	1962	346	>0.0	77,700
896	1322	626	-7.2	47,700
897	420	570	-31.4	51,300
898	662	428	-20.3	64,500
899	845	243	-15.3	113,000
900	624	703	-21.7	43,400
901	931	1094	-13.5	27,000
903	799	229	-16.3	121,000
904	765	520	-17.2	55,200
905	775	889	-17.0	34,800
907	888	824	-14.4	37,600
908	828	1303	-15.6	19,700
910	681	1544	-19.7	11,700
911	1544	301	-4.1	89,100
913	1606	387	-3.3	70,400
914	1237	688	-8.3	44,100
916	1442	749	-5.5	41,100
917	1260	367	-8.0	73,700
919	764	1541	-17.3	11,700
920	1133	1123	-9.7	25,900
921	1123	380	-9.8	71,500
923	829	242	-15.6	113,200
924	1131	318	-9.7	84,300
925	1441	874	-5.5	35,400
926	679	219	-19.7	128,200
927	1487	1191	-4.8	23,500
928	1082	775	-10.5	39,800
929	1231	816	-8.4	38,000
931	1609	670	-3.3	45,100
932	810	900	-16.0	34,400
933	965	520	-12.8	55,100
934	947	462	-13.2	60,600
936	865	843	-14.8	36,800
937	1421	1056	-5.9	28,400
939	1197	827	-8.8	37,500
941	1765	885	-1.5	35,000
942	602	472	-22.7	59,600
943	312	498	<-35.0	57,100
944	993	491	-12.1	57,700
945	1300	269	-7.5	100,300
946	630	423	-21.6	65,100
947	187	736	<-35.0	41,600
948	1380	344	-6.5	78,200
949	1766	665	-1.5	45,400
950	1038	193	-11.3	151,000
951	860	152	-14.9	213,000
952	957	701	-13.0	43,400
954	503	547	-27.6	53,000
955	1938	712	>0.0	42,900
957	1010	816	-11.8	37,900
958	768	174	-17.2	174,900
960	596	419	-23.0	65,700
961	557	409	-24.8	67,100
962	887	320	-14.4	83,900
963	564	334	-24.5	80,500
964	969	1155	-12.8	24,800
965	671	255	-20.0	106,600
966	1204	798	-8.7	38,700
967	910	154	-13.9	210,300
968	609	1048	-22.3	28,700
969	1285	206	-7.7	138,900
970	822	232	-15.8	119,300
971	976	437	-12.6	63,400
972	403	567	-32.6	51,600
974	279	495	<-35.0	57,400
975	844	981	-15.3	31,200
976	1124	295	-9.8	91,100
977	994	664	-12.1	45,400
978	1612	642	-3.2	46,700
979	749	1141	-17.7	25,300
980	1064	642	-10.8	46,700
981	1197	911	-8.8	33,900
983	1762	1508	-1.6	12,800
984	1344	317	-6.9	84,700
985	1024	1105	-11.5	26,600
987	739	1159	-17.9	24,600
988	816	555	-15.9	52,400
990	785	361	-16.7	74,900
991	1159	317	-9.3	84,500
992	1090	928	-10.4	33,300
993	1030	701	-11.5	43,400
994	847	811	-15.2	38,200
995	902	461	-14.1	60,700
996	888	847	-14.4	36,600
997	1815	579	-0.9	50,700
998	1205	504	-8.7	56,500
999	617	289	-22.0	93,100
1000	968	290	-12.8	92,700
1001	970	771	-12.7	40,000
1002	1736	478	-1.9	58,900
1003	643	1184	-21.1	23,700
1006	822	487	-15.8	58,100
1007	875	279	-14.6	96,400
1009	291	644	<-35.0	46,600
1010	1386	745	-6.4	41,200
1011	459	541	-29.4	53,500
1012	679	661	-19.7	45,600
1013	1818	1128	-0.9	25,800
1014	1032	634	-11.4	47,200
1015	1629	994	-3.0	30,700
1016	1311	1134	-7.4	25,500
1017	1722	424	-2.0	65,000
1018	1015	743	-11.7	41,300
1020	1574	1219	-3.7	22,500
1021	781	484	-16.8	58,400
1022	1129	83	-9.7	591,300
1023	812	317	-15.9	84,800
1024	785	446	-16.7	62,400
1025	1290	739	-7.7	41,500

MSN	X	Y	CPKdl	SDSMW
1026	405	552	-32.5	52,600
1027	1298	848	-7.5	36,500
1028	856	547	-15.0	53,000
1030	1284	226	-7.7	123,200
1031	986	822	-12.3	37,700
1032	1547	403	-4.1	67,900
1033	1381	551	-6.4	52,700
1034	1525	496	-4.3	57,200
1035	1128	645	-9.7	46,500
1036	1226	274	-8.5	98,300
1039	1761	262	-1.6	103,600
1040	541	839	-25.7	36,900
1041	818	910	-15.8	34,000
1044	1036	485	-11.3	58,300
1045	1439	407	-5.5	67,300
1047	1540	250	-4.2	109,200
1048	1576	635	-3.7	47,100
1049	1089	411	-10.4	66,700
1050	949	1040	-13.2	28,900
1051	426	818	-31.1	37,800
1052	1583	1385	-3.6	16,900
1053	779	1092	-16.8	27,000
1054	1613	620	-3.2	48,000
1055	1380	377	-6.5	72,000
1056	284	663	<-35.0	45,500
1058	1261	746	-8.0	41,200
1060	393	605	-33.3	49,000
1061	1817	645	-0.9	46,600
1062	1245	746	-8.2	41,200
1064	1258	792	-8.1	39,000
1065	705	934	-18.9	33,000
1066	1181	734	-9.0	41,800
1067	529	658	-26.3	45,800
1068	508	696	-27.4	43,700
1069	1898	604	-0.3	49,100
1071	873	609	-14.7	48,700
1073	1768	1128	-1.5	25,800
1075	836	773	-15.4	39,900
1076	1863	861	-0.6	36,000
1078	826	566	-15.7	51,600
1081	971	483	-12.7	58,500
1083	1697	202	-2.3	142,300
1085	1157	794	-9.4	38,900
1090	620	910	-21.9	34,000
1092	1867	597	-0.5	49,500
1093	2019	894	>0.0	34,600
1094	1546	538	-4.1	53,700
1095	1545	477	-4.1	59,100
1098	61	835	<-35.0	33,000
1099	1954	237	>0.0	116,000
1101	588	1048	-23.3	28,600
1102	1050	667	-11.1	45,200
1103	457	797	-29.5	38,800
1105	1884	532	-0.4	54,200
1106	1714	649	-2.1	46,300
1107	1717	546	-2.1	53,100
1108	1976	722	>0.0	42,400
1111	547	1066	-25.3	28,000
1112	1348	621	-6.9	48,000
1115	1385	762	-6.4	40,400
1116	1078	816	-10.6	38,000
1117	975	787	-12.6	39,300
1118	1202	933	-8.7	33,100
1119	1022	1076	-11.6	27,600
1120	1905	616	-0.3	48,300
1121	1512	1301	-4.5	19,700
1122	1114	677	-9.9	44,700
1123	1464	452	-5.1	61,700
1125	1048	857	-11.1	36,200
1126	1122	802	-9.8	38,600
1128	1722	892	-2.1	34,700
1133	1098	825	-10.2	37,500
1139	1830	569	-0.8	51,400
1147	764	1182	-17.3	23,800
1148	1968	724	>0.0	42,300
1153	921	1158	-13.7	24,700
1154	1594	864	-3.5	35,900
1161	637	400	-21.3	68,400
1162	623	397	-21.8	68,800
1163	665	397	-20.2	68,700
1168	564	528	-24.4	54,500
1170	552	529	-25.0	54,500
1171	538	524	-25.9	54,800
1172	545	514	-25.5	55,700
1174	1099	522	-10.2	55,000
1176	1304	586	-7.5	50,200
1177	1366	539	-6.6	53,700
1178	1608	702	-3.3	43,400
1179	1485	224	-4.8	124,900
1180	1459	224	-5.2	124,800
1181	1431	223	-5.7	125,100
1182	1407	223	-6.1	125,200
1183	1383	224	-6.4	124,700
1184	1454	182	-5.3	164,400
1185	1422	183	-5.8	162,600
1186	1394	182	-6.3	164,300
1189	1171	214	-9.2	131,800
1190	1457	286	-5.2	94,200
1191	686	1114	-19.5	26,200
1192	265	893	<-35.0	34,700
1193	403	1292	-32.6	20,000
1194	344	1275	<-35.0	20,600
1195	505	1311	-27.6	19,400
1196	572	1293	-24.1	20,000
1197	639	1502	-21.2	13,000
1198	637	1402	-21.3	16,300
1199	614	1407	-22.1	16,200
1200	637	1431	-21.3	15,400
1201	1095	1394	-10.3	16,600
1202	1719	1545	-2.1	11,600
1203	791	668	-16.5	45,200
1204	964	1021	-12.9	29,700
1205	313	195	<-35.0	148,700
1208	306	194	<-35.0	149,800
1209	320	197	<-35.0	147,400
1210	326	197	<-35.0	146,600
1211	394	294	-33.2	91,400
1212	402	294	-32.7	91,200
1214	386	294	-33.7	91,400
1215	641	329	-21.2	81,600
1216	660	329	-20.4	81,600
1217	914	266	-13.8	101,800
1218	873	245	-14.7	112,000
1219	970	372	-12.7	72,900
1220	1021	298	-11.6	90,100
1221	1392	205	-6.3	139,500
1222	1354	203	-6.8	141,800
1223	1362	205	-6.7	139,500
1224	673	540	-19.9	53,600
1225	614	542	-22.1	53,400
1226	603	539	-22.6	53,600
1227	696	623	-19.2	47,800
1228	707	628	-18.9	47,500
1229	475	447	-28.7	62,300
1230	466	1282	-29.0	20,400
1231	759	1461	-17.4	14,400
1232	1324	1170	-7.2	24,200
1233	1583	1005	-3.6	30,300
1234	1865	809	-0.6	38,200
1235	1812	817	-1.0	37,900
1236	1411	703	-6.0	43,400
1237	1392	682	-6.3	44,500
1238	794	410	-16.4	66,900
1239	769	407	-17.1	67,300
1240	740	406	-17.9	67,500
1241	743	511	-17.8	55,900
1242	713	510	-18.7	56,000
1243	682	509	-19.6	56,100
1244	663	504	-20.3	56,500
1245	565	582	-24.4	50,500
1246	547	577	-25.3	50,800
1247	530	576	-26.3	50,900
1249	516	572	-27.0	51,200
1250	973	536	-12.7	53,900
1251	607	532	-22.4	54,200
1252	665	529	-20.2	54,400
1253	899	766	-14.1	40,200
1254	1311	746	-7.4	41,200
1255	1300	761	-7.5	40,400
1257	1838	712	0.0	42,900
1258	1806	718	-1.0	42,600
1259	1727	715	-2.0	42,700
1260	1629	713	-3.0	42,800
1261	1555	717	-4.0	42,600
1262	1468	717	-5.0	42,600
1263	1413	722	-6.0	42,400
1264	1340	717	-7.0	42,600
1265	1263	717	-8.0	42,600
1266	1182	720	-9.0	42,500
1267	1110	717	-10.0	42,600
1268	1055	717	-11.0	42,600
1269	999	717	-12.0	42,600
1270	959	715	-13.0	42,700
1271	905	712	-14.0	42,900
1272	857	714	-15.0	42,800
1273	810	705	-16.0	43,300
1274	774	711	-17.0	42,900
1277	737	708	-18.0	43,100
1278	702	711	-19.0	42,900
1279	671	710	-20.0	43,000
1280	645	710	-21.0	43,000
1281	617	707	-22.0	43,100
1282	595	704	-23.0	43,300
1283	573	700	-24.0	43,500
1284	552	695	-25.0	43,700
1285	536	694	-26.0	43,800
1286	515	687	-27.0	44,200
1287	496	683	-28.0	44,400
1288	467	669	-29.0	45,200
1289	447	667	-30.9	45,300
1290	427	655	-31.0	45,900
1291	412	655	-32.0	45,900
1292	397	652	-33.0	46,100
1293	381	654	-34.0	46,000
1294	365	653	-35.0	46,100
1295	348	653	<-35.0	46,100

Table 2. Table of some identified proteins

POP name	Protein name	MSN's	Basis for identification
IDS:3_ALPHA_HDDH	3-α-hydroxysteroid-dihydrodiol-dehydrogenase, an enzyme of steroid metabolism	137, 159	Pure protein and antibody provided by Dr. T.M. Penning, Department of Pharmacology, School of Medicine, University of Pennsylvania.
IDS:ACTIN_BETA	β cellular actin, a cytoskeletal protein	38	Homologous position with respect to other mammalian systems
IDS:ACTIN_GAMMA	γ cellular actin, a cytoskeletal protein	68	Homologous position with respect to other mammalian systems
IDS:ALBUMIN	Serum albumin, mature form.	21, 28, 33	Predominance in rat plasma
IDS:APO_A-I	Apo A-I plasma lipoprotein, mature form (tentative).	236, 463	Presence in rat plasma, regulation by some lipid-lowering drugs
IDS:CALMODULIN	Calmodulin, an acidic cytosolic calcium-binding protein	123, 649	Homologous position with respect to other mammalian systems
IDS:CATALASE	Catalase (peroxisomal)	54, 61, 106	Presence in purified peroxisomes, similarity in position to mouse catalase
IDS:CPKSPOTS	Spots contributed by the CPK charge standards (not rat liver proteins)	1257 - 1295	
IDS:CPS	Carbamoyl phosphate synthase	114, 157, 167, 174, 1184, 1185, 1186, 1222	Pure protein provided by Dr. Margaret Marshall, Department of Pharmacology, Medical School, University of Wisconsin - Madison.
IDS:CYTOCHROME_B5	Cytochrome b5	87, 477	Pure protein provided by Dr. Andrew Parkinson, Department of Pharmacology, Toxicology and Therapeutics, University of Kansas Medical Center
IDS:FABP-L	Liver fatty-acid binding protein	. 227	Pure protein provided by Dr. Nathan Bass, Department of Medicine, University of California School of Medicine, San Francisco
IDS:HMG-COA_SYNTHASE	Cytosolic HMG-CoA Synthase	133, 144, 235, 413	Antibody provided by Dr. Michael Greenspan, Merck Sharp & Dohme Research Laboratories, Rahway, NJ
IDS:LAMIN_B	Lamin B, a nuclear protein	415, 734	Homologous position with respect to other mammalian systems
IDS:MITCON:1	Mitcon:1 (F1 ATPase β subunit), a mitochondrial inner membrane	17, 49, 71, 340, 1245, 1246, 1247, 1249	Homologous position with respect to other mammalian systems, presence in mitochondria
IDS:MITCON:2	Mitcon:2, a mitochondrial matrix stress protein equivalent to E.	15, 25, 110, 1241, 1242, 1243, 1244	Homologous position with respect to other mammalian systems, presence in mitochondria
IDS:MITCON:3	Mitcon:3, a mitochondrial matrix stress protein, likely analog of	18, 35, 226, 600, 1238, 1239, 1240	Homologous position with respect to other mammalian systems, presence in mitochondria
IDS:NADPH_P450_RED	NADPH cytochrome P-450 reductase, frequently co-induced with P-450's	175, 251, 812	Pure protein provided by Dr. Andrew Parkinson, Department of Pharmacology, Toxicology and Therapeutics, University of Kansas Medical Center
IDS:PDI	Protein disulphide isomerase 1	168, 1170, 1171, 1172	Sequence information obtained by R.M. Van Frank, Lilly Research Laboratories, Indianapolis
IDS:PLASMA_PROTEINS	Rat plasma proteins observed in liver	21, 28, 33, 44, 72, 102, 115, 197, 236, 246, 248, 257, 293, 332, 347, 364, 369, 419, 432, 463, 468, 518, 562, 605, 623, 666, 667, 725, 738, 790, 865, 903, 926	Plasma coelectrophoresis studies
IDS:PRO-ALBUMIN	Serum albumin precursor	47, 93	Relative position to mature albumin, presence in microsomes
IDS:PYRCARBOX	Pyruvate carboxylase	179, 1180, 1181, 1182, 1183	Pavlica, R.J., et al., BBA (1990) *1022* 115-125.
IDS:SOD	Superoxide dismutase	135	Sequence information obtained by R.M. Van Frank, Lilly Research Laboratories, Indianapolis
IDS:TUBULIN_ALPHA	α tubulin, a cytoskeletal protein	56, 132, 1224, 1252	Homologous position with respect to other mammalian systems
IDB:TUBULIN_BETA	β tubulin, a cytoskeletal protein	50, 1225, 1226, 1251	Homologous position with respect to other mammalian systems

e 3. Computed pI's of two sets of carbamylated protein standards: Rabbit muscle CPK and human hemoglobin (Hb)

Protein Name	PIR Name	#ASP 3.9	#GLU 4.1	#HIS 6.0	#LYS 10.8	#ARG 12.5	NH2- 7.0	Calc pI	Real CPK
Rabbit muscle CPK	KIRBCM	28	27	17	34	18	1	6.84	0.0
		28	27	17	33	18	1	6.67	-1
		28	27	17	32	18	1	6.54	-2
		28	27	17	31	18	1	6.42	-3
		28	27	17	30	18	1	6.31	-4
		28	27	17	29	18	1	6.21	-5
		28	27	17	28	18	1	6.12	-6
		28	27	17	27	18	1	6.03	-7
		28	27	17	26	18	1	5.94	-8
		28	27	17	25	18	1	5.85	-9
		28	27	17	24	18	1	5.76	-10
		28	27	17	23	18	1	5.67	-11
		28	27	17	22	18	1	5.58	-12
		28	27	17	21	18	1	5.48	-13
		28	27	17	20	18	1	5.39	-14
		28	27	17	19	18	1	5.29	-15
		28	27	17	18	18	1	5.20	-16
		28	27	17	17	18	1	5.12	-17
		28	27	17	16	18	1	5.04	-18
		28	27	17	15	18	1	4.96	-19
		28	27	17	14	18	1	4.89	-20
		28	27	17	13	18	1	4.83	-21
		28	27	17	12	18	1	4.77	-22
		28	27	17	11	18	1	4.71	-23
		28	27	17	10	18	1	4.66	-24
		28	27	17	9	18	1	4.61	-25
		28	27	17	8	18	1	4.56	-26
		28	27	17	7	18	1	4.52	-27
		28	27	17	6	18	1	4.48	-28
		28	27	17	5	18	1	4.44	-29
		28	27	17	4	18	1	4.40	-30
		28	27	17	3	18	1	4.36	-31
		28	27	17	2	18	1	4.32	-32
		28	27	17	1	18	1	4.29	-33
		28	27	17	0	18	1	4.25	-34
		28	27	17	0	18	0	4.22	-35
Hb-beta, human	HBHU	7	8	9	11	3	1	7.18	
		7	8	9	10	3	1	6.79	
		7	8	9	9	3	1	6.53	-1.8
		7	8	9	8	3	1	6.32	-3.2
		7	8	9	7	3	1	6.13	-5.3
		7	8	9	6	3	1	5.96	-7.2
		7	8	9	5	3	1	5.78	-10.0
		7	8	9	4	3	1	5.59	-12.3
		7	8	9	3	3	1	5.37	-15.5
		7	8	9	2	3	1	5.14	-18.0
		7	8	9	1	3	1	4.91	-21.0
		7	8	9	0	3	1	4.71	-25.5
		7	8	9	0	3	0	4.54	-27.2

Table 4. Computed pI's of some known proteins related to measured CPK pI's

	Protein Name	PIR Name	#ASP 3.9	#GLU 4.1	#HIS 6.0	#LYS 10.8	#ARG 12.5	Calc pI	Real CPK
0	Creatine phospho kinase (CPK), rabbit muscle	KIRBCM	28	27	17	34	18	6.84	0.0
1	Fatty acid-binding protein, rat hepatic	FZRTL	5	13	2	16	2	7.83	-3.0
2	b2-microglobulin, human	MGHUB2	7	8	4	8	5	6.09	-5.0
3	Carbamoyl-phosphate synthase, rat	SYRTCA	72	96	28	95	56	5.97	-5.5
	Proalbumin (serum albumin precursor), rat	ABRTS	32	57	15	53	27	5.98	-6.2
	Serum albumin, rat	ABRTS	32	57	15	53	24	5.71	-9.0
	Superoxid dismutase (Cu-Zn, SOD), rat	A26810	8	11	10	9	4	5.91	-9.2
	Phospholipase C, phophoinositide-specific (?), rat	A28807	34	42	9	49	21	5.92	-9.2
	Albumin, human	ABHUS	36	61	16	60	24	5.70	-11.5
	Apo A-I lipoprotein, rat	A24700	18	24	6	23	12	5.32	-13.7
	proApo A-I lipoprotein, human	LPHUA1	16	30	6	21	17	5.35	-14.3
	NADPH cytochrome P-450 reductase, rat	RDRTO4	41	60	21	38	36	5.07	-15.6
	Retinol binding protein, human	VAHU	18	10	2	10	14	5.04	-16.9
	Actin beta, rat	ATRTC	23	26	9	19	18	5.06	-17.2
	Actin gamma, rat	ATRTC	20	29	9	19	18	5.07	-16.6
	Apo A-I lipoprotein, human	LPHUA1	16	30	5	21	16	5.10	-17.5
	Apo A-IV lipoprotein, human	LPHUA4	20	49	8	28	24	4.88	-19.7
	Tubulin alpha, rat	UBRTA	27	37	13	19	21	4.66	-19.8
	F1ATPase beta, bovine	PWBOB	25	36	9	22	22	4.80	-21.0
	Tubulin beta, pig	UBPGB	26	36	10	15	22	4.49	-22.5
	Protein disulphide isomerase (PDI), rat hepatic	ISRTSS	43	51	11	51	9	4.07	-25.0
	Cytochrome b5, rat	CBRT5	10	15	6	10	4	4.59	-26.0
	Apo C-II lipoprotein, human	LPHUC2	4	7	0	6	1	4.44	-30.5
	Amino acid pI assumed in calulation:		3.9	4.1	6.0	10.8	12.5		

...Wirth
...Luo
...ori Fujimoto
...C. Bisgaard
...D. Olson

...atory of Exp...
...ogenesis.
...al Cancer In
...al Institutes
...da.

...ndence: Dr. P
...National Car
...52, USA

...ons: 2-D PA
... HLE, hum:
... weight; NE
...8, Nonidet P-
...de; RLE, rat

...riftsgesellsch.

JOURNAL OF BIOLUMINESCENCE AND CHEMILUMINESCENCE VOL 4 59–78 (198

High Specific Activity Chemiluminescent and Fluorescent Markers: their Potential Application to High Sensitivity and 'Multi-analyte' Immunoassays

Roger Ekins*, Frederick Chu and Jacob Micallef
Department of Molecular Endocrinology, University College and Middlesex School of Medicine, University of London, Mortimer Street, London W1N 8AA, UK

The sensitivities of immunoassays relying on conventional radioisotopic labels (i.e. radioimmunoassay (RIA) and immunoradiometric assay (IRMA)) permit the measurement of analyte concentrations above *ca* 10^7 molecules/ml. This limitation primarily derives, in the case of 'competitive' or 'limited reagent' assays, from the 'manipulation errors arising in the system combined with the physicochemical characteristics of the particular antibody used; however, in the case of 'non-competitive' systems, the specific activity of the label may play a more important constraining role. It is theoretically demonstrable that the development of assay techniques yielding detection limits significantly lower than 10^7 molecules/ml depends on:

(1) the adoption of 'non-competitive' assays designs;
(2) the use of labels of higher specific activity than radioisotopes;
(3) highly efficient discrimination between the products of the immunological reactions involved.

Chemiluminescent and fluorescent substances are capable of yielding higher specific activities than commonly used radioisotopes when used as direct reagent labels in this context, and both thus provide a basis for the development of 'ultra-sensitive', non-competitive, immunoassay methodologies. Enzymes catalysing chemiluminescent reactions or yielding fluorescent reaction products can likewise be used as labels yielding high effective specific activities and hence enhanced assay sensitivities.

A particular advantage of fluorescent labels (albeit one not necessarily confined to them) lies in the possibility they offer of revealing immunological reactions localized in 'microspots' distributed on an inert solid support. This opens the way to the development of an entirely new generation of 'ambient analyte' microspot immunoassays permitting the simultaneous measurement of tens or even hundreds of different analytes in the same small sample, using (for example) laser scanning techniques. Early experience suggests that microspot assays with sensitivities surpassing that of isotopically based methodologies can readily be developed.

Keywords: Ultrasensitive immunoassay; fluorescent microspot immunoassay; confocal microscopy

*Author for correspondence.

0884–3996/89/030059–20$10.00

INTRODUCTION

Immunoassay methods relying on radioisotopic labels have played a major role in medicine and other biologically related fields (agriculture, veterinary science, the food and pharmaceutical industries, etc.) during the past two decades. Their importance has derived from the exploitation both of the 'structural specificity' characterizing antibody–antigen reactions and the 'detectability' of isotopically-labelled reagents, the latter permitting observation of the binding reactions between exceedingly small concentrations of the key reactants involved. The combination of these features has endowed radioimmunoassay methods with unique specificity and sensitivity characteristics, and accounts for their ubiquitous use throughout modern medicine and biology. However, in the past few years, interest has increasingly focused on so-called 'alternative', non-radioisotopic, immunoassay methods; such techniques are based on essentially identical analytical principles but differ in the markers used to label the particular immunoreactant (antibody or analyte) whose distribution between bound and free moieties (following the basic analytical reaction) constitutes the assay 'response'. The reasons for this interest may be grouped under four headings:

(1) Environmental; logistic; economic; practicality and convenience, etc. (i.e. 'non-scientific).
(2) The attainment of higher sensitivity.
(3) The development of 'immunosensors' and 'immunoprobes'.
(4) The development of 'multi-analyte' assay systems.

Our own reasons for developing non-isotopic techniques fall principally under headings (2) and (4), and this presentation will centre primarily on the concepts which underlie our immunoassay development strategy in these areas.

THE ATTAINMENT OF 'ULTRA-HIGH' IMMUNOASSAY SENSITIVITY

Though, as indicated above, the sensitivity of radioisotopically based immunoassay methods has constituted one of the principal foundations of their widespread use over the past 25 years, a fundamental reason for their replacement stems, paradoxically, from the current requirement to develop microanalytical techniques which are superior to them in this particular respect. Radioisotopic methods are, in practice, limited to the measurement of analyte concentrations above about 10^8–10^9 molecules/ml (i.e. approx 0.15–1.5 pmol/l)(Dakubu *et al.*, 1984). However, in certain fields (e.g. virology, tumour detection) there is a particular need to detect or measure molecular concentrations below this level. The factors which determine immunoassay sensitivity have been extensively discussed (Ekins *et al.*, 1968, 1970a; Ekins, 1978; Jackson *et al.*, 1983; Dakubu *et al.*, 1984; Ekins, 1985). Nevertheless, some of the underlying concepts are still frequently misunderstood and merit brief discussion in the present context.

The concept of sensitivity

One major source of past confusion has been disagreement regarding the concept of 'sensitivity' itself, many authors equating assay sensitivity with the slope of the dose–response curve (Yalow and Berson, 1970a, b; Berson and Yalow, 1973; see also Ekins *et al.*, 1970b, Tait, 1970). It is now widely agreed that the notion that a steeper dose–response curve implies greater sensitivity is erroneous. The invalidity of this belief is clearly revealed by the fact that the relative magnitudes of the responses yielded by two assay systems is dependent on the particular variable which is chosen to represent the response (see Fig. 1(a))(Ekins, 1976). For this and other reasons, it has long been recognized that the 'sensitivity' of an assay can only be satisfactorily represented by its lower limit of detection (Fig. 1(b)), and this concept is now embodied in all internationally agreed definitions of the term. An essentially identical definition is as the precision (i.e. standard deviation) of measurement of zero dose, since this quantity determines the least quantity distinguishable from zero and hence the assay detection limit. The sensitivity of an assay is thus represented by the zero-dose intercept of the 'precision profile' (Fig. 2(a)) when the latter is expressed in terms of standard deviation rather than of coefficient of variation (Ekins, 1983a). In short, the more sensitive of two assays is the one yielding greater precision of the zero dose estimate (Fig. 2(b)).

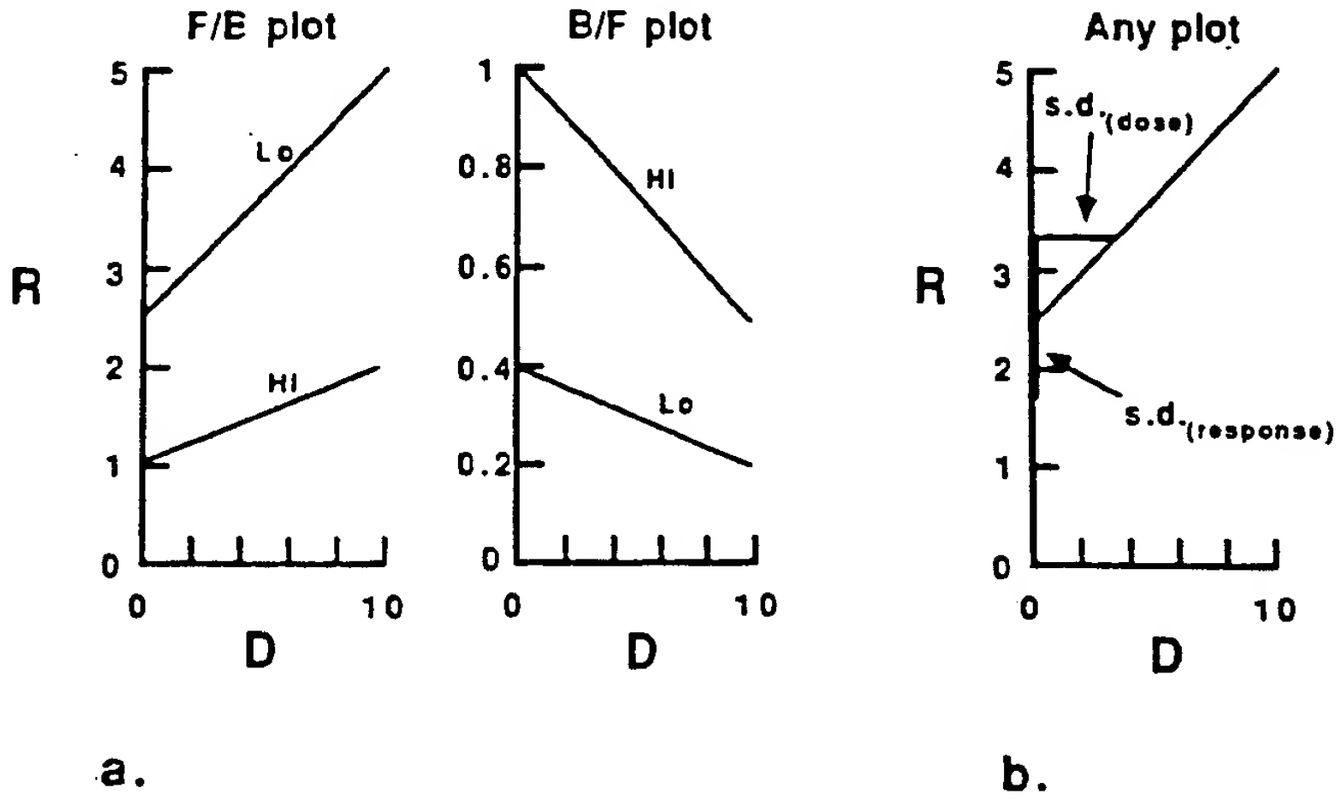

Figure 1. (a) Diagrammatic representation of conventional RIA dose–response curves for systems using high (hi) and low (lo) antibody concentrations plotted in terms of free-bound (F/B) and bound/free (B/F) labelled antigen. Note that the use of a lower amount of antibody yields a dose–response curve of greater slope in the F/B plot, but of lower slope in the B/F plot. It is impossible to decide, on the basis of the data shown in this figure, which concentration of antibody yields the assay system of higher sensitivity. (b) The sensitivity of an assay is essentially represented by the minimum detectable dose, i.e. the SD of the dose measurement ($SD_{(dose)}$) at zero dose. This is given by the SD of the response ($SD_{(response)}$) divided by the dose–response curve slope at zero dose (i.e. $(SD_{(response)}) \times dD/dR)_0$). This quantity is unaffected by the choice of the coordinate frame used to plot the dose–response curve. (Note: it is common to multiply $(SD_{(dose)})_0$ by an arbitrary factor to increase the confidence level attaching to the minimum detectable dose estimate, though, since no agreement exists regarding the value of this factor, this unnecessary step merely adds to confusion when the relative sensitivities of two assay procedures are compared.)

'Competitive' and 'non-competitive' ('limited reagent' and 'excess reagent') assays

A second important misconception in this area is the notion that immunoassays relying on the use of *labelled antibodies* (e.g. immunoradiometric assays, IRMA) are *ipso facto* more sensitive than those which rely on the use of *labelled 'analyte'* (e.g. radioimmunoassays, RIA); furthermore the grounds originally advanced for the claimed superiority of labelled antibody methods (Miles and Hales, 1968) were partially based on false concepts of sensitivity, and thus failed to identify the *true* reasons why certain assay designs are

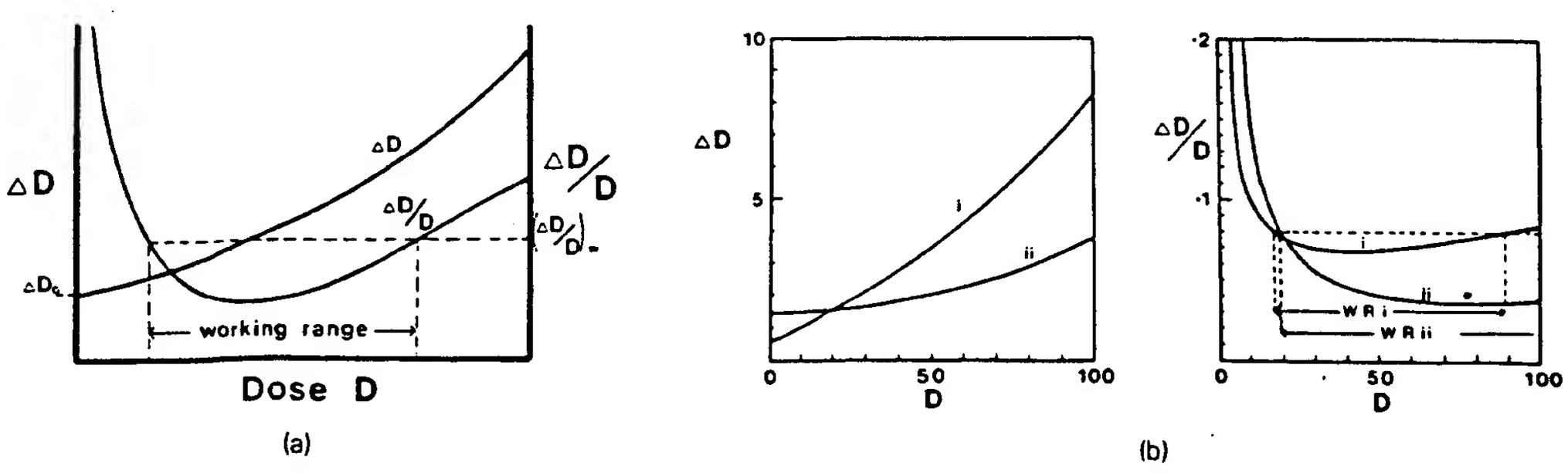

Figure 2. (a) The 'precision profile' of an assay portrays the error in the dose measurement as a function of dose. The error may be represented, *inter alia*, by the absolute error (ΔD; e.g. SD of D) or the relative error ($\Delta D/D$; e.g. CV of D). $(\Delta D)_0$, the error in the measurement of zero dose, represents the sensitivity of the assay. The working range may be defined as the range of dose values within which $\Delta D/D$ is less than an 'acceptable' value set by the investigator. (b) The more sensitive of the two assays (assay I) intercepts the ΔD axis at a lower value. However, assay II is more precise at higher values of dose, and has a wider working range.

potentially capable of yielding far higher sensitivity than others. This issue likewise merits clarification.

The purely pragmatic sub-classification of immunoassays into labelled antibody and labelled analyte methods diverts attention from a more fundamental divide in immunoassay methodology, which relates to the optimal concentration of antibody required in an assay system to maximize its sensitivity. In certain assay designs (which may be termed '*limited reagent*' or '*competitive*') the optimal concentration tends to zero; conversely in others (which may be termed '*excess reagent*' or '*non-competitive*') the concentration tends to infinity. It should be particularly emphasized that the optimal antibody concentration is essentially governed, not only by the physicochemical characteristics of the antibody–analyte binding reaction, but also by the errors incurred in measurement of the assay response. Were an assay system to be totally error-free, *no* antibody concentration would be optimal, and the distinction between competitive and non-competitive methodologies would thus not arise.

Though it is inappropriate in this presentation to discuss in detail the statistical and physicochemical theory underlying this fundamental divergence in immunoassay design (see Ekins *et al.*, 1968, 1970a; Jackson *et al.*, 1983), the reason for it can perhaps be more readily understood if the basic principles of immunoassay are portrayed in a somewhat different way from that in which they are usually presented. All immunoassays essentially depend upon measurement of the 'fractional occupancy' by analyte of antibody binding sites following reaction of analyte with antibody (see Fig. 3(a)). Those techniques which implicitly rely on measurement of residual, *unoccupied*, binding sites optimally necessitate the use of concentrations of antibody tending to zero, and may be termed 'competitive', conversely those in which *occupied* sites are directly measured necessitate use of high antibody concentrations and are termed 'non-competitive' (Fig. 3(b)). This emphasizes that the differences in assay design characterizing so-called competitive and non-competitive methods are essentially unrelated to which component (if any) of the reaction system is labelled. Indeed immunoassays in which *no label of any kind is involved* can, on identical grounds; be subdivided into those of 'limited reagent' (or 'competitive') and 'excess reagent' (or 'non-competititve') design. Thus the distinction between these two forms of immunoassay simply reflects differences in the way that fractional antibody occupancy is determined, and the fact that it is generally undesirable—for reasons of accuracy—to measure a *small* quantity by estimating the difference between two *large* quantities. When an immunoassay relies on the measurement of unoccupied antibody binding sites, the total amount of antibody used in the system must be small to minimize error in the resulting (indirect) estimate of occupied sites.

Figure 3. The distinction between 'non-competitive' (above) and 'competitive' immunoassays (below) reflects how antibody binding-site occupancy is measured. Labelled antibody methods are 'non-competitive' if occupied sites of the (labelled) antibody are measured, but are 'competitive' (below right) when *unoccupied* sites are measured. Labelled antigen (below left) or labelled anti-idiotypic antibody methods (below centre) rely on measurement of sites *unoccupied* by analyte, and are therefore invariably of 'competitive' design.

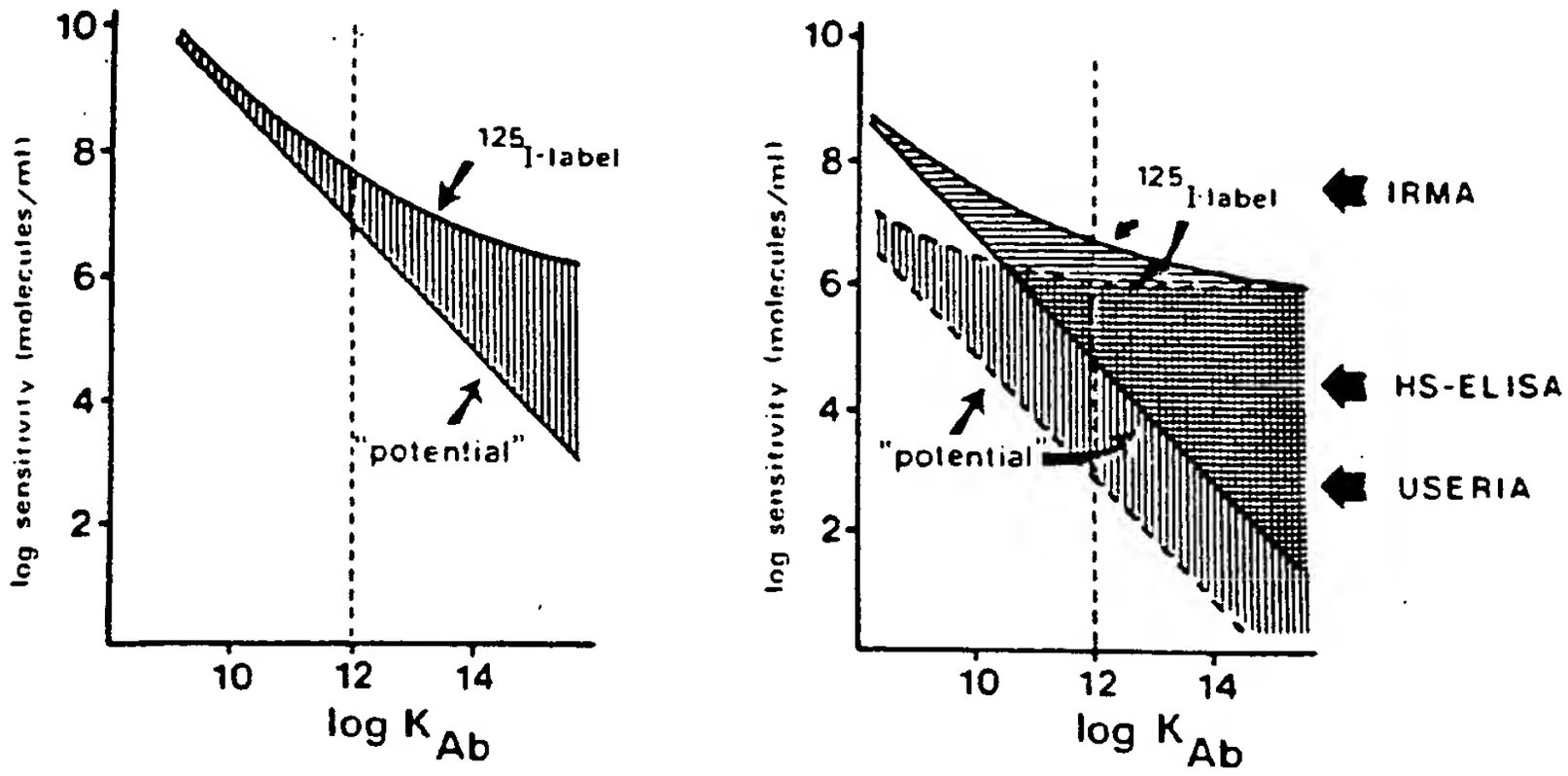

Figure 4. Curves showing the theoretically predicted relationship between antibody affinity and the sensitivities achievable using 'competitive' and 'non-competitive' assay strategies. The 'potential' sensitivity curves assume the use of infinite specific activity labels; the sensitivities achievable using ^{125}I-labelled antigen or antibody are also shown. Shaded areas indicate the sensitivity loss due to errors in measurement of the label. Curves relating to 'competitive' assays assume a 1% error in measurement of the response variable arising from 'experimental' errors (i.e. errors other than those inherent in label measurement *per se*). Non-competitive curves assume 'non-specific binding' of labelled antibody of 0.01% and 1% (lower and upper curves) respectively. Arrows indicate sensitivities claimed for typical non-competitive immunoassay methodologies.

Conversely, when occupied sites are measured *directly*, this particular constraint does not arise; indeed, considerable advantage often derives from using relatively large amounts of antibody in the system.

Sensitivity of 'competitive' and 'non-competitive' immunoassays

Competitive and non-competitive immunoassays differ significantly in many of their performance characteristics in consequence of the differences in optimal antibody concentration on which they rely. Most particularly they differ in their potential sensitivities. Figure 4. portrays the sensitivities predicted theoretically as a function of antibody binding affinity, making realistic assumptions regarding the experimental errors incurred in reagent manipulation, 'non-specific' binding of labelled antibody, etc., and assuming the use of optimal reagent concentrations (Ekins, 1985). Amongst other concepts illustrated in the figure is the much greater assay sensitivity *potentially* attainable (using an antibody of given affinity) by adoption of a non-competitive approach. In short, whereas the maximal sensitivity realistically achievable using a competitive design is in the order of 10^7 molecules/ml (using antibody of the highest affinity found in practice), a non-competitive method is capable of yielding sensitivities some orders of magnitude greater than this. However, Fig. 4 also demonstrates that, assuming the use of high affinity antibodies (i.e. $\sim 10^{11}$–10^{12} l/M), maximal sensitivities yielded by isotopically based techniques (whether relying on labelled antibody (IRMA) or labelled analyte (RIA), or whether of competitive or non-competitive design) are closely comparable, i.e. of the order of 10^7–10^8 molecules/ml.

This limitation is a manifestation of the fact that, in the case of the non-competitive methods, an important constraint on assay sensitivity is (under certain circumstances) the 'specific activity' of the label used. On the other hand, limitation of assay sensitivity due to the low specific activity of radioisotopic labels does *not* often arise, in practice, in the case of competitive assays, whose sensitivity is generally restricted by other factors (Ekins, 1985). The fundamental significance of this conclusion is that, only by the use of labels possessing specific activities higher than those of the commonly used radioisotopes *in assays of non-competitive design*, can current

sensitivity limits be breached. Conversely, use of a higher specific activity label in a *competitive* assay will usually have no significant effect on its sensitivity (assuming experimental errors incurred in reagent manipulation of the magnitude generally encountered in practice).

High specific activity non-isotopic labels

The term 'specific activity' is conventionally applied, in the case of radioisotopic labels, to denote the number of radioactive disintegrations per unit time per unit weight of the isotope or labelled compound. In the present context, use of the term is widened to signify 'detectable events' per unit time per unit weight of labelled material. Thus it can be used to indicate the rate of photon emission by a chemiluminescent or fluorescent label, or the rate of conversion of substrate molecules—by an enzyme label—to molecules of a detectable product. The importance of the concept derives from the fact that 'signal measurement error' (i.e. error in the measurement of the label *per se*) is a contributory factor in limiting assay sensitivity, and may—when other sensitivity-constraining factors are reduced—become dominant. Furthermore, when extending the sensitivities of immunoassay systems beyond their present limits, the numbers of molecules involved are low, and statistical errors incurred in counting individual 'detectable events', and the time required to count them, may assume a particular importance.

Table 1 compares the specific activities of potentially useful labels with that of ^{125}I. All are of relevance in the context of this volume since chemiluminescent and fluorescent labels can be used to label antibodies (or antigens) directly; alternatively, enzyme labels catalysing reactions yielding chemiluminescent signals or fluorescent products can be utilized.

Table 1. Relative specific activities of various isotopic and non-isotopic labels. Note that, though the specific activity of ^{125}I-labelled reagents does not, in practice, significantly limit the sensitivity of competitive assays (see Fig. 4), the lower specific activity of ^{3}H may severely restrict the sensitivity of competitive assays (e.g. of steroid hormones) which rely on the use of this particular radioisotope

Specific Activities	
^{125}I:	1 detectable event/sec/7.5 × 10^6 labelled molecules.
^{3}H:	1 detectable event/sec/5.6 × 10^8 labelled molecules.
Enzymes:	Determined by enzyme 'amplification factor' and detectability of reaction product.
Chemiluminescent labels	1 detectable event/labelled molecule.
Fluorescent labels:	Many detectable events/labelled molecule.

The importance of background in non-competitive immunoassays

A second important factor governing the sensitivity of non-competitive labelled-antibody immunoassays is the 'background' or 'blank' signal emitted in the absence of analyte, since error in the measurement of this signal is clearly a major determinant of the error in measurement of zero dose. Amongst contributors to the background signal are the 'noise' of the measuring instrument itself, 'ambient' signal generators (such as, in 'sandwich' immunoassays, solid 'capture-antibody' supports or, in the case of radioisotopic methods, cosmic ray and other extraneous radiation sources) and 'non-specifically bound' labelled antibody. Minimization of each of these components is essential for maximal sensitivity: mere arithmetic subtraction of background is of absolutely no benefit in this context.

Non-specific binding of antibody is of particular interest, since the magnitude of this contribution is dependent, *inter alia*, on the amount of labelled antibody used in the system, and the duration of its exposure to analyte. Thus increasing the amount of labelled antibody increases the amount of such antibody bound to analyte; however, it may also increase the non-specifically bound moiety to a greater proportional extent, and thus cause a net reduction in sensitivity. This effect underlies the loss in sensitivity at higher antibody concentrations depicted in Fig. 5 (reproduced from Jackson *et al.*, 1983). This phenomenon also underlies the relationship between sensitivity and the affinity constant of the labelled antibody depicted in Fig. 4. The possession by labelled antibody of a high affinity constant implies that a

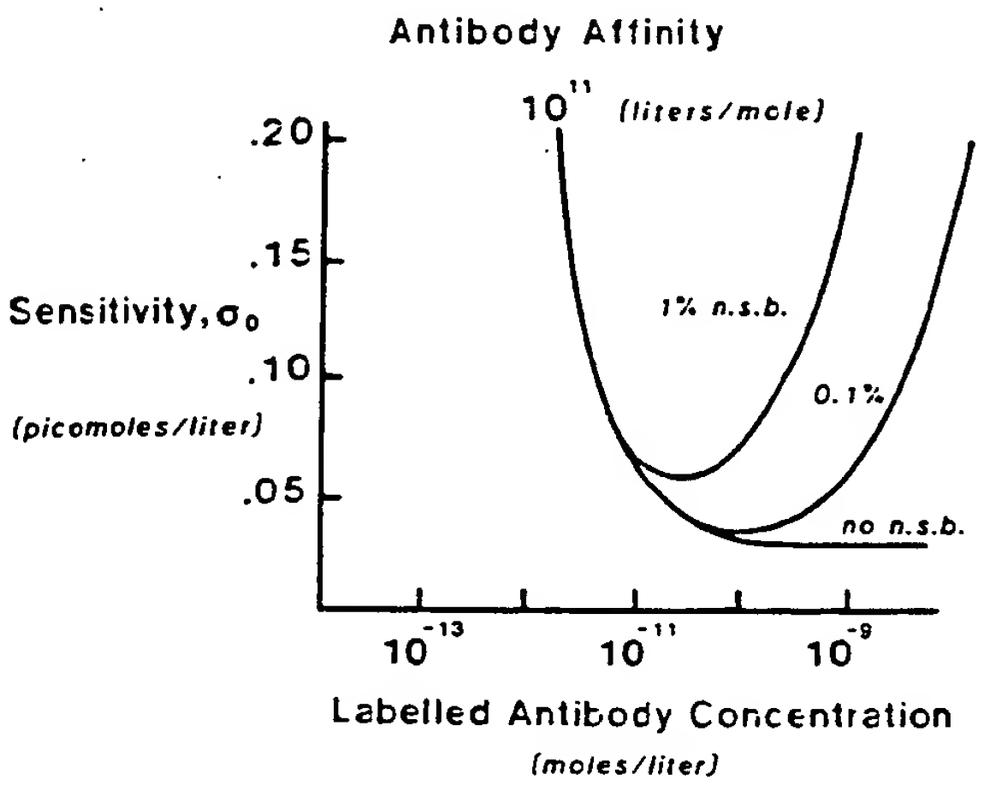

Figure 5. Assay sensitivity (represented by the standard deviation of the zero dose measurement, σ_0), plotted as a function of the concentration of labelled antibody (of affinity 10^{11} L/M) used in the assay, assuming different levels of non-specific binding of labelled antibody. (Note: an irreducible instrument background has been assumed in the computations represented; this limits the ultimate sensitivity attainable, regardless of the concentration of antibody used.)

lower concentration is required to yield the same level of analyte binding, albeit with reduced non-specific binding, thus increasing assay sensitivity

In summary, the high sensitivity of non-competitive labelled antibody methods derives essentially from their permitted use of optimal concentrations of antibody which (provided non-specific binding of labelled antibody is low) are generally considerably greater than in competitive methods, *not* from the fact that the antibody is labelled. Labelled antibody methods generally *fall* in sensitivity as the concentration of antibody is reduced towards zero, ultimately yielding a sensitivity theoretically identical to that of competitive methods (Rodbard and Weiss, 1973). (Paradoxically, early exponents of labelled antibody methods, whilst claiming them to be of higher sensitivity, also concluded that their sensitivity was *increased* by reduction in the amount of labelled antibody used (Woodhead *et al.*, 1971). This incorrect conclusion—based on observation of effects on the slope of the dose-response curve—exemplifies the many fallacies encountered in the immunoassay field stemming from confusion regarding the concept of sensitivity discussed above.) Finally it should be emphasized that maximization of the sensitivity of a non-competitive immunoassay generally implies the selection of reagent concentrations and other experimental conditions such that the [analyte signal/background] ratio (i.e. s/b) is maximized. However, this simple relationship disregards statistical considerations which arise when the numbers of detectable events are very low, and a more appropriate objective may, under these circumstances, be maximization of the ratio s^2/b (Loevinger and Berman, 1951).

Other performance characteristics of competitive and non-competitive immunoassays

Non-competitive designs also display a number of other advantages deriving from the relatively high antibody concentrations on which they generally rely. These include increased reaction speeds (and hence shorter incubation times), decreased vulnerability to certain environmental effects (which cause variations in binding affinity between antibody and analyte), reduced sensitivity-dependence on high antibody binding affinity, etc.

Nevertheless a price has to be paid for these benefits; this includes the greater tendency of a large amount of antibody to bind molecules differing from, but with structural resemblance to, the analyte itself, implying a loss of assay *specificity*. This effect generally necessitates the use, whenever possible, of an 'immunoextraction' procedure using a second 'capture' antibody (usually directed against a different binding site, or 'epitope') as shown in Fig. 3(b). This technique—the 'sandwich' or 'two-site' immunoassay (Wide, 1971)—thus potentially combines the twin virtues of ultra-high sensitivity and specificity (together with short reaction time), features of crucial importance in many diagnostic situations (for example, in the detection of AIDS viral antigens). (Note, however, that the loss of specificity inherent in non-competitive assay designs implies that they are less readily applicable to the measurement of analytes of small molecular size, which cannot be simultaneously bound by two different antibodies directed against different antigenic sites on the molecule. Such analytes are generally more appropriately measured using 'competitive' assay methods.)

Development of ultra-sensitive immunoassay methodologies

The perception that the development of 'ultra-sensitive' immunoassay systems (i.e. systems surpassing conventional RIA methods in sensitivity) depends on (a) reliance on 'excess reagent' or 'non-competitive' assay designs; (b) the use of non-isotopic labels displaying higher specific activities than commonly used radioisotopes; (c) the development of efficient separation systems (ensuring minimization of non-specific antibody binding, and hence of signal 'backgrounds'), and (d) dual or multi-antibody analyte-recognition systems (exemplified by 'sandwich' or two-site assays) to maintain/increase assay specificity, has formed the basis of our own laboratory's immunoassay development since the early to mid-1970s (Ekins, 1978). This led us, *inter alia*, to an immediate recognition (Ekins, 1979, 1980) of the importance of the *in vitro* techniques of monoclonal antibody production pioneered by Köhler and Milstein (1975), which are currently the subject of bitter patent disputes in the USA (Ezzell, 1986, 1987a,b), and which may be expected in Europe.

Meanwhile, of the candidate labels for use in this context, both chemiluminescent and fluorescent labels offer many attractions. The development of stable, highly chemiluminescent, acridinium esters by McCapra and his colleagues (McCapra *et al.*, 1977) has subsequently been exploited by Weeks *et al* (1983, 1984) and, more recently, by several commercial kit manufacturers; other workers have used more conventional chemiluminescent compounds to label immunoassay reagents (see, for example, Kohen *et al.*, 1984, 1985; Barnard *et al.*, 1985). Yet others have relied on enzyme labels to catalyse chemiluminogenic (Whitehead *et al.*, 1983) and fluorogenic (Shalev *et al.*, 1980) reactions as indicated above. Detailed description of these various methodologies is presented by others in this volume and need not be duplicated here.

Common to all the 'ultra-sensitive' immunoassay methodologies relying on such alternative labels is their dependence on a non-competitive, labelled antibody, assay strategy whenever appropriate; however, for the reasons indicated above, *competitive* methods continue to be generally employed for the measurement of analytes of small molecular size (e.g. therapeutic drugs, steroid and thyroid hormones, etc.). Nevertheless, the convenience (from a manufacturing viewpoint, and for other technical reasons) of relying on standard labelling procedures has meant that, even in these cases, labelled antibody techniques are increasingly preferred. Though the commercial kits based on these various labels differ to a minor extent in sensitivity, specificity, convenience, etc., such differences are at least partially attributable to differences in the physicochemical characteristics of the antibodies used in the kits, and to other 'immunological' factors unconnected with the particular nature of the label *per se*.

Despite the obvious attractions of chemiluminescent techniques in an immunoassay context, the use of fluorescent labels combined with sophisticated time-resolution techniques for their detection (a concept arising from discussions with J. F. Tait in 1970) appeared to us (in the mid-1970s) to offer more exciting long-term possibilities for a number of reasons. These naturally included attainment of the enhanced specific activities and high signal to background ratios required for ultra-sensitive immunoassay as indicated above. However, more importantly, fluorescence techniques also appeared to provide a simple route to the development of 'multi-analyte' assay systems of the kind described below.

In pursuance of this strategy, we began collaboration with LKB/Wallac, *ca* 1976–77, in the development of the instrumentation and technology required to develop such methods. Fortunately a group of fluorescent substances generally known as the lanthanide chelates (including, in particular, the chelates of europium, samarium and terbium facilitate such development, possessing prolonged fluorescence decay times (~10–1000 μs), large Stokes shift (~300 nm) and other desirable physical characteristics which permit the construction of relatively cheap instrumentation for their measurement (Marshall *et al.*, 1981; Hemmilä *et al.*, 1983). The fluorescent properties of the lanthanide chelates may be compared with those of a conventional fluorophor such as fluorescein which is characterized by a much smaller Stokes shift (~28 nm), and a fluorescent decay time and emission spectrum which imply that it is less readily distinguished from fluorescent substances present in blood (such as bilirubin) or in plastic sample holders. The unique fluorescence characteristics of the lanthanide chelates thus permit them to be

measured in the presence of a fluorescence background (deriving from extraneous sources) which, in practice, approaches zero. Fig. 6 illustrates the basic concepts involved in pulsed-light, time-resolved, fluorescence measurement, which form the basis of the DELFIA immunoassay system currently marketed by LKB/Wallac.

Though it is inappropriate to pursue this subject in greater detail, attention should also be drawn to the possibilities offered by phase-resolved fluorimetry. This permits separate identification of fluorophores differing in fluorescence lifetime by their exposure to a sinusoidally modulated exciting light source, and observation of their demodulated, phase-shifted, light emission (McGown and Bright, 1984). This technique offers the possibility both of the development of homogeneous assays (relying on a difference in fluorescence decay time of bound and free forms of the fluorescent-labelled molecule), and of discriminating between two labelled antibodies in the context of multi-analyte 'ratiometric' immunoassay as discussed below.

'AMBIENT ANALYTE' IMMUNOASSAY

Before proceeding to a discussion of the development of multi-analyte assays, another important concept, termed 'ambient analyte immunoassay' (Ekins, 1983b), must first be examined. This term is intended to describe a type of immunoassay system which, unlike unconventional methods, measures the analyte *concentration* in the medium to which an antibody is exposed, being essentially independent both of sample volume, and of the amount of antibody present. This concept is illustrated in Fig. 7, and relies on the physicochemically-based proposition that, when a 'vanishingly small' amount of antibody (preferably, but not essentially, coupled to a solid support) is exposed to an analyte-containing medium, the resulting (fractional) occupancy of antibody binding sites solely reflects the ambient analyte concentration. Clearly the binding by antibody of analyte results in a depletion of the amount of analyte in the surrounding medium, but provided the proportion so bound is small (i.e. less than, for example, 1% of the total), such disturbance can be ignored. (This effect is closely analogous to that caused by the introduction of a thermometer into a medium possessing a much larger thermal capacity; the temperature disturbance caused by the thermometer itself is negligible and can, in these circumstances, be disregarded.)

The principles of ambient analyte assay derive from the recognition that *all* immunoassays essentially depend upon measurement of the 'fractional occupancy' by analyte of antibody binding sites following reaction of analyte with antibody as discussed above (Figs 3. (a) and (b)). The fractional occupancy of ('monospecific' or 'monoclonal') antibody binding sites in the presence of varying analyte concentrations, plot-

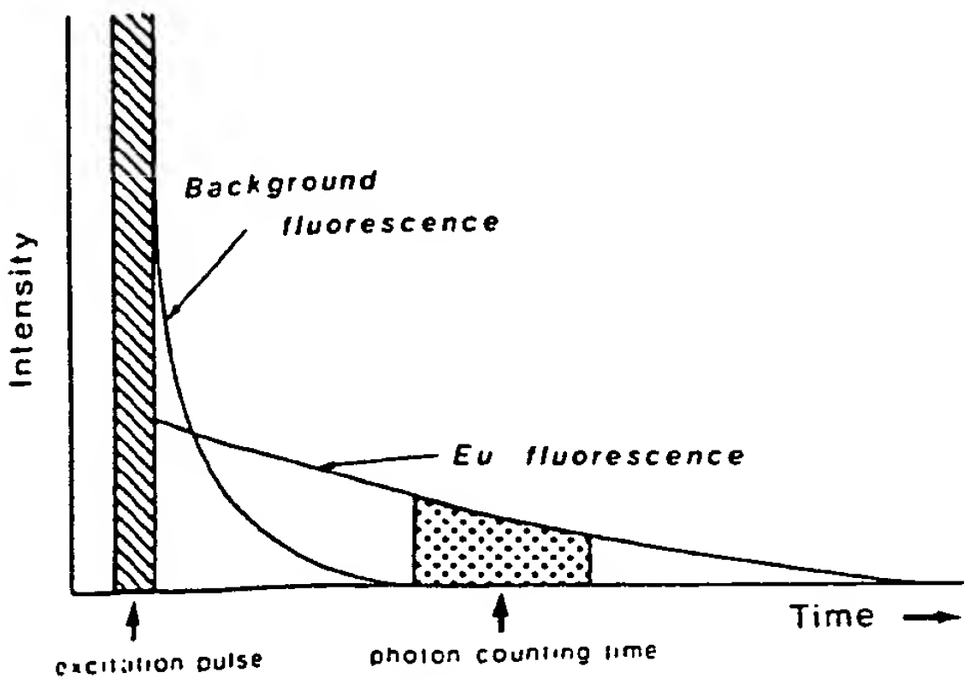

Figure 6. Basic principles of pulse-light, time resolved fluorescence. Fluorescence emitted by the fluorophor (typically a europium chelate) is distinguished from background fluorescence, which decays more rapidly.

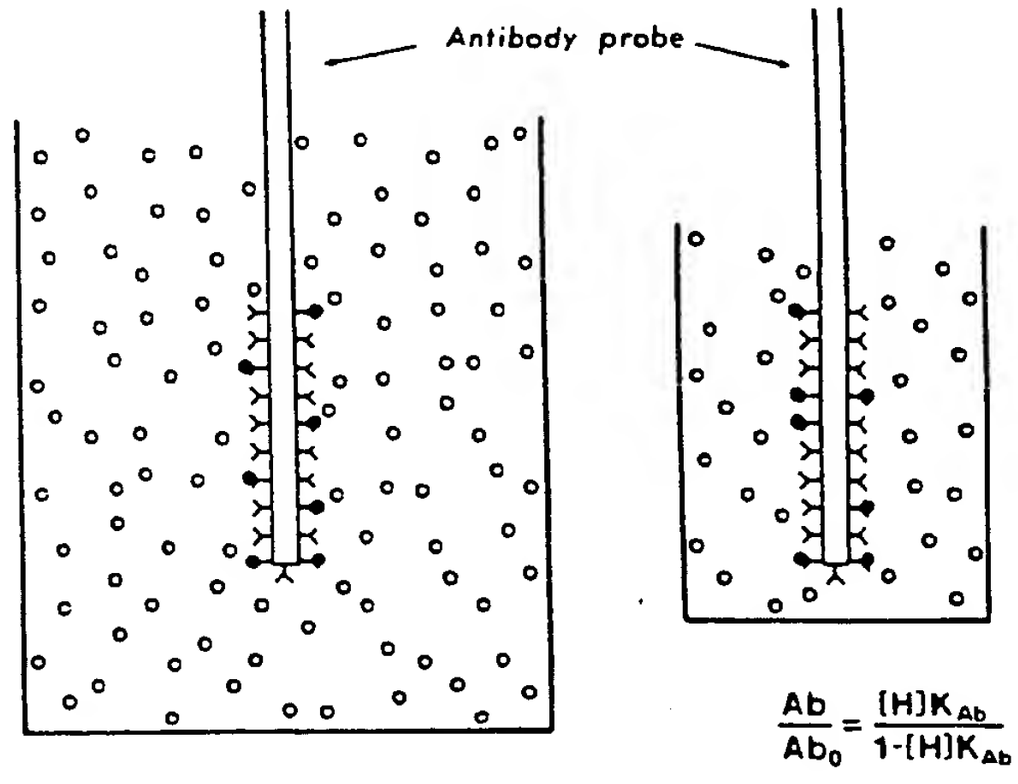

Figure 7. Basic principle of 'ambient analyte' immunoassay (AAI). The fractional occupancy (F) of a vanishingly small amount of antibody (of affinity K) is determined by the analyte concentration in the medium ([An]).

ted against antibody concentration, is portrayed in Fig. 8. The fraction of analyte bound is also plotted in this figure. (Note: for the sake of generality, all concentrations in this figure are expressed in terms of $1/K$, where K is the affinity constant of the antibody. For example, if $K = 10^{11}$ L/M, a concentration of $0.1 \times 1/K$ represents 0.1×10^{-11} M/L, or $0.1 \times 10^{-11} \times 10^{-3} \times 6.02 \times 10^{23} = 6.02 \times 10^{8}$ molecules/ml.)

It should be particularly noted that, at antibody concentrations of less than *ca* $0.01 \times 1/K$ antibody fractional occupancy is essentially dependent solely on the analyte concentration in the medium, and is independent of variations in antibody concentration. This reflects the fact that this concentration of antibody binds less than approximately 1% of the analyte in the medium, irrespective of its concentration. This implies, for example, that the introduction of 10, 100, or 1000 antibody molecules into a medium containing billions of analyte molecules will result, in each case, in virtually identical fractional antibody binding-site occupancy, the upper limit of antibody concentration being determined by the antibody affinity constant. (An antibody concentration of $0.01 \times 1/K$ is a hundred-fold less than that ($1 \times 1/K$) necessary to bind 50% of a 'trace' amount of analyte (see Fig. 8), claimed by Berson and Yalow (1973) as maximizing assay 'sensitivity' (i.e. the slope of the dose–response curve when expressed in terms of bound/free labelled analyte). This false conclusion has subsequently become incorporated into the mythology of radioimmunoassay design which, regrettably, a majority of kit manufacturers continue to accept.)

The ambient analyte assay concept was originally exploited in the original development of what has come to be known as 'two-step' free hormone immunoassay (Ekins *et al.*, 1980), but it is clear that it is of far wider application, and can, in particular, be utilized in the construction of immunosensors and immunoprobes. One such example is a probe for the measurement of salivary steroids that is currently being developed in our laboratory. Comprising a small antibody-coated plastic 'dipstick' comparable in size and shape to a clinical thermometer, this device is intended to permit the measurement of salivary steroid levels without requiring the collection of saliva. However, the concept also underlies our approach to multi-analyte immunoassay, also under development in our laboratory.

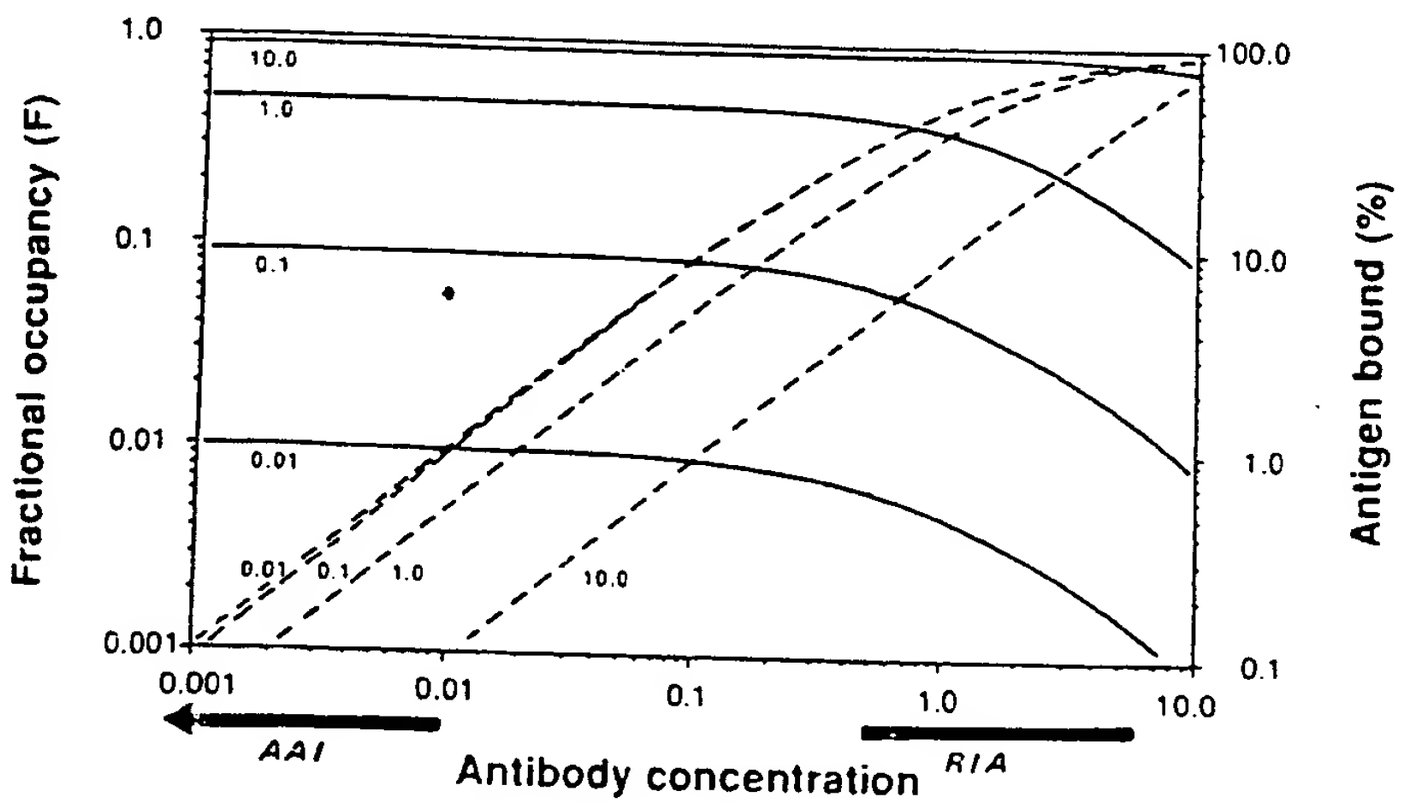

Figure 8. Fractional antibody binding-site occupancy (F) plotted as a function of antibody binding-site concentration for different values of analyte (antigen) concentration [An]. The percentage binding of analyte to antibody (b) is also shown. All concentrations are expressed in units of $1/K$. Note that for antibody concentrations of less than $0.01/K$ (approximately), percentage binding of analyte is <1%, and fractional binding-site occupancy is essentially unaffected by variations in antibody concentration extending over several orders of magnitude, being governed solely by [An]. Note that radioimmunoassays and other 'competitive' immunoassays are commonly designed using antibody concentrations approximately $0.5/K$–$1/K$ or above (implying $b_0 > 30\%$), in accordance with the precepts of Berson and Yalow (e.g. Berson and Yalow, 1973).

MULTI-ANALYTE 'RATIOMETRIC' IMMUNOASSAY SYSTEMS

The concepts relating to ambient analyte immunoassay and assay sensitivity outlined above are both exploited in our present development of a random access, multi-analyte, immunoassay technology capable of measuring, in the same small sample, virtually any number of individual analytes from selected analyte 'menus' (e.g. a hormone menu, viral antigen menu, an allergen menu, etc.). Many examples of a need to measure a multiplicity of different analytes in the same sample exist in medical diagnosis, for example, in the routine diagnosis of thyroid disease, where it is frequently necessary to measure a number of different hormones and thyroid-related proteins. At present, clinicians frequently experience difficulty in deciding on the best sequence of tests to arrive at a correct diagnosis. Such problems would be overcome were all relevant analytes measurable at a cost comparable to the cost of measurement of a single substance. Our own immediate objective is the development of a technology permitting the measurement of complete 'hormone profiles' using a single small blood sample. However, the need for 'multi-analyte', or 'random access' measurement is not confined to medical diagnosis: it also arises, for example, in the pharmaceutical industry (where there exists a requirement to ensure the purity of protein drugs synthesized by recombinant DNA techniques), in the food industry and elsewhere. Though still at an early stage, our approach to the achievement of this objective can be briefly indicated.

Multi-analyte assay: general principles

As discussed above, the notion of ambient analyte assay simultaneously introduces two extremely important and novel concepts: (a) that an estimate of analyte concentration can be based upon the use of an infinitesimal amount of 'sampling' antibody, and (b) that such an estimate derives from a direct measurement of fractional antibody occupancy by analyte, irrespective of the exact amount of antibody used. It should be emphasized that the latter proposition is valid only in the context of ambient analyte assay, and is *not* true in current conventional immunoassay systems (in which fractional antibody occupancy depends both upon the amount of antibody in the system, and sample volume—see Fig. 8). In short, exposure of a small number of antibody molecules (in the form, for example, of a 'microspot' located on a solid support) to an analyte-containing fluid results in occupancy of antibody binding sites in the microspot reflecting the analyte concentration in the medium. Following such exposure, the antibody-bearing probe may be removed and exposed to a 'developing' solution containing a high concentration of an appropriate second antibody directed against either a second epitope on the analyte molecule if this is large (i.e. the occupied site), or against unoccupied antibody binding sites in the case of small analyte molecules (see Fig. 3(b)). (Note: an antibody simulating antigen, and reacting with unoccupied binding sites, is described as a 'mirror-image anti-idiotypic antibody'; the use of such an antibody instead of labelled antigen is convenient but not essential, and is suggested here merely to simplify illustration of the basic concepts involved.)

Subsequently, an estimate of binding-site occupancy of the 'sampling' (solid phase) antibody located in the microspot may be derived by measurement of the ratio of signals emitted by the two antibodies forming the dual-antibody 'couplets'. This can be conveniently achieved by labelling the 'sampling' and 'developing' antibodies with different labels, for example, a pair of radioactive, enzyme or chemiluminescent markers. Fluorescent labels are nevertheless particularly useful in this context because, by the use of optical scanning techniques, they permit arrays of different antibody 'microspots' distributed over a surface, each directed against a different analyte, to be individually examined, thus enabling multiple assays to be simultaneously carried out on the same small sample. Fig. 9 illustrates these basic ideas, and Fig. 10 such an array.

Microspot immunoassay sensitivity: theoretical considerations

The notion that it is, in principle, possible to measure an analyte concentration using a microspot of antibody comprising a number of antibody molecules in the range *ca* 10^1–10^6 is likely, at first sight, to appear surprising, and may, indeed, provoke scepticism regarding the assay sensitivities potentially attainable using this approach. Clearly a number of factors, such as the sensitivity

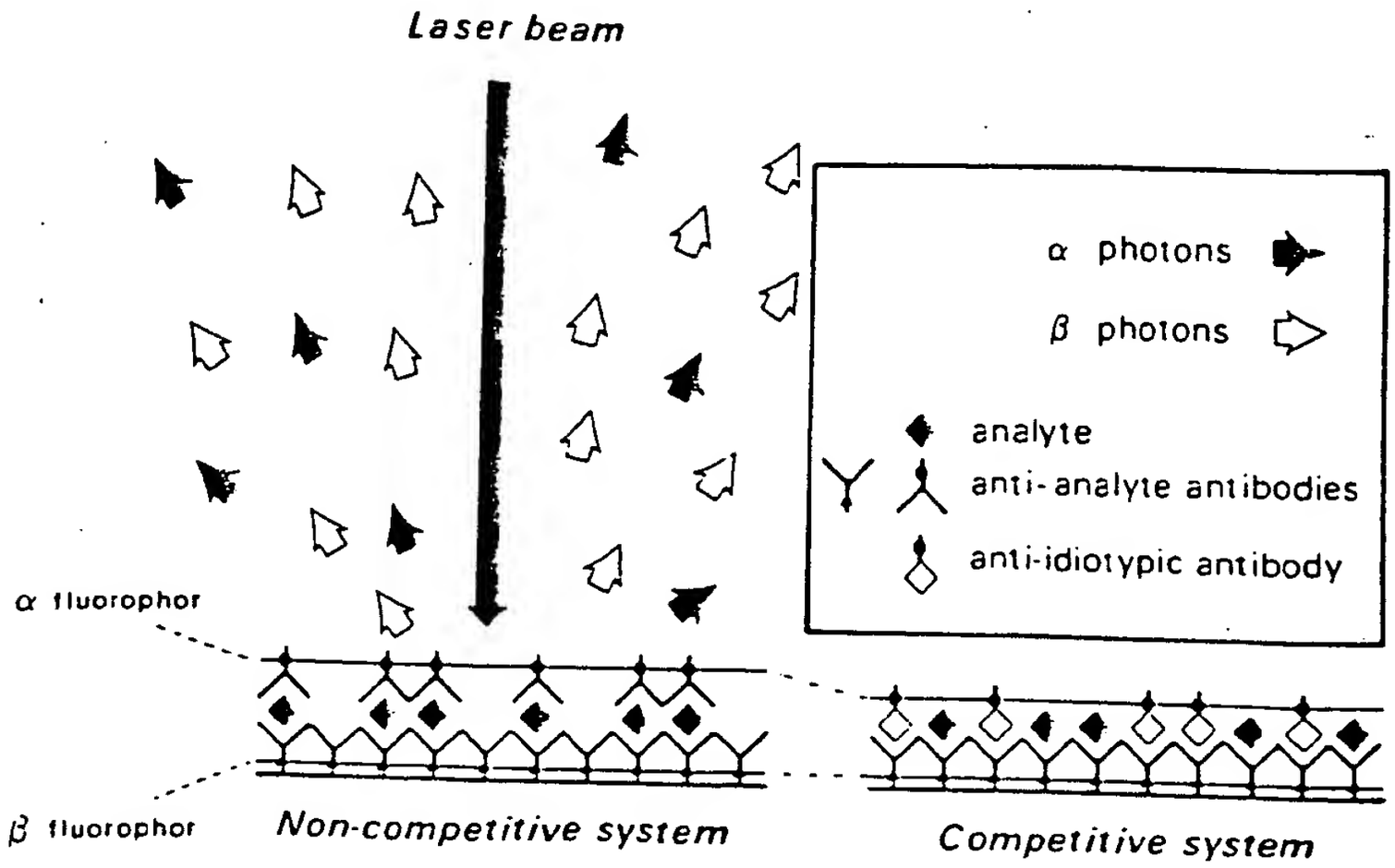

Figure 9. Basic principle of dual-label, ambient-analyte, immunoassay relying on fluorescent labelled antibodies. The ratio of α and β fluorescent photons emitted reflects the value of F (see Figs 5 and 6) and is solely dependent on the analyte concentration to which the probe has been exposed. It is unaffected by the amount or distribution of antibody coated (as a monomolecular layer) on the probe surface.

of the signal measuring equipment, the density of antibody molecules on the surface of the solid support, etc., are likely to play a part in determining final assay sensitivity. Such factors are, in turn, dependent on the efficiency with which the particular labels used can be detected, the adsorption properties of antibody supports, etc. Though these are obviously variable, reasonable estimates can be made of the order of sensitivities likely to be achieved on the basis of some simple theoretical calculations. To clarify the following discussion, it is assumed that 'sensing' antibody can be uniformly and consistently coated on a solid matrix at a standard density, implying that only the 'developing' antibody need be labelled and measured in order to ascertain fractional occupancy of sensing antibody binding sites.

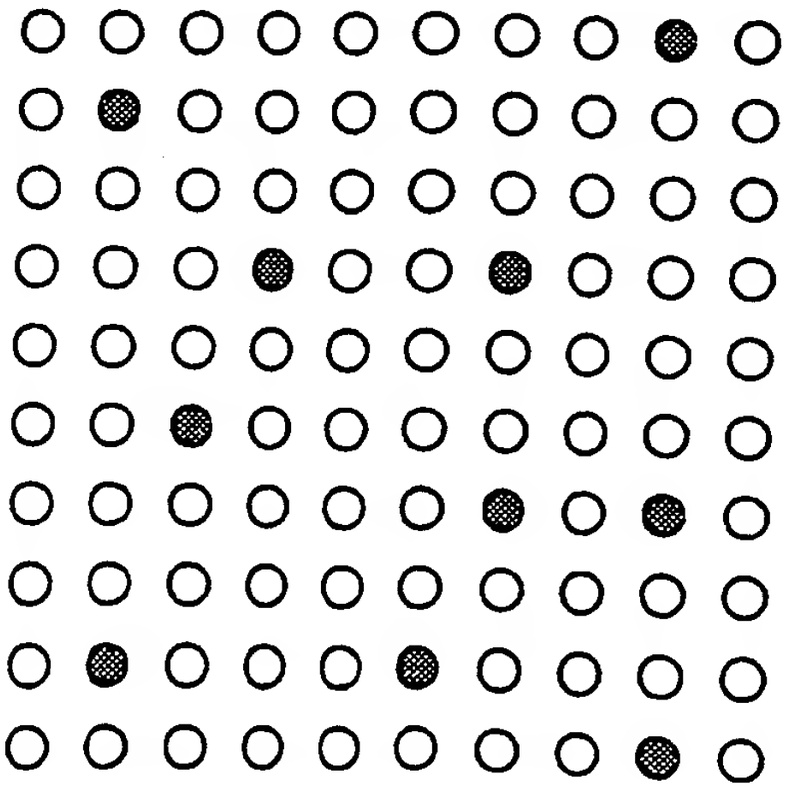

Figure 10. 'Multi-analyte' antibody array. Each antibody 'microspot' represents a 'vanishingly small' amount of antibody directed against an individual analyte.

Fig. 11 illustrates the surface of an antibody microspot, of surface area $A(\mu m^2)$, and (uniformly) coated with antibody of affinity K(L/M) in a monomolecular layer of density D(molecules/μm^2). Let us assume that the spot is exposed to an analyte-containing medium of volume v(ml), and containing an analyte concentration C molecules/ml. The molecular concentration of antibody in the system is thus given by AD/v. (Note: the fact that antibody is situated on the surface of a solid support, and not evenly distributed throughout the medium, does not affect the extent of analyte binding at thermodynamic equilibrium, assuming that antibody binding sites are not impeded in their reactions and have not been damaged during the coating process.)

Meanwhile, fractional occupancy (F) of antibody binding sites by analyte (at equilibrium) is

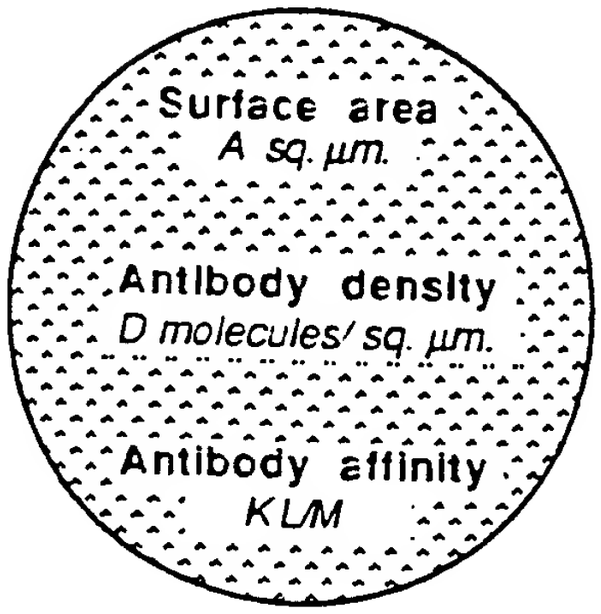

Avogadro's number:
N molecules/M

Figure 11. Microspot ambient-analyte immunoassay. The microspot shown is assumed to be uniformly coated with antibody, though if the dual-labelled antibody 'ratiometric' approach shown in Fig. 9 is adopted, uniform coating is not essential. The minimum fluid volume for ambient analyte assay conditions to prevail (enabling adoption of the ratiometric approach) is shown. Minimum test sample volume (M/S): $A \times D \times K \times 10^5/N$

given by the equation:

$$F^2 - F(1/q + p/q + 1) + p/q = 0 \qquad (1)$$

where p = analyte concentration, q = antibody concentration (both expressed in units of $1/K$).

Thus, for antibody binding site concentrations $\rightarrow 0$ (i.e. $q < 0.01$), $F \approx p/(1 + p)$; (see Fig. 8).

Likewise, the fraction of analyte bound by antibody (f) at equilibrium is given by the equation:

$$f^2 - f(1/p + q/p + 1) + q/p = 0 \qquad (2)$$

Thus, for analyte concentration $\rightarrow 0$ (i.e. $p < 0.01$), $f \approx q/(1 + q)$; (see Fig. 8). Furthermore, when $q < 0.01$, and when $p \geqslant 0$, $f < 0.01$.

Expressed in units of $1/K$; the concentration (q) in the assay of 'sensing' antibody situated on the microspot is given by $DAK/(\nu \times 6 \times 10^{20})$, (since Avogadro's constant, expressed as the number of molecules/mmol, is 6×10^{20} (approximately)). The fraction of an analyte concentration $\rightarrow 0$ which will be bound to the spot is therefore $DAK/(\nu \times 6 \times 10^{20} + DAK)$, implying that the number of analyte molecules bound to the spot is given by $\nu CDAK/(\nu \times 6 \times 10^{20} + DAK)$.

Case 1: sandwich (two-site) assay. Following incubation of sample with antibody, we assume the sample is removed, and the microspot then exposed to a volume V(ml) of a solution of a second, labelled, 'developing' antibody of affinity K^* (L/M) at a concentration given by Q (expressed in units of $1/K^*$).

The fraction of analyte bound by labelled antibody (F^*) at equilibrium is given by the equation:

$$F^{*2} - F^*(1/P + Q/P + 1) + Q/P = 0 \qquad (3)$$

where P represents the analyte concentration in the developing-antibody solution, expressed in units of $1/K^*$, i.e. $\nu CDAKK^*/[(\nu \times 6 \times 10^{20} + DAK)V \times 6 \times 10^{20}]$.

Assuming $P < 0.01$, $F^* \approx Q/(1 + Q)$. (For example, if $Q = 1$, the fraction of analyte molecules bound by labelled antibody = 0.5 approximately). Thus, since the number of analyte molecules bound to the spot is given by $\nu CDAK/(\nu \times 6 \times 10^{20} + DAK)$, the number of analyte molecules labelled by the second, developing, antibody is given by $\nu CDAKQ/[(\nu \times 6 \times 10^{20} + DAK)(1 + Q)]$, and the surface density of such molecules is given by $\nu CDKQ/[(\nu \times 6 \times 10^{20} + DAK)(1 + Q)]$. Moreover, assuming that $DAK \ll \nu \times 6 \times 10^{20}$ (i.e. that the amount of antibody in the system is such that 'ambient assay' conditions prevail, then the surface density (D^*) of developing-antibody molecules = $CDKQ/[(6 \times 10^{20})(1 + Q)]$ approximately. It should be noted that D^* is independent of both ν and V, also that the ratio $D^*/D = C \times KQ/[(6 \times 10^{20})(1 + Q)] = C \times$ constant.

If the minimum detectable surface density of developing-antibody molecules (i.e. σ_{D0}^*, the standard deviation of the measurement of D^* when $C = 0$) is given by D^*_{min} (molecules/μm^2) and C_{min} represents the minimum detectable analyte concentration in the test sample, then,

disregarding non-specific binding of developing antibody within the microspot area,

$$C_{min} = D^*_{min} \times [(6 \times 10^{20})(1 + Q)]/DKQ \quad (4)$$

For example, if $Q = 1$, $D = 10^5$ molecules/μm^2, $K = 10^{11}$ L/M and $D^*_{min} = 20$ molecules/μm^2, then $C_{min} = 2.4 \times 10^6$ molecules/ml $= 10^{-15}$ M/L. It should be noted, in this example, the fractional occupancy of the sensing antibody binding sites by the minimum detectable analyte concentration is 0.04%.

Case 2: anti-idiotypic antibody ('competitive') assay. In this case, we assume that, following removal of the sample, the microspot is exposed to a volume V(ml) of a solution of (for example) a second, labelled, anti-idiotypic antibody reacting with *unoccupied* sites on the sensing antibody. Using similar reasoning as above, we may likewise assume that the fraction of such sites which become occupied by the anti-idiotypic 'developing' antibody is given by $Q/(1 + Q)$, where Q is the developing-antibody concentration. However, the minimum detectable surface density of anti-idiotypic antibody is not, in a competitive design, the critical determinant of assay sensitivity; this parameter is essentially governed by the precision of the density measurement.

From Eq. (1), the fraction of sites *unoccupied* by analyte $= 1/(1 + p)$, and the fraction occupied by anti-idiotypic antibody $= Q/(1 + p)(1 + Q)$. Thus, if the CV in the measurement of anti-idiotypic antibody is ε, the standard deviation is $\varepsilon Q/(1 + p)(1 + Q)$. This term also represents the SD in the estimate of the fraction of sites *occupied* by analyte. Since the total number of antibody binding sites in the spot is DA, the SD in the estimate of occupied sites as $p \rightarrow 0$ (i.e. σD^*_0) approximates $\varepsilon DAQ/(1 + Q)$; the SD in the occupied site surface-density estimate is thus $\varepsilon DQ/(1 + Q)$. But the SD in the measurement of fractional binding-site occupancy when $p \rightarrow 0$ defines D_{min}, and hence the minimum detectable analyte concentration in the test sample as indicated in Eq (4).

Thus

$$C_{min} = D_{min} \times [(6 \times 10^{20})(1 + Q)]/DKQ \quad (5)$$

$$= \varepsilon DQ/(1 + Q) \pm [(6 \times 10^{20})(1 + Q)]\, DKQ \quad (6)$$

$$= \varepsilon/K \times (6 \times 10^{20}) \quad (7)$$

For example, if values of $Q = 1$, $D = 10^5$ molecules/μm^2, and $K = 10^{11}$ L/M are assumed as in the non-competitive example considered above, and the CV in the measurement of anti-idiotypic antibody density in the microspot is 1% (i.e. $\varepsilon = 0.01$), then $D_{min} = 500$ molecules/μm^2, and $C_{min} = 6 \times 10^7$ molecules/ml $= 10^{-13}$ M/L. Fractional occupancy of the sensing antibody binding sites by the minimum detectable analyte concentration is, in this example, 1%. It should be noted that the sensitivity limit of ε/K (expressed in molar terms) is identical to that previously established for conventional 'competitive' assays (Ekins and Newman, 1970), and which underlies the predictions represented in Fig. 4.

Such considerations appear to suggest (a) that microspot assay sensitivities superior to those obtainable by conventional radioisotopically based immunoassays are achievable, and (b) that sensitivities yielded by non-competitive microspot assays are likely to be considerably greater than those of corresponding competitive microspot assays. It must be emphasized, however, that, though such predictions are likely to prove correct, assumptions regarding the performance of the labels and signal-measuring instrument used are incorporated in the simple theoretical analysis discussed above. Such factors are clearly of importance in determining overall microspot immunoassay performance.

Practical implementation

The concepts discussed above are clearly exploitable using a variety of antibody labels, including chemiluminescent labels; however, our preliminary studies have been based on the use of conventional fluorophores, since the technology of simultaneous measurement of dual fluorescence from small areas is already well established. Because this volume centres on chemiluminescence, we shall provide only a brief indication of our initial experimental work in this area, which is currently based on the use of commercially available confocal microscopes.

Instrumentation: the laser scanning confocal microscope. In laser scanning confocal fluoresc-

ence microscopy, a small area of the specimen is illuminated by a focused laser beam; the fluorescence photons emanating solely from this area are, in turn, focused onto a photon detector. Both the intensity of illumination and the efficiency of light collection diminish rapidly with distance from the focal plane (Fig. 12). At the 'confocal' point, the projection of the illumination pinhole and the back-projection of the detector pinhole coincide. Such systems contrast with conventional epi-fluorescence methods, where the specimen is exposed to an essentially uniform flux of illumination (White *et al.*, 1987).

Sensitivity of current instruments. Typically, fluorescence photons emanating from the laser-illuminated area are detected by a low dark-current photomultiplier. Electrons spontaneously emitted by the photomultiplier photocathode contribute to the background signal of the instrument, and must, for highest sensitivity, be minimized. Fortunately the overall design of such instruments permits the photomultiplier photocathode to be of very small area, so that this particular source of background noise is not only small, but can be expected to reduce in relative importance with future improvement in photomultiplier design. Meanwhile current instruments already display very high sensitivity of detection of fluorescent signals. For example, the confocal microscope manufactured by Zeiss is claimed to display a lower detection limit for fluorescein of about ten molecules/μm^2 (Ploem, 1986). Most commercially available FITC-labelled IgG attains a fluorophore/protein molar ratio of ~4; thus the detection limit (D^*_{min}) of the Zeiss microscope is ~2–3 FITC-labelled IgG molecules/μm^2. This implies an analyte-concentration detection limit of ~2.4×10^5 molecules/ml for a two-site assay, assuming the same parameter values as used in the examples discussed above, or 2.4×10^4 molecules/ml using a 'sensing' antibody of affinity 10^{12} L/M.

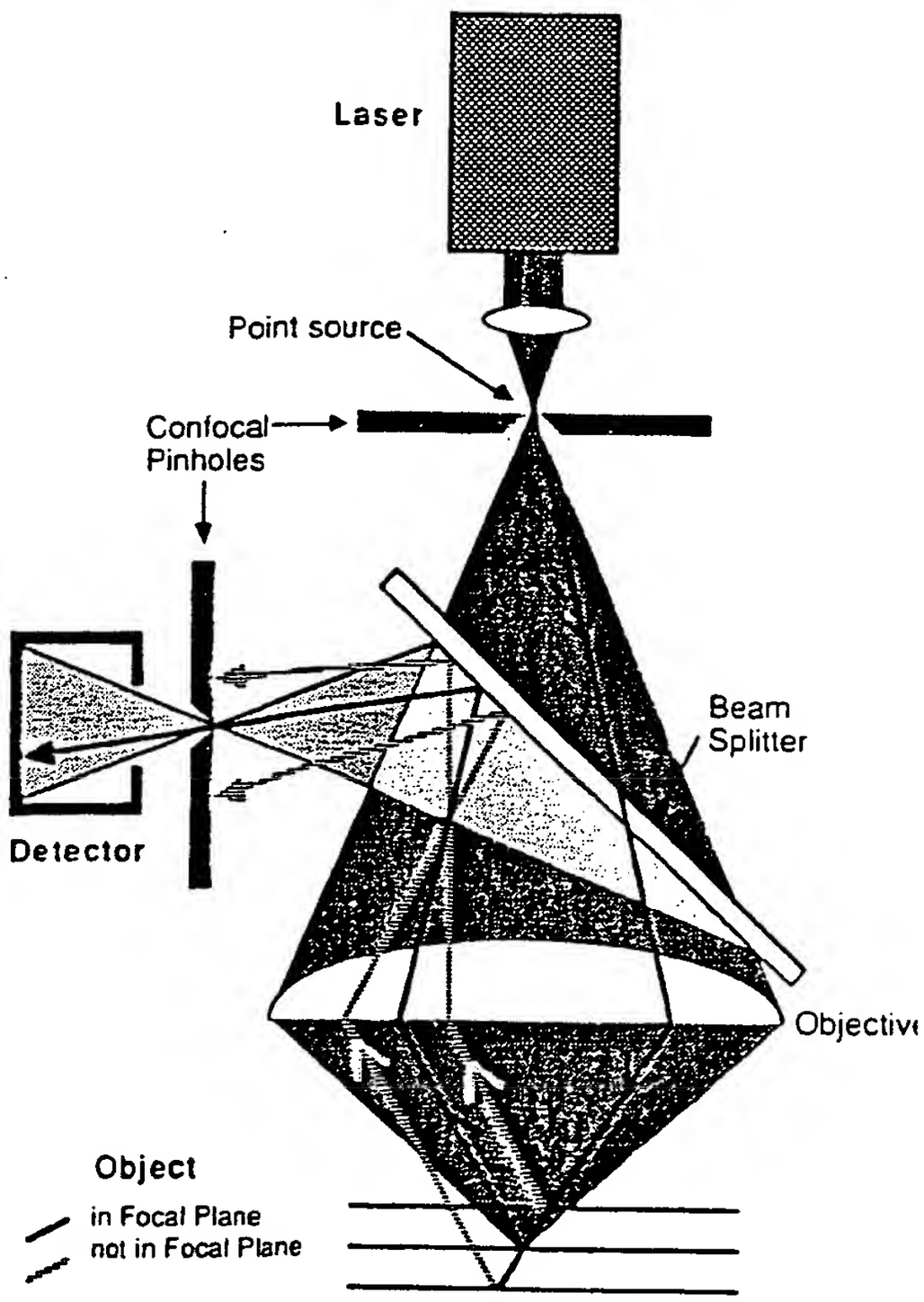

Figure 12. Principle of the confocal microscope. Illuminating light is focused at a point in the focal plane. Reflected light from this point is focused onto a detector. A complete two-dimensional image of structures within the focal plane is obtained by scanning the selected area of interest, and may be stored in a microcomputer for video display

Another comparable instrument is the Bio-Rad/Lasersharp laser scanning confocal microscope, which we are currently using in the development of 'ratiometric' multi-analyte assay methodology in accordance with the principles outlined above (see Fig. 13). The argon laser in this system possesses two excitation lines at 488 and 514 nm. It is thus particularly efficient for the excitation of blue/green emitting fluorophores such as FITC (which displays an excitation maximum at 492 nm). However, it is considerably less efficient in the excitation of red-emitting fluorophores such as Texas red (excitation maximum 596 nm). However, the ratiometric immunoassay principle permits considerable variation in detection efficiencies of the two labels relied on since, *inter alia*, the specific activities of the two labelled antibody species forming the antibody couplets can be chosen to yield optimal signal ratios in the region of unity. Thus inefficiency of the argon laser in exciting red emitting fluorophores is not necessarily a major handicap in the present context.

Though the current Lasersharp instrument relies on a conventional microscope rather than a purpose-designed optical system (and appears to

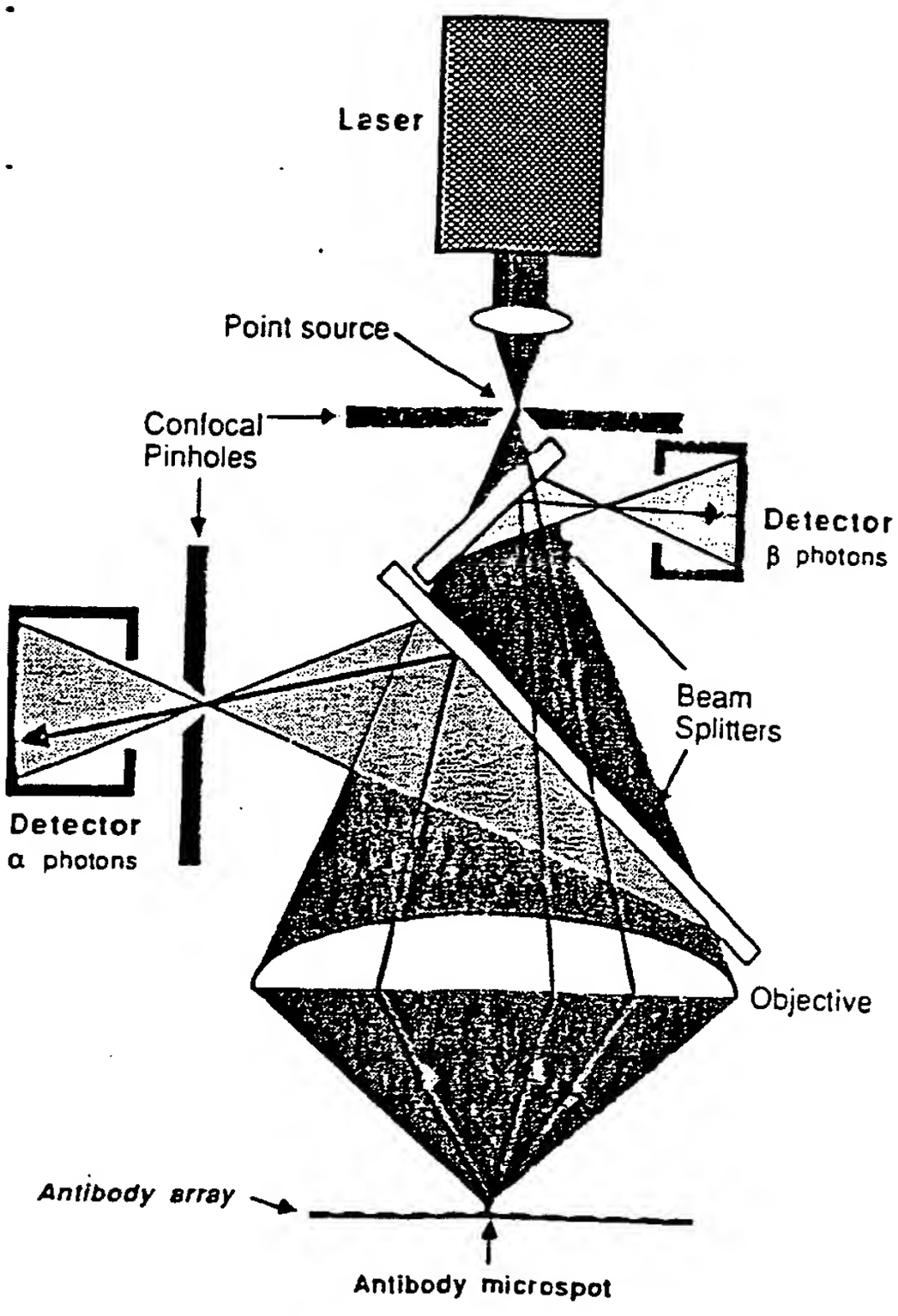

Figure 13. Dual-channel confocal fluorescence microscope permitting simultaneous measurement of the fluorescence signals from two fluorophors situated at the focal point. By scanning the antibody array, the ratio of signals from each antibody microspot may be determined

be less sensitive), it permits quantification of fluorescence signals generated from microspots of selected area. Initial studies have revealed that, under conditions that are not necessarily optimal, the instrument is capable of detecting approximately twenty-five FITC-labelled IgG molecules/μm^2, scanning an area of $\sim 50\,\mu m^2$ (Fig. 14). It must be stressed that neither of these confocal microscopes are designed specifically for routine ratiometric multi-analyte immunoassay use, and it can be anticipated that future instruments constructed specifically for this purpose are likely to prove both cheaper and more sensitive.

Other instruments. The MPM 200 Microscope Photometer manufactured by Zeiss of West Germany is anticipated to become available shortly. This photometer is claimed to be highly versatile: it can be used in transmission and reflection modes, and as a highly sensitive fluorimeter. The measuring field can be varied in shape and size for optimum adjustment to the specimen structure. More generally, the technology of sensitive light measurement is improving rapidly in response to needs in astronomy, the space program etc., such technology clearly being readily exploitable in a multi-analyte immunoassay context using light-generating labels in accordance with the broad principles presented here.

Solid antibody supports. On the basis of the theoretical considerations discussed above, it is evident that solid antibody supports for multi-analyte immunoassay use should display a capacity to adsorb a high surface density of antibody combined with low intrinsic signal-generating properties (for example, low intrinsic fluorescence), thus minimizing background. We have examined a number of materials, including polypropylene, Teflon, cellulose and nitrocellulose membranes and microtitre plates (clear polystyrene plates from Nunc; black, white and clear polystyrene plates from Dynatech with these criteria in mind. White Dynatech Microfluor microtitre plates, formulated specially for the detection of low fluorescence signals, yield high signal-to-noise ratios and have therefore been provisionally used in our developmental studies.

Surface density of antibody coating. Preliminary experiments using Microfluor plates have revealed that it is possible to coat them with antibody at a surface density of at least 5×10^4 IgG molecules/μm^2 (Fig. 15). Moreover nearly all antibody molecules so deposited appear to retain immunological activity (Fig. 16).

Verification of the 'ratiometric' imunoassay concept. Our primary intention, in initial studies, has been establishment of the basic conditions which, using a particular instrument, can be anticipated on theoretical grounds to yield high assay sensitivity. Though the setting up of individual microspot immunoassays has thus appeared to us to be of secondary importance during the initial stages of our studies, we have nevertheless

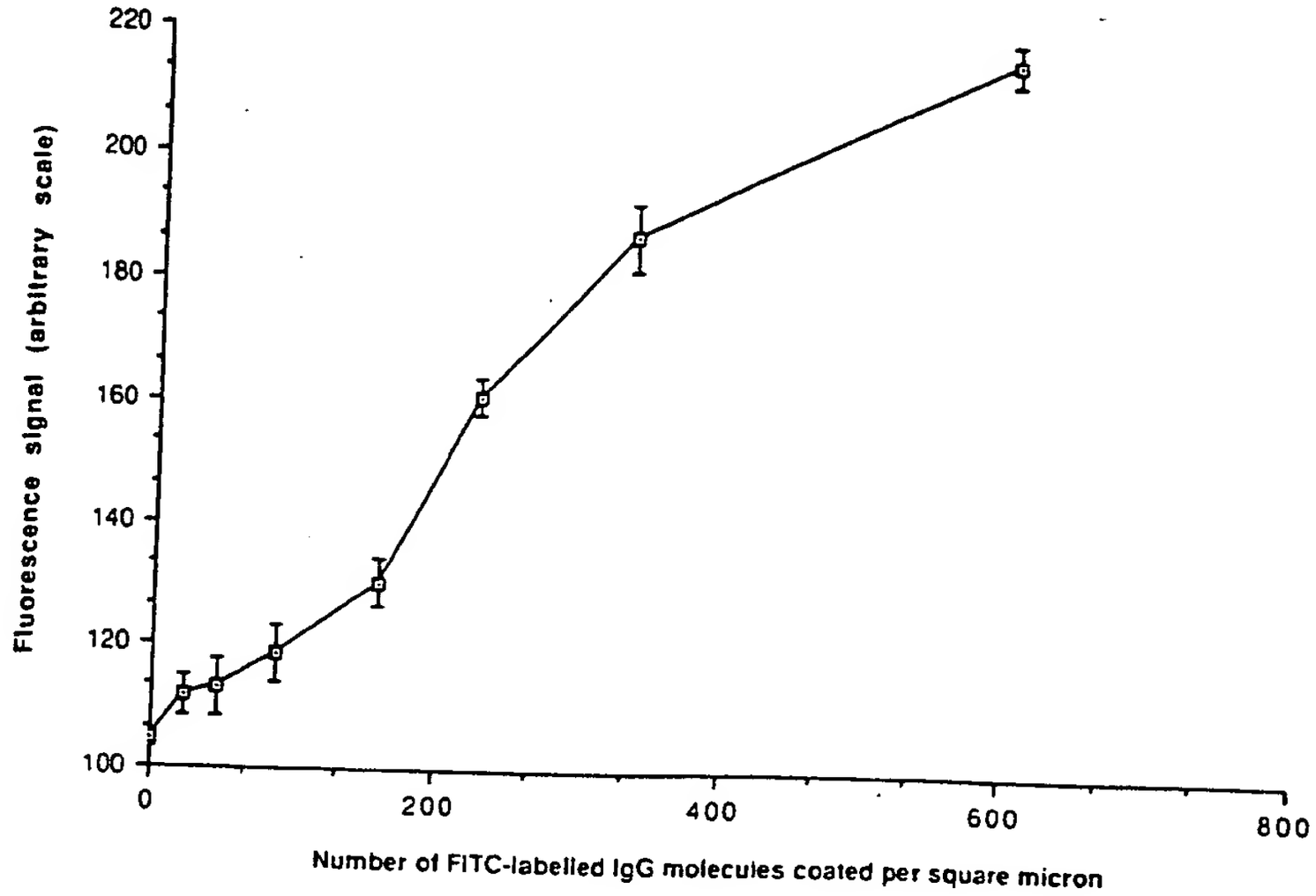

Figure 14. Fluorescence signal (arbitrary units), measured using the Bio-Rad/Lasersharp scanning confocal microscope, plotted as a function of the density of fluorescein-labelled IgG molecules (number of molecules/μm^2) deposited on Dynatech Microfluor white microtitre plates

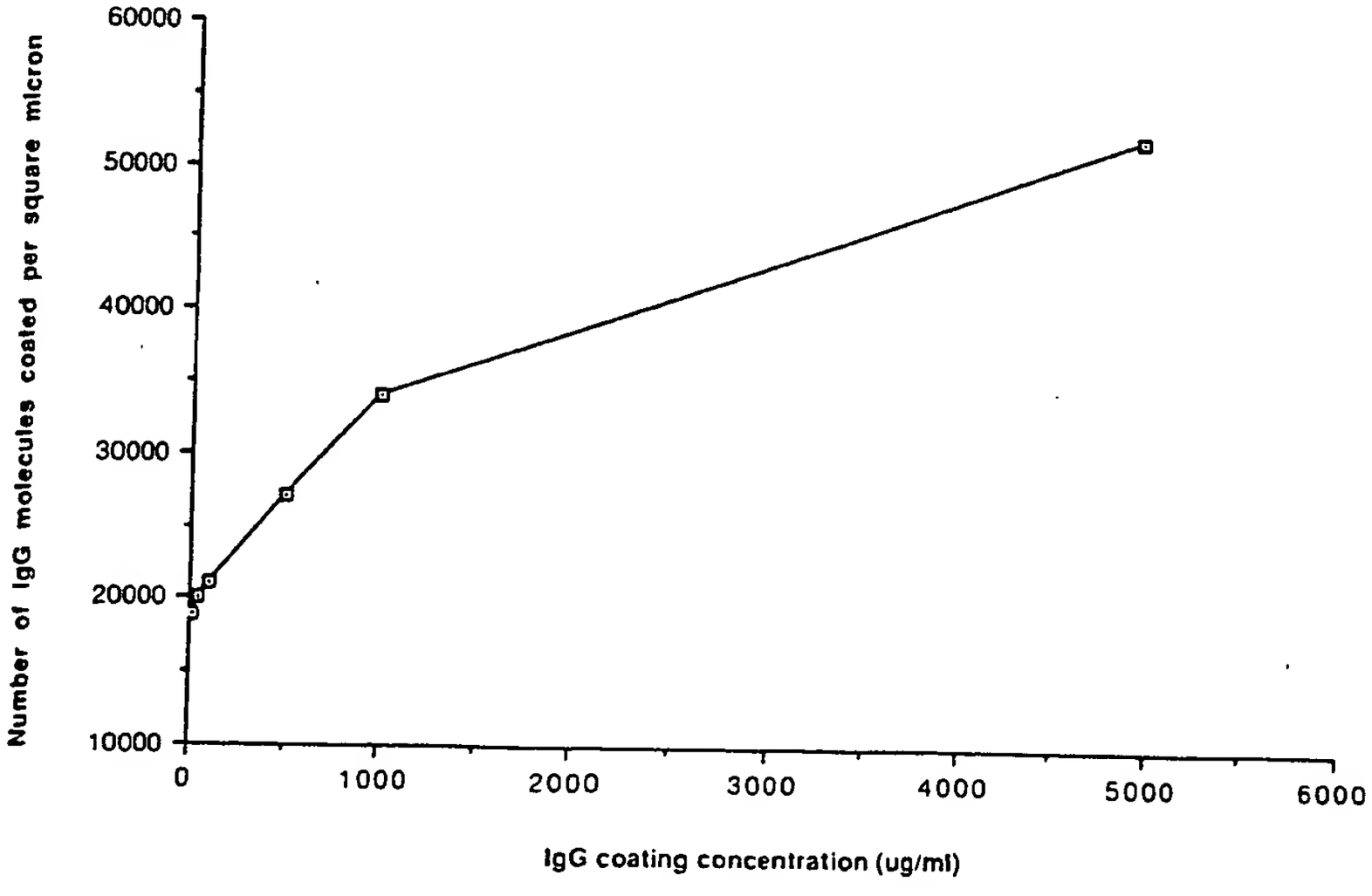

Figure 15. Surface density of IgG molecules (number of molecules/μm^2) deposited on Dynatech Microfluor white plates plotted as a function of IgG concentration ($\mu g/ml$) in the coating solution

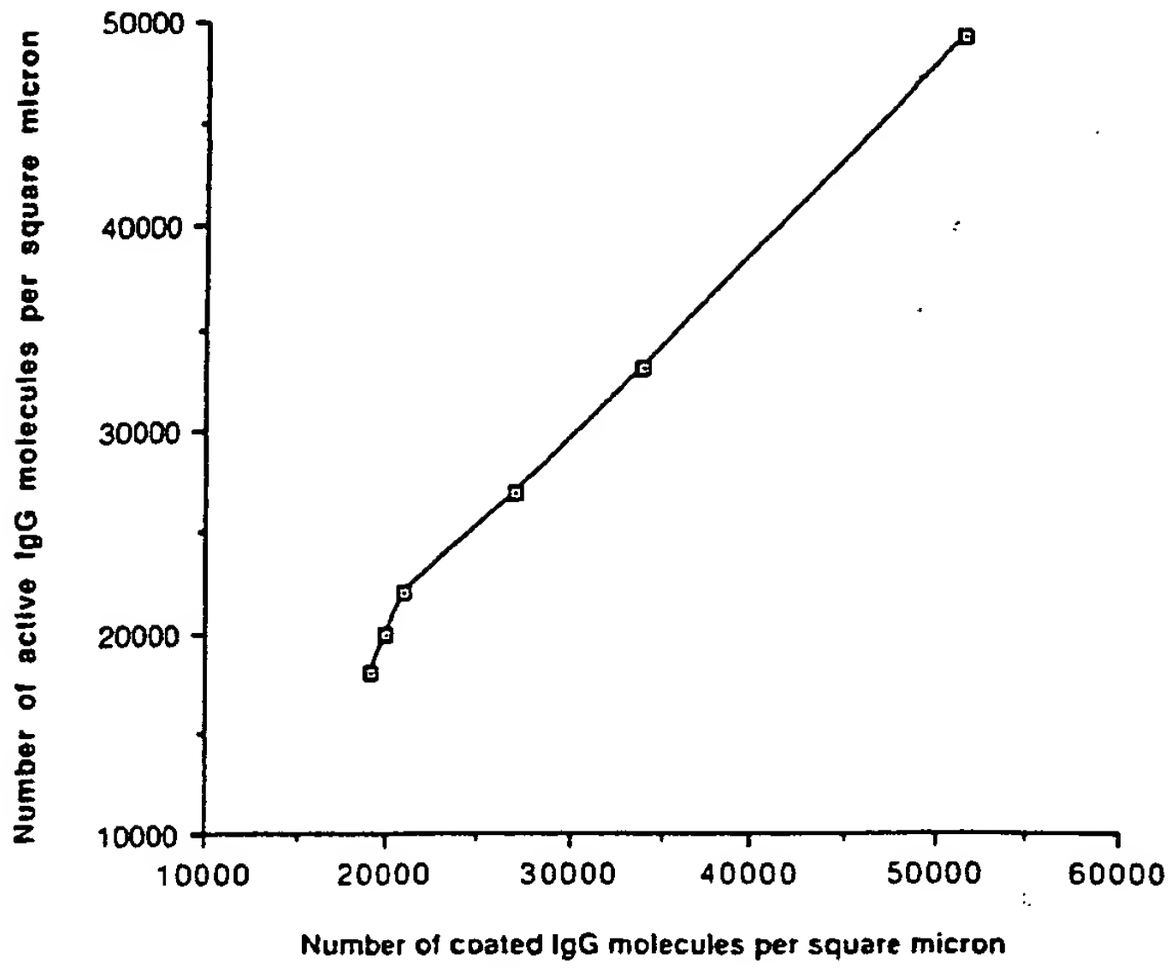

Figure 16. Surface density of immunoreactive IgG molecules (number of molecules/μm^2) plotted as a function of the total surface density of IgG (number of molecules/μm^2) on Dynatech Microfluor white microtitre plates

thought it useful to confirm the validity of our general concepts by comparing the performance of certain assays when constructed in microspot format and when conventionally designed. For example, we have compared a dual-labelled tumour necrosis factor (TNF) ratiometric assay system using Texas red and FITC-labelled antibodies with an optimized IRMA system using identical antibodies but with the second antibody ^{125}I-labelled. Although unoptimized, the ratiometric microspot assay yielded formal sensitivity values closely approaching that of the conventional, optimized, IRMA. Although verifying the general concepts underlying ratiometric microspot immunoassay methodology, further work is required to achieve the considerably greater sensitivity that theory predicts as achievable using optimized reagent concentrations and improved instrumentation.

CONCLUSION

As indicated above, differentiation of the fluorescent signals yielded by two fluorophores can be readily achieved solely on the basis of wavelength differences, and this approach has been relied on entirely in our preliminary studies. However, other physical techniques exploiting differences in decay time of two or more fluorescence emissions (using, for example, a pulsed or sinusoidally modulated laser source, and time– or phase-resolving detectors) are available, and can be expected both to further reduce background and to improve signal resolution, thus increasing assay sensitivity and precision. These considerations aside, the basic technology involved closely resembles that employed in domestic compact disk recorders and other similar data-storage devices, the obvious difference being that light emitted from each of the discrete zones forming the antibody-array is fluorescent rather than reflected, and yields chemical rather than physical information. Indeed, our preliminary studies suggest that highly sensitive immunoassays using antibody microspots of surface area approximating 50 μm^2 are achievable, implying that some 2,000,000 different immunoassays could, in principle, be accommodated on a surface area of 1 cm^2. Though non-specific binding of a multiplicity of developing antibodies would probably prohibit the use of antibody arrays of this order, it is evident that the technology is capable of encompassing analyte numbers of the kind likely to be useful in practice.

The development of multi-analyte assay systems of this kind can be anticipated to bring about

fundamental changes in medical diagnosis and many other biologically related areas. Systems capable of measuring every hormone and other endocrinologically related substance within a single small sample of blood are within technological reach, providing data which, when analysed with the aid of computer-based 'expert' pattern-recognition systems, are likely to reveal endocrine deficiences only dimly perceived using current 'single-analyte' diagnostic procedures. Such systems also provide a means to the development of a 'random access' immunoassay methodology, permitting the selection of any desired test or combination of tests from an extensive analyte menu. Clearly the accommodation of a wide range of individual immunoassays on a small immunoprobe (comparable in its overall physical dimensions with a few drops of blood) is likely to totally transform the logistics of immunodiagnostic testing, and genuinely represents, in our view, 'next generation' immunoassay methodology.

Acknowledgement

These studies are being generously supported by The Wolfson Foundation.

REFERENCES

Barnard, G. J. R., Kim, J. B. and Williams, J. L. (1985). Chemiluminescence immunoassays and immunochemiluminometric assays. In *Alternative Immunoassays*, Collins, W. P. (Ed.), John Wiley, Chichester, pp. 123–152.

Berson, S. A. and Yalow, R. S. (1973). Measurement of hormones—radioimmunoassay. In *Methods in Investigative and Diagnostic Endocrinology, 2A*, Berson, S. A. and Yalow, R. S. (Eds), North Nolland/Esevier, New York, pp. 84–135.

Dakubu, S., Ekins, R., Jackson, T. and Marshall, N. J. (1984). High sensitivity, pulsed light time-resolved fluoroimmunoassay. In *Practical Immunoassay. The State of the Art*, Butt, W. R. (Ed.), Marcel Dekker, New York, pp. 71–101.

Ekins, R. P. (1976). General principles of hormone assay. In *Hormone Assays and their Clinical Application*, Loraine, J. A. and Bell, E. T. (Eds), Churchill Livingstone, Edinburgh, pp. 1–72.

Ekins, R. P. (1978). The future development of immunoassay. In *Radioimmunoassay and Related Procedures in Medicine 1977*, IAEA, Vienna, pp.241–275.

Ekins, R. P. (1979). Radioassay methods. In *Radiopharmaceuticals II: Proceedings, 2nd International Symposium on Radiopharmaceuticals*, 19–22 March 1979, Seattle, Washington, Sorenson, J. A. (Ed), Society of Nuclear Medicine, New York, pp. 219–240.

Ekins, R. P. (1980). More sensitive immunoassays. *Nature*, **284**, 14–15.

Ekins, R. P. (1983a). The precision profile: its use in assay design, assessment and quality control. In *Immunoassays for Clinical Chemistry*, Hunter, W. M. and Corrie, J. E. T. (Eds), Churchill Livingstone, Edinburgh, pp. 76–105.

Ekins, R. P. (1983b). Measurement of analyte concentration. *British Patent* no. 8224600.

Ekins, R. (1985). Current concepts and future developments. In *Alternative Immunoassays*, Collins, W. P. (Ed.), John Wiley, Chichester, pp. 219–237.

Ekins, R. P. and Newman, B. (1970). Theoretical aspects of saturation analysis. In *Karolinska Symposia on Research Methods in Reproductive Endocrinology. 2nd Symposium: Steroid Assay by Protein Binding*, Diczfalusy, E. (Ed.), The Reproductive Endocrinology Research Unit, Karolinska sjukhuset Stockholm. pp. 11–36.

Ekins, R. P., Newman, B. and O'Riordan, J. L. H. (1968). Theoretical aspects of 'saturation' and radioimmunoassay. In *Radioisotopes in Medicine: In Vitro Studies*, Hayes, R. L., Goswitz, F. A. and Murphy, B. E. P. (Eds), Oak Ridge Symposia, USAEC, Oak Ridge, Tennessee, pp. 59–100.

Ekins, R. P., Newman, B. and O'Riordan, J. L. H. (1970a). Saturation assays. In *Statistics in Endocrinology*, McArthur, J. W. and Colton, T. (Eds), MIT Press, Cambridge, MA, pp. 345–378.

Ekins, R. P., Newman, B. and O'Riordan, J. L. H. (1970b). Competitive protein-binding assays. Discussion. In *Statistics in Endocrinology*, McArthur, J. W. and Colton, T. (Eds), MIT Press, Cambridge, MA, pp. 379–392.

Ekins, R. P., Filetti, S., Kurtz, A. B. and Dwyer, K. (1980). A simple general method for the assay of free hormones (and drugs); its application to the measurement of serum free thyroxine levels and the bearing of assay results on the 'free thyroxine' concept. *J. Endocrinol.*, **85**, 29–30.

Ezzell, C. (1986). Hybritech versus Abbott. *Nature*, **324**, 506.

Ezzell, C. (1987a). Judge confirms injunction in sandwich assay patent suit. *Nature*, **326**, 532.

Ezzell, C. (1987b). Hybritech wins court injunction over sandwich assays. *Nature*, **327**, 5.

Hemmilä, I., Dakubu, S., Mukkala, V.-M., Siiteri, H. and Lovgren, T. (1983). Europium as a label in time-resolved immunofluorometric assays. *Anal. Biochem.*, **137**, 335–343.

Jackson, T. M., Marshall, N. J. and Ekins, R. P. (1983). Optimisation of immunoradiometric (labelled antibody) assays. In *Immunoasays for Clinical Chemistry*, Hunter, W. M. and Corrie, J. E. T. (Eds), Churchill Livingstone, Edinburgh, pp. 557–575.

Kohen, F., Bayer, E. A., Wilchek, M., Barnard, G., Kim, J. B., Collins, W. P., Beheshti, I., Richardson, A. and McCapra, F. (1984). Development of luminescence-based immunoassays for haptens and for peptide hormones. In *Analytical Applications of Bioluminescence and Chemiluminescence*, Kricka, L., Stanley, P. E., Thorpe, G. H. G. and Whitehead, T. P. (Eds), Academic Press, New York, pp. 149–158.

Kohen, F., Pazzagli, M., Serio, M., DeBoever, J. and Vanderkerckhove, D. (1985). Chemiluminescence and bioluminescence immunoassay. In *Alternative Immunoassays*, Collins, W. P. (Ed). John Wiley, Chichester, pp. 103–121.

Köhler, G. and Milstein, C. (1975). Continuous culture of

fused cells secreting specific antibody. *Nature*, 256, 495–497.

Loevinger, R. and Berman, M. (1951). Efficiency criteria in radioactive counting. *Nucleonics*, 9, 26.

Marshall, N. J., Dakubu, S., Jackson, T. and Ekins, R. P. (1981). Pulsed-light, time-resolved, fluoroimmunoassay. In *Monoclonal Antibodies and Developments in Immunoassay*, Albertini, A. and Ekins, R. (Eds), Elsevier/ North Holland, Amsterdam, pp. 101–108.

McCapra, F., Tutt, D. E. and Topping, R. M. (1977). Assay method utilizing chemiluminescence. *British Patent no.* 1, 461, 877.

McGown, L. B. and Bright, F. V. (1984). Phase-resolved fluorescence spectroscopy. *Anal. Chem.*, 56, 1400–1417.

Miles, L. E. H. and Hales, C. N. (1968). An immunoradiometric assay of insulin. In *Protein and Polypeptide Hormones, Pt. I*, Margoulies, M. (Ed.), Excerpta Medica, Amsterdam, pp. 61–70.

Ploem, J. S. (1986). New instrumentation for sensitive image analysis of fluorescence in cells and tissues. In *Applications of Fluorescence in the Biological Sciences*, Tayer, D. L., Waggoner, A. S., Lanni, F., Murphy, R. and Birge, R. (Eds), Alan R. Liss, New York, pp. 289–300.

Rodbard, D. and Weiss, G. H. (1973). Mathematical theory of immunometric (labelled antibody) assay. *Analyt. Biochem.*, 52, 10–44.

Shalev, A., Greenberg, G. H. and McAlpine, P. J. (1980). Detection of attograms of antigen by a high sensitivity enzyme-linked immunosorbent assay (HS-ELISA) using a fluorogenic substrate. *J. Immunol. Methods*, 38, 125–139.

Tait, J. F. (1970). Competitive protein-binding assays. Discussion. In *Statistics in Endocrinology*, McArthur, J. W. and Colton, T. (Eds), MIT Press, Cambridge, MA. pp. 379–392.

Weeks, I., McCapra, F., Campbell, A. K. and Woodhead, J. S. (1983). Immunoassays using chemiluminescent labelled antibodies. In *Immunoassays for Clinical Chemistry*, Hunter, W. M. and Corrie, J. E. T. (Eds), Churchill Livingstone, Edinburgh, pp. 525–530.

Weeks, I., Campbell, A. K., Woodhead, S. and McCapra, F. (1984). Immunoassays using chemiluminescent labels. In *Practical Immunoassay. The State of the Art*, Butt, W. R. (Ed.), Marcel Dekker, New York, pp. 103–116.

White, J. G., Amos, W. B. and Fordham, M. (1987). An evaluation of confocal versus conventional imaging of biological structures by fluorescence light microscopy. *J. Cell Biol.*, 105, 41–48.

Whitehead, T. P., Thorpe, G. H., Carter, T. J., Groucutt, C. and Kricka, L. J. (1983). Enhanced luminescence procedure for sensitive determination of peroxidase-labelled conjugates in immunoassay. *Nature*, 305, 158–159.

Wide, L. (1971). Solid phase antigen-antibody systems. In *Radioimmunoassay Methods*, Kirkham, K. E. and Hunter, W. M. (Eds), Churchill Livingstone, Edinburgh, pp. 405–418.

Woodhead, J. S., Addison, G. M., Hales, C. N. and O'Riordan, J. L. H. (1971). Discussion. In *Radioimmunoassay Methods*, Kirkham, K. E. and Hunter, W. M. (Eds), Churchill Livingstone, Edinburgh, pp. 467–488.

Yalow, R. S. and Berson, S. A. (1970a). Radioimmunoassays. In *Statistics in Endocrinology*, McArthur, J. W. and Colton, T. (Eds), MIT Press, Cambridge, MA. pp. 327–344.

Yalow, R. S. and Berson, S. A. (1970b). Cmpetitive protein-binding assays. Discussion. In *Statistics in Endocrinology*. McArthur, J. W. and Colton, T. (Eds), MIT Press, Cambridge, MA. pp. 379–392.